University of Alberta

An investigation of the abundance and molecular characteristics of organic matter in glacier systems

by

Joel D. Barker

©

A thesis submitted to the Faculty of Graduate Studies and Research
in partial fulfillment of the requirements for the degree of

Doctor of Philosophy

Department of Earth and Atmospheric Sciences

Edmonton, Alberta
Spring 2007

Library and Archives Canada

Published Heritage Branch

395 Wellington Street
Ottawa ON K1A 0N4
Canada

Bibliothèque et Archives Canada

Direction du Patrimoine de l'édition

395, rue Wellington
Ottawa ON K1A 0N4
Canada

Your file Votre référence
ISBN: 978-0-494-29647-9
Our file Notre référence
ISBN: 978-0-494-29647-9

NOTICE:
The author has granted a non-exclusive license allowing Library and Archives Canada to reproduce, publish, archive, preserve, conserve, communicate to the public by telecommunication or on the Internet, loan, distribute and sell theses worldwide, for commercial or non-commercial purposes, in microform, paper, electronic and/or any other formats.

The author retains copyright ownership and moral rights in this thesis. Neither the thesis nor substantial extracts from it may be printed or otherwise reproduced without the author's permission.

AVIS:
L'auteur a accordé une licence non exclusive permettant à la Bibliothèque et Archives Canada de reproduire, publier, archiver, sauvegarder, conserver, transmettre au public par télécommunication ou par l'Internet, prêter, distribuer et vendre des thèses partout dans le monde, à des fins commerciales ou autres, sur support microforme, papier, électronique et/ou autres formats.

L'auteur conserve la propriété du droit d'auteur et des droits moraux qui protège cette thèse. Ni la thèse ni des extraits substantiels de celle-ci ne doivent être imprimés ou autrement reproduits sans son autorisation.

In compliance with the Canadian Privacy Act some supporting forms may have been removed from this thesis.

While these forms may be included in the document page count, their removal does not represent any loss of content from the thesis.

Conformément à la loi canadienne sur la protection de la vie privée, quelques formulaires secondaires ont été enlevés de cette thèse.

Bien que ces formulaires aient inclus dans la pagination, il n'y aura aucun contenu manquant.

Canada

Abstract

Reports of viable microbial populations in basal ice and subglacial meltwater, and evidence of subglacial microbial metabolism, challenges the conceptual model of an abiotic subglacial environment. Glaciers overrun organic matter (OM) during advance, and supraglacially-derived OM is routed subglacially through moulins and crevasses in supraglacial meltwater. Subglacial OM may support heterotrophic microbial metabolism. Heterotrophy affects the abundance and molecular characteristics of OM exported to downstream environments in glacier meltwater and OM abundance and characteristics affects aquatic ecology. Glaciers are water sources to rivers globally. Increased glacier melt in response to climate warming will increase OM export from glaciers to downstream ecosystems. Given the importance of OM abundance and characteristics to downstream aquatic ecology, an understanding of the abundance and behaviour of OM in glacier systems is important. Few studies have addressed the topic of OM export from glaciers, and a direct assessment of OM abundance and characteristics in glacier systems is lacking. The purpose of this thesis is to quantify OM abundance in a range of glacier environments, characterize OM that is stored within and exported from glacier systems and determine the factors that influence the OM flux to downstream environments. To address these objectives, the abundance, fluorescence and infrared absorption characteristics of OM in glacier meltwater and ice were investigated at John Evans Glacier and Outre Glacier, Canada, and Victoria Upper Glacier, Antarctica.

Dissolved organic carbon was detected in all of these glaciers (0.06 – 46.6 ppm). The fluorescence characteristics of dissolved organic carbon in meltwater and ice indicates that several organic pools exist subglacially which are of microbial and terrestrial provenance. OM mobilization from these pools is influenced by subglacial meltwater flow routing. The infrared characteristics of particulate organic carbon in basal ice indicates that there is a microbial component to OM in basal ice regardless of potential source OM.

The export of microbially-derived OM to downstream ecosystems represents the export of labile OM from glacier systems. This export may contribute to a positive feedback with climate warming as an increased OM flux in meltwater increases heterotrophy in glacially-fed rivers and increases the flux of CO_2 to the atmosphere.

Acknowledgements

My words are clumsy and my writing likely isn't much better, so I can only hope that the people below will have some sort of appreciation of the depth of my gratitude.

First of all, thank you Dr. Martin Sharp. You introduced me to the world of glaciology and polar research back as an undergrad and I cannot thank you enough for that. Through your own efforts and generosity you've presented me with incredible opportunities for which I am grateful. Throughout the years you have selflessly provided me with guidance, and I appreciate that. Thanks too to the Sharp family. Not only are you excellent hosts, but you also serve as an example that yes, a family can flourish despite the demands that field work and travel exert on the dynamic. I can't tell you how much of a comfort this is.

Thank you Dr. Vince St. Louis. Your support and advice at crucial times, and your indomitable humour, definitely made a difference.

Thank you Dr. Sean Fitzsimons. I learned an incredible amount from you, not only in the fine art of digging tunnels, but also in the fine art of managing crises and maintaining the balance.

Thank you Bud Rickhi, for being there. Lessons learned from you have made this all possible. I owe you a huge dept of gratitude.

So many other people have contributed over the years. Among them: Dr. Ray Turner, thank you for your encouragement and enthusiasm, and use of your spectrofluorometer. Dr. Thomas Stachel, thank you for the use of your FTIR. John Orwin, thanks for being such a good friend. Lindz and Inka, thanks for your support and enthusiasm for what I was doing. Chris, Rosie and Shannon, thanks for friendship. We miss you guys. Dr. John England and Katherine, thanks for afternoons on the pond. Dr. Alex Wolfe, thank you for your encouragement and stimulating discussions. To Drs. Berry Lyons and Yo Chin at OSU. Thanks for your patience and I look forward to the upcoming year. To Ryan, Aby, Chris and Becki thanks for your friendship and support in Columbus. To Mark Skidmore, thanks for your support and for getting this whole thing started.

Particularly, I would like to acknowledge the following people, who have made such an important contribution to life outside of work. Lana and Nigel (and now Madeline), your support and friendship over the years has made such a difference. From helping lug flooded carpet in 30 degrees to being there with a unwavering support, Sam and I are so appreciative and hold you both in high esteem. Melissa and Serge, your friendship has also made a huge difference. We definitely don't see you guys enough. Gabe and Jane, your friendship has also made a huge difference. From helping build a deck in the rain, to taking in the fireworks on Canada Day, you've made it fun.

A huge thank you to my Mum, Dad and sister. I never would have considered starting the PhD, and wouldn't have finished it were it not for your unwavering support. You've always been there, through thick and thin, and I cannot hope to express how much that means to me.

Most importantly, thank you to my wife Sam. You inspire me. Anything that I've accomplished is as much a result of your contribution as it is of my own. None of this means a thing if you're not here to share it with me, and I'm so glad that you are.

Table of Contents

Chapter 1. Introduction **1**
1.1. Context and Rationale 1
1.2. Background 2
1.2.1. Organic matter in aquatic systems 2
1.2.2. Organic matter in glacier systems 3
1.2.3. Glacier hydrologic systems 4
1.2.3.1. Cold based glaciers 5
1.2.3.2. Polythermal glaciers 6
1.2.4. Glacier microbiology 6
1.3. Thesis Outline 7
1.4. References 10

Chapter 2. Abundance and dynamics of dissolved organic carbon in glacier systems **15**
2.1. Introduction 15
2.2. Field Sites and Methodology 17
2.2.1. Field sites 17
2.2.2. Sampling 20
2.2.3. Analysis 20
2.3. Results and Discussion 21
2.3.1. John Evans Glacier 21
2.3.2. Outre Glacier 24
2.3.3. Victoria Upper Glacier 26
2.4. Summary and Conclusion 28
2.5. References 30

Chapter 3. Using synchronous fluorescence spectroscopy and Principal Components Analysis (PCA) to monitor dissolved organic matter (DOM) dynamics in a glacier system **39**
3.1. Introduction 39
3.2. Field Site and Methodology 41
3.2.1. Outre Glacier 41
3.2.2. Sampling 42
3.2.3. Fluorescence analysis 43
3.2.4. Principal Components Analysis 44
3.3. Results 45
3.3.1. TOTAL PCA 45
3.3.2. PCA by environment 46
3.3.2.1. Subglacial 46
3.3.2.2. Marginal 46
3.3.2.3. Alpine Stream 47
3.3.2.4. Basal 47
3.3.2.5. South Glacier 47
3.3.2.6. Supra 48
3.3.3. PC shape interpretation 48
3.3.4. PC loadings 51
3.4. Interpretation 53
3.5. Summary and Conclusions 58
3.6. References 60

Chapter 4. An investigation of particulate and dissolved organic matter in basal ice.... 75
4.1. Introduction.... 75
4.2. Field Sites.... 76
4.3. Sampling and Methods.... 77
4.3.1. Basal ice sampling.... 77
4.3.1.1. JEG.... 77
4.3.1.2. VUG.... 78
4.3.2. Sample preparation and analysis.... 79
4.3.2.1. Micro-FTIR.... 79
4.3.2.2. Fluorescence analysis.... 81
4.4. Results and Interpretation.... 81
4.4.1. Micro-FTIR.... 81
4.4.2. Synchronous fluorescence.... 84
4.5. Discussion.... 85
4.6. Summary and Conclusions.... 91
4.7. References.... 94

Chapter 5. Synthesis and Discussion.... 103
5.1. OM abundance in glacier systems.... 103
5.1.1. Meltwater.... 103
5.1.2. Ice.... 104
5.2. OM Characteristics.... 105
5.2.1. Meltwater.... 105
5.2.2. Ice.... 107
5.3. Factors that influence the flux of OM exported from glacier systems to downstream aquatic environments.... 108
5.4. Conclusions.... 109
5.4.1. Implications for global carbon cycling.... 110
5.5. Directions for future research.... 112
5.6. References.... 114

List of Tables

Table 2.1. DOC abundance at John Evans Glacier, Outre Glacier and Victoria Upper Glacier 33

Table 3.1. Synchronous fluorescence peak designation 72

Table 3.2. Correlation matrix for PC scores 73

Table 3.3. Proposed source of each PC 74

Table 4.1. Absorbance band assignments 102

List of Figures

Fig. 2.1. Dissolved organic carbon concentrations and emission fluorescence at John Evans Glacier, 2001 33

Fig. 2.2. Outre Glacier a) dissolved organic carbon concentrations, b) supraglacial and subglacial synchronous spectra, c) basal ice and non-glacial spectra, d) average subglacial synchronous spectrum 34

Fig. 2.3. 270/370 nm ratio relative to the time of daily minimum discharge at Outre Glacier 35

Fig. 2.4. Dissolved organic carbon concentrations in ice at Victoria Upper Glacier 36

Fig. 2.5. Synchronous spectra from ice samples at Victoria Upper Glacier 37

Fig. 2.6. 276/370 nm ratio in ice along a transect from glacier ice to basal ice at Victoria Upper Glacier 38

Fig. 3.1. Location of the Outre Glacier field site 63

Fig. 3.2. Photographs showing that a) Outre Glacier terminates below treeline and b) that the main subglacial meltwater channel is confined by an N-channel 64

Fig. 3.3. The average synchronous fluorescence spectrum from Outre Glacier 65

Fig. 3.4. TOTAL PCA factor scores vs. spectral wavelength 66

Fig. 3.5. The spectral waveform for the PCs from each environment 67

Fig. 3.6. The relationship between the shape of each TOTAL PC and the shape of individual spectra that load strongly on them. 68

Fig. 3.7. TOTAL PC factor loadings 69

Fig. 3.8. Synchronous spectra loading on TOTAL PCs 2, 3 and 4 relative to TOTAL PC1 70

Fig. 3.9. a) manually recorded water depth in the proglacial stream at Outre Glacier, b) air temperature record from Stewart, B.C. 71

Fig. 4.1. The co-isotope plot for John Evans Glacier tunnel ice samples 95

Fig. 4.2. The glacier ice/basal ice transition at VUG 95

Fig. 4.3. OM that has been eluted from the GF/F filter paper 96

Fig. 4.4. The average FTIR spectrum for all of the basal ice samples from Victoria Upper Glacier and John Evans Glacier 96

Fig. 4.5. The CH_2/CH_3 ratio for Victoria Upper Glacier and John Evans Glacier POM samples 97

Fig. 4.6. The synchronous spectra and FTIR spectra for basal ice samples from Trench 1 at Victoria Upper Glacier 98

Fig. 4.7. The synchronous spectra and FTIR spectra for basal ice samples from Trench 2 at Victoria Upper Glacier 99

Fig. 4.8. The synchronous spectra and FTIR spectra for basal ice samples from the 10 m section at John Evans Glacier 100

Fig. 4.9. The synchronous spectra and FTIR spectra for basal ice samples from the 12 m section at John Evans Glacier 101

List of Acronyms

CP/MAS	cross polarization/magic angle sample
DCM	dichloromethane
DOC	dissolved organic carbon
DOM	dissolved organic matter
EEM	emission excitation matrix
EPS	extracellular polymeric substance
EPR	electron paramagnetic resonance
FTIR	Fourier transform infrared
IR	infrared
JEG	John Evans Glacier
NMR	nuclear magnetic resonance
OC	organic carbon
OM	organic matter
PC	principal component
PCA	principal components analysis
POC	particulate organic carbon
POM	particulate organic matter
VUG	Victoria Upper Glacier

List of Symbols

λ_{em}	emission wavelength
λ_{ex}	excitation wavelength
$\Delta\lambda$	wavelength offset

Chapter 1: Introduction

1.1. Context and Rationale.

Organic matter (OM) mediates the biogeochemistry and bioavailability of metals (e.g. Cabaniss, 1992), affects water column optical properties (e.g. Kowalczuk et al., 2005), and functions as a substrate for heterotrophic metabolism (Arnosti et al., 2005) in aquatic ecosystems. Processes that produce, consume and/or transform OM influence aquatic ecosystem carbon cycling (McKnight et al., 2003) because the abundance and molecular composition of OM will determine its environmental function (e.g. Kaplan and Newbold, 2003, Arnosti, 2003). The importance of OM molecular composition in aquatic environments has made the molecular characterization of OM a major theme in aquatic system research (e.g. Findlay and Sinsabaugh, 2003; Thurman, 1985).

OM abundance and molecular characteristics are a function of its organic source material and biogeochemical history (e.g. Stedmon et al, 2003). For example, the primary source of OM to freshwater aquatic systems is plant matter and its degradation by biotic and abiotic processes during transport determines its molecular characteristics and ecological function. By understanding OM sources and the processes by which it is biogeochemically altered in aquatic systems, it may be possible to predict how OM will function in downstream ecosystems and contribute to the ecosystem carbon budget (e.g. Hedges et al., 1994).

"Glaciers across the globe are important sources of water for many important rivers – rivers upon which people depend for drinking water, agriculture and industrial purposes" (Achim Steiner, Executive Director of the United Nations Environment Programme (2007)). Despite the importance of glaciers to downstream aquatic environments, little is known about the abundance, sources, and characteristics of OM within, and exported from, glacier systems. Recent work by Sharp et al. (1999) and Skidmore et al. (2000, 2005) shows that viable microbial populations exist in subglacial environments and highlights the possibility that OM is biogeochemically produced, consumed and/or transformed in glacier systems. Given the importance of OM abundance and molecular characteristics to downstream aquatic ecology, an understanding of the abundance and behaviour of OM in glacier systems is important.

Glacier systems have been ignored by studies seeking to quantify and characterize aquatic system OM and there have been few studies that address OM in glacier environments (e.g. Lafreniere

and Sharp, 2004). Thus the sources, distribution, abundance and molecular characteristics of OM in glacier settings are poorly understood. The facts that 1) glaciers supply freshwater to major rivers globally, 2) viable subglacial heterotrophic microbial communities may produce, consume and or alter OM which is exported to downstream aquatic ecosystems, 3) increased glacier melt in response to global climate warming will increase the flux of glacier meltwater to downstream ecosystems, 4) the abundance and molecular characteristics of OM exert a fundamental influence on aquatic ecosystem processes, highlight the need to determine whether significant quantities of OM are exported from glacier systems, and if so, to determine the abundance and characteristics of glacier system OM. The purpose of this thesis is to 1) quantify the abundance of OM in a range of glacier environments; 2) characterize OM that is both stored within and exported from glacier systems; 3) determine the factors that influence the flux of OM that is exported from glacier systems to downstream aquatic environments.

1.2. Background.

1.2.1. Organic matter in aquatic systems.

OM is frequently expressed in terms of organic carbon (OC) content (Kaplan and Newbold, 2003) and a distinction is made between the dissolved phase (DOC) and the particulate phase (POC). DOC or DOM (dissolved OM) is operationally defined as that OM which passes through a filter with a pore size between 0.2 – 0.7 μm (Benner, 2003). DOM is the primary substrate supporting microbial growth and respiration in aquatic ecosystems, so factors that affect the quantity and molecular characteristics of DOM will exert a major influence on ecosystem structure and function.

The abundance and molecular characteristics of the organic source material, and the effect of subsequent heterotrophic biogeochemical processing of that source material, determine the quantity and molecular characteristics of OM. In most aquatic systems, the source of the bulk OM is readily identified. For example, OM in river systems is predominantly derived from surrounding vegetation and soils, whereas oceanic OM is primarily derived from phytoplankton. This difference in OM source is reflected in the molecular characteristics of the respective aquatic OM, where river system OM is characterized by a relative abundance of vascular plant-derived aromatic moieties and oceanic OM is characterized by a relatively high abundance of phytoplankton-derived amino acids and neutral sugars (Benner, 2003). The subsequent biogeochemical alteration of the source OM is selective as active microbial populations

mineralize the more easily metabolized compounds. For example, the relative abundance of recalcitrant vascular plant-derived aromatic moieties in river DOM is accentuated by biogeochemical activity as soil microbes mineralize the more labile compounds (such as plant-derived carbohydrates) during OM transport to rivers (Benner, 2003).

The microbial degradation of DOM is a function of the chemical composition of DOM and the characteristics of the microbial population present. Microbes metabolize relatively small monomeric compounds, such as free amino acids, more easily than larger polymeric molecules which require the extracellular enzymatic breakdown before they can be transported across the cell membrane (Arnosti, 2003). Likewise, an organic compound will be mineralized if it fulfills the metabolic requirements of the microbes present. It is in this way that OM is both a control on, and a product of, microbial metabolism in aquatic ecosystems.

1.2.2. Organic matter in glacier systems.

Glacier systems are aquatic environments for which the incorporation of source OM and subsequent biogeochemical alterations are poorly understood. Conceptually, the glacier OM system can be described as follows: Glaciers overrun OM in soils and vegetation during periods of advance (e.g. Humlum et al., 2005, Bergsma et al., 1884). This overrun OM contributes to the subglacial OM pool. The subglacial OM pool can be supplemented by supraglacially-derived OM, which is the product of microbial activity in the supraglacial snowpack and cryoconite holes (cylindrical depressions which result from the melting of supraglacial sediment into the glacier surface) or of the deposition of wind-blown sediment on the glacier surface. This OM can be delivered to the glacier bed by ice flow, or by transport in supraglacial meltwater that is routed through the glacier via moulins and crevasses. A third potential source of OM to the subglacial pool results from OM which is released by ice melt at the glacier bed due to the geothermal heat flux or a raising of the pressure melting point due to the pressure exerted by the overlying ice mass. OM is exported from the glacier system by subglacial meltwater flow or supraglacial meltwater runoff to proglacial streams. OM can also be sequestered by entrainment onto the base of the glacier during the formation of basal ice (e.g. by refreezing of subglacial waters). Thus, hydrological processes in the supraglacial, englacial and subglacial environments may influence the incorporation of OM into a glacier system and its subsequent export to downstream environments.

1.2.3. Glacier hydrologic systems.

Within the subglacial environment, hydrological conditions will influence OM distribution, mobilization and/or storage, and exchange between the englacial and subglacial OM pools in the same way that hydrological conditions influence the distribution and mobilization of glacial sediment and dissolved ions (e.g. Sharp et al., 1995). In temperate glaciers (glaciers with liquid water at the bed throughout the year) the circulation of subglacial meltwater is controlled by the hydraulic pressure gradient (Hooke, 1989). Assuming the absence of established subglacial meltwater flow-paths, subglacial meltwater is distributed across a broad area of the bed at the beginning of the melt season when subglacial meltwater sources are restricted to subglacial ice melt and release from subglacial storage (e.g. Willis et al., 1993). Subglacial water volumes and flow velocities are relatively small and subglacial water pressure is relatively high. This type of subglacial flow condition is described as a "distributed" system (Hubbard and Nienow, 1997). As the melt season progresses and supraglacial meltwater is delivered to the glacier bed through moulins and crevasses, subglacial meltwater channels begin to develop and form an arborescent channelized network (the "channelized" drainage system) extending back from the glacier terminus toward the point sources of supraglacial meltwater input to the subglacial meltwater drainage system (Nienow et al., 1998). As the supraglacial meltwater input increases with increasing snow and ice melt, these channels increase in volume either by excavation into the bed (Nye, 1973) or, more commonly, frictional melting upward into the glacier sole (Rothlisberger, 1972). Channel enlargement results in a decrease in channel hydraulic pressure and a pressure gradient develops from the more distal areas towards the main channels, which results in subglacial meltwater circulation towards the main channels (Paterson, 1994). Meltwater discharge from glaciers is primarily a function of meteorological forcing on supraglacial melt and tends to show a diurnal discharge hydrograph in response to daily radiative cycles (e.g. Hannah, 2000). This diurnal fluctuation, in turn, causes a fluctuation in hydraulic pressure within the subglacial channelized system so that periods of increased supraglacial meltwater flux to the channelized system result in increased channel pressures with the result that flow occurs from the main channels to the distributed system. This condition persists until pressures in the channelized system decrease relative to distributed drainage system hydraulic pressure either by channel enlargement or a decrease in the supraglacial meltwater flux to the subglacial hydrologic system. At that point. flow from the distributed system to the channelized system is re-established. In this way, hydrologic exchange can occur between the channelized and distributed meltwater drainage systems beneath temperate glaciers (e.g. Hubbard et al., 1995).

By definition, temperate glaciers have liquid water at the bed throughout the year (Paterson, 1994, pg. 205). However, not all glaciers are temperate and two other types of glacier are generally recognized on the basis of their subglacial thermal (and thus hydrological) regimes: cold-based and polythermal glaciers.

1.2.3.1. Cold-based glaciers.

By definition, the temperature of ice throughout a cold-based glacier is below the pressure melting point (due to low overlying air temperatures, high rates of vertical advection of cold surface ice to the bed, or an ice mass which is too thin to raise basal pressures above the pressure melting point, or a combination of the three). However, liquid water can exist as a film at the ice-rock interface (e.g. Cuffey et al., 1999) or boundaries between ice crystals (Alley et al., 1986). Liquid water at the bed exists as an interfacial film that occurs between ice and "foreign solids" (Cuffey et al., 1999). This film is formed by a reduction in the chemical potential close to the foreign solid which lowers the melting point. The existence of dissolved solutes in the water further depresses the melting point thus maintaining the water film. The existence of this film at the interface between the glacier sole and the underlying substrate is believed to induce sliding of cold-based glaciers over the bed (e.g. Cuffey et al., 1999). The circulation of liquid water within a cold-based glacier occurs when the water film at the bed intersects grain boundaries in the overlying ice. Variations in the hydraulic pressure field will induce water circulation along grain boundaries and the basal film and thus transport fine sediment (e.g. Cuffey et al., 1999), dissolved solutes and nutrients throughout the glacier. In cases where a cold-based glacier overruns water saturated sediment, the upward flow of water through the sediment pore spaces towards the freezing front may occur and result in the formation of basal ice (e.g. Christoffersen and Tulaczyk, 2003). In this case, a combination of increased fluid pressure (due to the overriding glacier) and any increase in solute concentration depresses the melting point of sediment pore water. The melting point can be depressed further by surface tension arising from curvature at the ice-water interface such as would occur with water flow through fine sediment (Christoffersen and Tulaczyk, 2003). If curvature exists at the ice-water interface, then a pressure gradient is created across the boundary due to interfacial effects (Fowler and Krantz, 1994) and the pore water pressure is decreased at the interface. This lowering of pore water pressure creates a hydraulic gradient which causes a net flow of pore water toward the freezing interface (Souchez

et al., 2004). Souchez et al. (2004) provide isotopic evidence in support of this mechanism of basal ice formation in two cold-based Antarctic glaciers (Mackay Glacier and Taylor Glacier).

1.2.3.2. Polythermal glaciers.

Polythermal glaciers exhibit both temperate and cold-based thermal regimes (e.g. Blatter and Hutter, 1991). As a result, glaciers characterized by a temperate thermal regime may be closely associated with zones where the ice is below the freezing point (i.e. "cold" ice). (e.g. Copland and Sharp, 2001). The distribution of temperate and cold ice in a polythermal glacier is dependent on several factors. For example, cold ice will persist where the mean annual temperature is below 0 °C whereas temperate ice may form whenever the melting point is lowered below the freezing point. An example of a mechanism for lowering the melting point include pressure melting at the bed beneath thick ice (e.g. Blatter, 1987). In the case of a polythermal glacier which exhibits a basal temperate zone, subglacial drainage system behaviour is characterized by a distributed meltwater drainage system prior to the initiation of the supraglacial meltwater flux through crevasses and moulins during the melt season (Bingham et al, 2005). If supraglacial meltwater penetrates to the bed and flows to the temperate zone, hydraulic pressures in the temperate zone increase as flow is inhibited from discharging down-gradient by a cold-based margin. This pressure increases until it exceeds the mechanical strength of the surrounding cold ice, thereby fracturing it. Propagation of these fractures provides a low resistance pathway through which the subglacial meltwater is routed and erupts onto the glacier surface and proglacial floodplain. As meltwater continues to flow through these fractures, they enlarge by frictional heating and due to their higher capacity, grow at the expense of those with smaller capacity. Subsequent subglacial drainage system re-organization occurs in a manner similar to that observed in temperate systems as a more hydraulically efficient channelized subglacial hydrologic system is established.

1.2.4. Glacier microbiology.

The concept of subglacial biogeochemistry is relatively new. Prior to the report by Sharp and coworkers (1999) of viable bacterial populations in subglacial meltwater and basal ice, abiotic weathering reactions were widely considered to be characteristic of subglacial environments (Raiswell, 1984). Subglacial environments are considered to be extreme environments for microbial life. For example, the subglacial environment is largely oligotrophic, cold, and permanently dark (Skidmore et al., 2005). However, subglacial environments also present

conditions that would favour microbial colonization such as insulation by the overlying ice mass from temperature fluctuations across the freezing point, the presence of liquid water in subglacial sediment or at ice grain boundaries, and organic carbon and nutrients in overrun soils and sediment and subglacially routed supraglacial OM (Sharp et al., 1999).

Microbes have been identified from the supraglacial snowpack (Carpenter et al., 2000) and cryoconite holes (Mueller and Pollard, 2004), as well as from accreted ice above subglacial Lake Vostok (Priscu et al., 1999) and subglacial basal ice and meltwater in aretic and alpine glaciers (Skidmore et al., 2005). Furthermore, evidence that subglacial microbial populations are active is mounting. For example, Skidmore et al. (2005) report that microbial populations that corresponded with observed aqueous geochemistry were recovered from two glaciers in different geological settings. Wadham et al. (2004) used sulphur and oxygen stable isotopes to show that microbial sulphate reduction occurs beneath Finsterwalderbreen, a polythermal glacier in Svalbard. A study by Hodson et al. (2005) at two polythermal glaciers at Svalbard show that supraglacial microbial nitrification and ammonia assimilation in cryoconite holes have produced a supraglacial dissolved organic nitrogen and particulate nitrogen flux and that subglacial denitrification and sulphate reduction is occurred. Furthermore, the analysis of 16s rRNA genes from subglacial, supraglacial and proglacial samples indicates that autochthonous subglacial microorganisms exist (Bhatia et al., 2006). These findings suggest that microbes function subglacially and that microbially mediated chemical reactions occur in, and may be unique to, subglacial environments.

1.3. Thesis Outline.

This thesis is presented as a series of three papers, outlined below, with a final chapter that draws together the main conclusions. Each chapter (Chapters 2-4) is written as an individual manuscript. The objectives of each paper are outlined below:

Paper 1: to quantify DOC abundance and to characterize DOC using fluorescence spectroscopy in a range of glacial sub-environments.

The abundance and fluorescence characteristics of DOC are investigated at John Evans Glacier, and Outre Glacier, Canada, and Victoria Upper Glacier, Antarctica. Each of these glaciers is characterized by different thermal and hydrological regimes and has different potential DOC

sources. The fluorescence characteristics of DOC are a consequence of DOC molecular characteristics. Where possible, samples of supraglacial runoff, glacier ice, basal ice and subglacial meltwater were collected. The DOC concentration in each sample was measured (high temperature combustion and non-dispersive infrared (IR) detection) and emission and/or synchronous fluorescence spectroscopy were used to characterize the DOC from each environment.

DOC exists in detectable quantities (0.06 - 46.6 ppm) in these three glacier systems. The fluorescence characteristics of DOC vary between glaciers, between environments at the same glacier, and over time within a single glacier environment. The results indicate that the quality of available OM and glacier hydrological flow routing influence the characteristics of DOC. The presence of fluorescence indicating recently produced microbially-derived organic compounds indicates that microbial cycling of OC may be active in glacier systems including subglacial and englacial environments.

Paper 2: to characterize the variation in the molecular characteristics of DOM collected in glacier meltwater samples from an alpine glacier system (Outre Glacier) during a melt season.

In glacial runoff, DOM characteristics would be expected to change over the course of a melt season as glacier drainage system development mobilizes DOM from different OM pools. Principal Components Analysis (PCA) of synchronous fluorescence spectra was used to detect and describe changes in the DOM in meltwater from Outre Glacier.

For most of the melt season, the dominant component of DOM in subglacial meltwater is characterized by a tyrosine-like fluorophore. This DOM component is most likely derived from supraglacial snowmelt. During periods of high discharge, a second component of DOM becomes more prominent, which is humic in character and similar to DOM sampled from a nearby non-glacial stream. This DOM component is probably derived from a moss-covered soil environment that has been glacially overrun. It appears to be entrained into glacial meltwater when the supraglacial meltwater flux exceeds the capacity of the principal subglacial drainage channels and water floods areas of the glacier bed that are normally isolated from the subglacial drainage system. A second supraglacial source of DOM also appears to be mobilized during periods of high air temperatures. It is characterized by both humic and proteinaceous fluorophores and may be derived from drainage through supraglacial cryoconite holes.

Paper 3: to describe the molecular characteristics of DOM and a component of the particulate OM (POM) in two glacier systems that are expected to have contrasting OM sources (microbial vs. vascular plant OM).

Evidence of microbial populations in basal ice at Victoria Upper Glacier (VUG) and John Evans Glacier (JEG) suggests that there is a microbial component to basal ice OM. Microbially-derived (e.g. algae) OM is generally more labile than terrestrially-derived (e.g. vascular plant) OM and may represent a substrate for heterotrophic microbial metabolism in basal ice and in downstream environments when basal ice melts. JEG has a subglacial pool of terrestrially-derived OM (Barker et al., 2006; Chapter 2) so terrestrially-derived OM may have been incorporated into basal ice during accretion to the glacier sole. The purpose of this investigation is to describe the molecular characteristics of DOM and POM in basal ice from glaciers exhibiting potentially different types of organic parent material (VUG and JEG), with the goal of determining a) the relative contribution of microbial and terrestrial OM in basal ice and b) if the OM source (terrestrial vs. microbial) is different for DOM and POM. To accomplish these goals, the molecular characteristics of the dichloromethane (DCM)-extractable POM are examined by micro-Fourier Transform infrared (micro-FTIR) spectroscopy and the molecular characteristics of DOM are examined by fluorescence spectroscopy.

Both the DCM-extractable component of POM and DOM exhibit microbial characteristics. The molecular characteristics of POM vary spatially in VUG and JEG basal ice. The POM extract appears to be microbially-derived lipid and the presence of spectral absorbance indicating the presence of relatively abundant polysaccharide moieties suggests that the microbial lipid may be associated with extracellular polymeric substances (EPS) in the basal ice. This lipid component was present in all basal ice samples. The molecular characteristics of DOM in VUG and JEG basal ice varied spatially but was generally similar and exhibited strong fluorescence that is characteristic of tyrosine. The tyrosine-like fluorophore was present in all basal ice samples and is indicative of recent microbial activity. Thus, basal ice OM has a ubiquitous microbially-derived component regardless of the molecular characteristics of the potential organic parent material. While the organic parent material may be incorporated in basal ice, its distribution appears to be heterogeneous and its contribution to the basal ice OM minor.

1.4. References.

Alley, R.B. 1986. Grain growth in polar ice: I. Theory. *Journal of Glaciology* 32(112): 415-424.

Arnosti, C. 2003. Microbial extracellular enzymes and their role in dissolved organic matter cycling. In Findlay, S.E.G., Sinsabaugh, R.L. (eds). Aquatic Ecosystems: Interactivity of Dissolved Organic Matter. Academic Press, New York: 316-342.

Arnosti, C., Durkin, S., Jeffrey, W.H. 2005. Patterns of extracellular enzyme activities among pelagic marine microbial communities: implications for cycling of dissolved organic matter. *Aquatic Microbial Ecology* 38(2): 135-145.

Benner, R. 2003. Molecular indicators of the bioavailability of dissolved organic matter. In Findlay, S.E.G., Sinsabaugh, R.L. (eds). Aquatic Ecosystems: Interactivity of Dissolved Organic Matter. Academc Press, New York: 121-137.

Bergsma, B.M., Svoboda, J., Freedman, B. 1984. Entombed plant-communities released by a retreating glacier at central Ellesmere Island, Canada. *Arctic* 37(1): 49-51.

Bhatia, M., Sharp, M., Foght, J. 2006. Distinct bacterial communities exist beneath a High Arctic polythermal glacier. *Applied and Environmental Microbiology* 72(9): 5838-5845.

Bingham, R.G., Nienow, P.W., Sharp, M.J., Boon, S. 2005. Subglacial drainage processes at a High Arctic polythermal valley glacier. *Journal of Glaciology* 51(172): 15-24.

Blatter, H. 1987. On the thermal regime of an arctic valley glacier: a study of White Glacier, Axel Heiberg Island, N.W.T., Canada. *Journal of Glaciology* 33(114): 200-211.

Blatter, H., Hutter, K. 1991. Polythermal conditions in Arctic glaciers. *Journal of Glaciology* 37(126): 261-269.

Cabaniss, S.E. 1992. Synchronous fluorescence spectra of metal-fulvic acid complexes. *Environmental Science and Technology* 26(6): 1133-1139.

Carpenter, E.J., Lin, S., Capone, D.G. 2000. Bacterial activity in South Pole snow. *Applied and Environmental Microbiology* 66(10): 4514-4517.

Christoffersen, P., Tulaczyk, S. 2003. Response of subglacial sediments to basal freeze-on 1. Theory and comparison to observations from beneath the West Antarctic Ice Sheet. *Journal of Geophysical Research* 108(B4): 2222.

Copland, L., Sharp, M. 2001. Mapping thermal and hydrological conditions beneath a polythermal glacier with radio-echo sounding. *Journal of Glaciology* 47(157): 232-242.

Cuffey, K.M., Conway, H., Hallet, B., Gades, A.M., Raymond, C.F. 1999. Interfacial water in polar glaciers and glacier sliding at -17°C. *Geophysical Research Letters* 26(6): 751-754.

Findlay, S.E.G., Sinsabaugh, R.L. (eds). 2003. Aquatic Ecosystems: Interactivity of Dissolved Organic Matter. Academc Press, New York: 512 pp.

Fowler, A.C., Krantz, W.B. 1994. A generalized secondary frost heave model. *SIAM Journal of Applied Mathematics* 54(6): 1650-1675.

Hannah, D.M., Smith, B.P.G., Gurnell, A.M., McGregor, G.R. 2000. An approach to hydrograph classification. *Hydrological Processes* 14(2): 317-338.

Hedges, J.I., Cowie, G.L., Richey, J.E., Quay, P.D., Benner, R., Strom, M., Forsberg, B.R. 1994. Origins and processing of organic matter in the Amazon River as indicated by carbohydrates and amino acids. *Limnology and Oceanography* 39(4): 743-761.

Hodson, A.J., Mumford, P.N., Kohler, J., Wynn, P.M. 2005. The High Arctic glacial ecosystem: new insights from nutrient budgets. *Biogeochemistry* 72(2): 233-256.

Hooke, R. LeB. 1989. Englacial and subglacial hydrology: a qualitative review. *Arctic and Alpine Research* 21(3): 221-233.

Hubbard, B., Nienow, P. 1997. Alpine subglacial hydrology. *Quaternary Science Reviews* 16(9): 939-955.

Hubbard, B.P., Sharp, M.J., Willis, I.C., Nielsen, M.K., Smart, C.C. 1995. Borehole water-level variations and the structure of the subglacial system at Haut Glacier d'Arolla, Valais, Switzerland. *Journal of Glaciology* 41(139): 572-583.

Humlum, O., Elberling, B., Hormes, A., Fjordheim, K., Hansen, O.H., Heinemeier, J. 2005. Late-Holocene glacier growth in Svalbard, documented by subglacial relict vegetation and living soil microbes. *The Holocene* 15(3): 396-407.

Kaplan, A., Newbold, J.D. 2003. The role of monomers in stream ecosystem metabolism. In Findlay, S.E.G., Sinsabaugh, R.L. (eds). Aquatic Ecosystems: Interactivity of Dissolved Organic Matter. Academc Press, New York: 97-119.

Kowalczuk, P., Ston-Egiert, J., Cooper, W.J., Whitehead, R.F., Durako, M.J. 2005. Characterization of chromophoric dissolved organic matter (CDOM) in the Baltic Sea by excitation emission matrix fluorescence spectroscopy. *Marine Chemistry* 96(3-4): 273-292.

Lafreniere, M.J., Sharp, M.J. 2004. The concentration and fluorescence of dissolved organic carbon (DOC) in glacial and nonglacial catchments: interpreting hydrological flow routing and DOC sources. *Arctic, Antarctic and Alpine Research* 36(2): 156-165.

McKnight, D.M., Hood, E., Klapper, L. 2003. Trace organic moieties of dissolved organic material in natural waters. In Findlay, S.E.G., Sinsabaugh, R.L. (eds). Aquatic Ecosystems: Interactivity of Dissolved Organic Matter. Academc Press, New York: 71-96.

Mueller, D.R., Pollard, W.H. 2004. Gradient analysis of cryoconite ecosystems from two polar glaciers. *Polar Biology* 27(2): 66-74.

Nienow, P., Sharp, M., Willis, I. 1998. Seasonal changes in the morphology of the subglacial drainage system, Haut Glacier d'Arolla, Switzerland. *Earth Surface Processes and Landforms* 23(9): 825-843.

Nye, J.F. 1973. Water at the bed of a glacier. IUGG-AIHS Symposium on the Hydrology of Glaciers, Cambridge, 7-13 September 1969. *International Association of Scientific Hydrology Publication* 95: 189-194.

Paterson, W.S.B. 1994. The Physics of Glaciers, 3rd Ed. Pergamon Press, London: 480 pp.

Priscu, J.C., Adams, E.E., Lyons, W.B., Voytek, M.A., Mogk, D.W., Brown, R.L., McKay, C.P., Takacs, C.D., Welch, K.A., Wolf, C.F., Kirshtein, J.D., Avci, R. 1999. Geomicrobiology of subglacial ice above Lake Vostok, Antarctica. *Science* 286: 2141-2144.

Raiswell, R. 1984. Chemical models of solute acquisition in glacial meltwaters. *Journal of Glaciology* 30(104): 49-57.

Rothlisberger, H. 1972. Water pressure in intra- and subglacial channels. *Journal of Glaciology* 11(62): 177-203.

Sharp, M., Brown, G.H., Tranter, M., Willis, I.C., Hubbard, B. 1995. Comments on the use of chemically based mixing models in glacier hydrology. *Journal of Glaciology* 41(138): 241-246.

Sharp, M., Parkes, J., Cragg, B., Fairchild, I.J., Lamb, H., Tranter, M. 1999. Widespread bacterial populations at glacier beds and their relationship to rock weathering and carbon cycling. *Geology* 27(2): 107-110.

Skidmore, M., Anderson, S.P., Sharp, M., Foght, J., Lanoil, B.D. 2005. Comparison of microbial community composition of two subglacial environments reveals a possible role for microbes in chemical weathering processes. *Applied and Environmental Microbiology* 71(11): 6986-6997.

Skidmore, M.L., Foght, J.M., Sharp, M.J. 2000. Microbial life beneath a high Arctic glacier. *Applied and Environmental Microbiology* 66(8): 3214-3220.

Souchez, R., Samyn, D., Lorrain, R., Pattyn, F. Fitzsimons, S. 2004. An isotopic model for basal freeze-on associated with subglacial upward flow of pore water. *Geophysical Research Letters* 31: L02401.

Stedmon, C.A., Markager, S., Bro, R. 2003. Tracing dissolved organic matter in aquatic environments using a new approach to fluorescence spectroscopy. *Marine Chemistry* 82(3-4): 239-254.

Steiner, A. 2007. Worldwide Glacier Melting Underlined in Newly Released Data. *United Nations Environmental Programme, Division of Early Warning and Assessment (DEWA); Global Resource Information Database (GRID) – Europe*: http://www.grid.unep.ch/news/glacier_melting.php

Thurman, E.M. 1985. Organic geochemistry of natural waters. Martinus Nijhoff/Dr W. Junk Publishers, Boston: 497 pp.

Wadham, J.L., Bottrell, S., Tranter, M., Raiswell, R. 2004. Stable isotope evidence for microbial sulphate reduction at the bed of a polythermal high Arctic glacier. *Earth and Planetary Science Letters* 219(3-4): 341-355.

Willis, I.C., Sharp, M.J., Richards, K.S. 1993. Studies of the water balance of Midtdalsbreen, Hardangerjokulen, Norway. II. Water storage and runoff prediction. *Zeitschrift fur Gletscherkunde und Glazialgeologie* 27/28: 117-138.

Chapter 2: Abundance and dynamics of dissolved organic carbon in glacier systems.[1]

2.1. Introduction.

Advancing glaciers often override soils, sediment, and vegetation, and erode bedrock. Dissolved and particulate organic carbon (OC) from these sources may be incorporated into glacial sediments and basal ice (debris-rich ice formed at the glacier sole). OC may also enter the subglacial environment from sources on the glacier surface (supraglacial) and areas surrounding the glacier (ice-marginal) by transport in glacier ice or runoff. Potential supraglacial OC sources include wind-blown material and microbial populations that exist in the surface snowpack, cryoconite holes, and meltwater streams. The subglacial OC pool may provide a substrate for metabolism by microbial populations and is thus a potential source of CO_2 and acidity for subglacial weathering mechanisms. Subglacial microbial metabolism may alter the quality of OC such that OC released from glaciers in runoff may have different properties from the OC that enters the subglacial environment. The microbial alteration of OC has potentially important implications for downstream aquatic ecology because OC abundance and properties (e.g. reactivity) influence nutrient and contaminant transport and bioavailability, and determine its suitability as a substrate for microbial metabolism.

Fluorescence spectroscopy has been used to characterize dissolved organic carbon (DOC) in soil solutions (e.g. Fraser et al., 2001), and in lakes (e.g. McKnight et al., 1994), rivers (e.g. Stedmon et al., 2003) and oceans (e.g. Parlanti et al., 2000). Fluorescence arises when fluorescing species (fluorophores) that have been irradiated with electromagnetic energy relax from an excited state to a lower energy state (Penzer, 1980). The spectral characteristics of this fluorescence are related to the molecular structure of the relaxing molecule. The emission fluorescence technique excites a molecule at a predetermined wavelength with an excitation monochromator and monitors its fluorescent emission over a predetermined spectral interval with an emission monochromator. Emission scanning is used for samples with only one fluorophore or where the

[1] A version of this chapter was published as Barker, J.D., Sharp, M.J., Fitzsimons, S.J., Turner, R.J. 2006. Abundance and dynamics of dissolved organic carbon in glacier systems. *Arctic, Antarctic and Alpine Research*, 38(2): 163-172.

fluorescing conditions of the fluorophore of interest are known. The synchronous fluorescence technique involves synchronously scanning a sample with both the excitation and emission monochromators with a predetermined interval between the two monochromators. Synchronous fluorescence scanning has the advantage of reducing the spectral overlap in a sample that contains more than one fluorophore, such as DOC (e.g. Cabaniss and Shuman, 1987), thereby providing better spectral resolution for each individual fluorophore.

As an analytical technique, fluorescence spectroscopy has the advantage of being more sensitive and requiring a less concentrated sample than other techniques such as ^{13}C-nuclear magnetic resonance (NMR), Fourier-transform infrared (FTIR), or electron paramagnetic resonance (EPR) spectroscopy. Furthermore, very little sample preparation is required prior to fluorescence spectroscopic analysis.

The majority of DOC in natural waters is comprised of humic material (Aiken et al., 1985). Fulvic acids are the fraction of humic material that is water soluble at any pH. Previous investigations have shown that the position of the fluorescent emission peak of fulvic acids (400-600 nm at an excitation of 370 nm) is indicative of organic matter provenance. Fluorescence emission peaks at shorter wavelengths are indicative of fulvic acids that are derived from microbial biopolymers, while peaks at longer wavelengths are indicative of fulvic acids that are derived from terrestrial sources (e.g. plant and leaf litter biopolymers) (McKnight et al., 2001). Due to the predominantly lignin-based precursor material, terrestrially derived fulvic acids contain more aromatic carbon (25-30% of total carbon) than microbial fulvic acids (12-17% of total carbon) (McKnight et al., 2001). This shift in the fulvic acid region of the spectrum is also found in whole water samples (Donahue et al., 1998). Two DOC end members are commonly cited and used as standards for microbially and terrestrially derived humic substances (e.g. Mobed et al., 1996; Donahue et al., 1998; McKnight et al., 2001). Lake Fryxell (microbial) DOC displays a fluorescent emission peak at 443 nm, while Suwannee River (terrestrial) DOC has its emission peak at 462 nm.

The presence of emission peaks at specific wavelengths of a synchronous spectrum indicates the existence of electron donating fluorophores that can be used to characterize the DOC in a sample. For example, emission peaks in the range 250-300 nm (with an 18 nm difference between

excitation and emission monochromators [$\lambda_{em} = \lambda_{ex} + 18$ nm]) have been attributed to the presence of proteins (De Souza Sierra et al., 1994) that are indicative of compounds of recent biological origin (which are potentially relatively labile), whereas peaks in the range 400-500 nm are indicative of humic material (Miano et al., 1988; Chen et al., 2003), which is a more recalcitrant form of DOC.

As there have been few studies of DOC cycling in glacial environments (e.g. Lafreniere and Sharp, 2004), the sources, distribution, and biogeochemical transformations of DOC in these settings are poorly understood. We therefore investigated the abundance and fluorescence characteristics of DOC in three glacier systems with contrasting thermal and hydrological regimes and different potential DOC sources. The purpose of this paper is to quantify DOC abundance in a range of glacial sub-environments, and to characterize the DOC using emission and synchronous fluorescence spectroscopy.

2.2. Field Sites and Methodology.

2.2.1. Field Sites.

This paper presents results from the analysis of samples collected from three glacier systems: John Evans Glacier, Ellesmere Island, Canada (79°49′N, 74°00′W); Outre Glacier, British Columbia, Canada (56°14′N, 130°01′W); and Victoria Upper Glacier in the McMurdo Dry Valleys, Antarctica (77°16′S, 161°29′E).

John Evans Glacier is a polythermal glacier that overlies, and is surrounded by, predominantly carbonate bedrock and sediments in a region with sparse arctic tundra vegetation. Outflow of subglacial meltwater is confined to the period between late June and early August. The first subglacial water that emerges each year is solute-rich, suggesting a long subglacial residence time (Skidmore and Sharp, 1999). The solute concentrations in the subglacial meltwater decrease rapidly following the onset of subglacial outflow due to dilution by new surface meltwaters that are routed to the bed via moulins and crevasses (Boon and Sharp, 2003). Subglacial and supraglacial meltwater samples were collected once a day at John Evans Glacier during the 2001 ablation season (late June-late July). We attempted to monitor water level in the subglacial

channel as it emerged from beneath John Evans Glacier using a pressure transducer, but continuous bank erosion and stream migration prevented an accurate record from being obtained.

Outre Glacier is a temperate glacier in the coastal mountains of northern British Columbia that currently terminates below treeline in temperate rainforest. During its Little Ice Age advance it likely overran OC in forest soils and vegetation. Outre Glacier has retreated approximately 700 m during the last century, but its terminus is still located below treeline, so it may have a large subglacial OC pool that is characterized by both labile (e.g. microbially derived and non-vascular plant-derived biopolymers) and recalcitrant (e.g. vascular plant-derived biopolymers) organic matter. To allow comparison of the characteristics of DOC from glacierized and non-glacierized catchments, a small stream in a non-glacierized catchment located to the south of Outre Glacier was also sampled. Water samples from Outre Glacier were collected at approximate daily flow minima and maxima during the 2002 ablation season (early July-late August). Water from the non-glacial stream was sampled approximately once every two weeks over the same period. Outre Glacier basal ice was sampled once late in the field season and stored frozen until analysis. Subglacial stream water level was monitored continuously using a Levelogger (Solinst, Canada) pressure transducer that was fixed to a stable frame.

Victoria Upper Glacier is a cold-based glacier in a polar desert and is adjacent to a proglacial ice-covered lake, which may be a significant source of labile (e.g. algal) OC to the glacier if it has overrun lake sediment or water in the past. While soil OC concentrations in the Dry Valleys are low (<0.1%; Horowitz et al., 1972), DOC concentrations as high as 30 ppm have been reported in Dry Valley lakes and have been attributed to algal production (McKnight et al., 1991). Victoria Upper Glacier terminates in an ~50 m high ice cliff, the lower ~15 m of which is composed of basal ice. Souchez et al. (2004) proposed a mechanism by which the upward flow of pore water (and associated DOC) through saturated subglacial sediment allows freezing onto the sole of the bed of cold-based glaciers forming basal ice sequences such as those observed in Dry Valley glaciers. A proglacial accumulation of glacier ice that has calved from the glacier terminus has produced an apron which extends to an elevation of ~10-15 m and permits the sampling of both meteorically derived glacier ice and ~1-5 m of basal ice in the vicinity of the glacier ice/basal ice contact. Glacier and basal ice samples from Victoria Upper Glacier were collected in January 2003.

The thermal regime of glaciers determines the routing of water through them. Subglacially and supraglacially derived meltwaters circulate along the bed of both temperate and polythermal glaciers. Liquid water in cold-based glaciers is limited to thin films around entrained sediment (Cuffey et al., 1999) and gas bubbles (Dash et al., 1995) and at ice grain boundaries (Price, 2000). Glacier meltwater routing controls the distribution of water, oxygen and nutrients in the subglacial environment and will thus influence subglacial microbial activity and determine the type of microbe that colonizes a particular subglacial site (Tranter et al., 2005). Similarly, the physical and chemical characteristics of the ice mass will influence the distribution and chemical characteristics of liquid water within the ice. Thus, the quality and spatial distribution of available nutrients would also be expected to exert a significant influence on subglacial and englacial microbial activity. For example, a subglacial heterotrophic microbial population in a temperate glacier could use OC in both subglacially routed supraglacial meltwater and subglacial sediment for metabolism. Some of the OC flushed from the glacier surface into the subglacial environment would be expected to consist of microbial exudates produced by algal communities in the supraglacial snowpack. The subglacial sediment would be expected to consist of OC from overridden soil and vegetation. The overridden OC may be more widely distributed across the glacier bed than the supraglacially derived OC and may be quantitatively more significant and, therefore, potentially important to subglacial microbial communities. However, the overridden OC may contain a large percent per volume of recalcitrant lignin-derived biopolymers (from overridden vascular plants) that may not be efficiently used for subglacial microbial metabolism. Additionally, some of this OC may be located in areas of the subglacial environment that are oxygen limited and therefore not conducive to heterotrophic metabolism by some microbes. Though less widely distributed and less quantitatively significant, the more labile supraglacially derived algal exudates that are transported in more oxygenated supraglacially derived meltwater may represent the more significant source of OC to the subglacial heterotrophic communities. Thus, we hypothesize that in addition to glacier water flow routing, the characteristics and distribution of subglacial OC will influence subglacial microbial processes and influence the characteristics and abundance of DOC both within, and exported from, the glacier system. The choice of field sites, as described above, provides the opportunity to quantify and characterize OC in glaciers with different sources, distribution, and methods of entraining OC.

2.2.2. Sampling.

Whenever possible, supraglacial meltwater, glacier ice, basal ice, and subglacial meltwater were sampled at each site (Table 2.1). Liquid samples were collected in pre-rinsed amber glass bottles and filtered immediately through pre-combusted 0.7 μm GF/F filter papers using a pre-rinsed glass filtration apparatus. The filtrate was decanted in duplicate into acid washed and pre-combusted amber glass vials and stored in the dark at ~4°C until analysis. Ice samples were collected using ethanol-bathed and flame-sterilized chisels and aluminum collection trays, melted in the field, and filtered as described above.

2.3. Analysis.

One of each pair of duplicate samples was analyzed for DOC concentration by high-temperature combustion and non-dispersive infrared detection using a Shimadzu TOC-5000A Total Organic Carbon Analyzer equipped with a high-sensitivity platinum catalyst. Prior to analysis, each DOC sample was acidified to pH 2 using trace metal grade HCl and sparged for 5 min with TOC grade air to remove dissolved carbonate species from the sample. Each sample was analyzed in triplicate. Five replicates were analyzed if the coefficient of variation exceeded 2%. The detection limit was 0.05 ppm (Miller and Miller, 1988). Sample dilution with UV-sterilized and deionized water was required to measure the concentration of DOC when concentrations exceeded 2.4 ppm.

The second of each pair of duplicate samples was analyzed by either emission (John Evans Glacier) or synchronous (Outre Glacier and Victoria Upper Glacier) fluorescence spectroscopy. Synchronous spectroscopy was employed more frequently because of the broader range of information that the technique provides. Emission spectra were measured using a Shimadzu RF-1501 spectrofluorometer with a Xenon lamp as an excitation source. Synchronous spectra were obtained using a SPEX Fluorolog-3 spectrofluorometer equipped with both excitation and emission monochromators and a Xenon lamp. Scans were performed at 1 nm increments with a

0.1 s integration period using a 10 nm bandwidth and an 18 nm offset between monochromators (for synchronous scans). All samples were scanned at room temperature using quartz a glass cuvette with a 10 mm path length. All spectra were Raman corrected by subtracting the spectrum for deionized water under identical scanning conditions. Scans were dark corrected, and instrument output was normalized to the water Raman spectra to correct for lamp fluctuation (<0.08% over the course of the analysis). No inner filter corrections were applied for DOC concentrations below 2.4 ppm. In the event that sample DOC concentrations exceeded 2.4 ppm, the diluted sample that was used for DOC determination was used for spectroscopic analysis. All fluorescence spectra were normalized to the sample fluorescence peak spectral maximum to facilitate the comparison of sample fluorophore peak location between samples. Fluorescence spectra were also smoothed with a 12 point running average to reduce spectrofluorometer signal noise and facilitate fluorophore peak identification. Peaks were identified by calculating the first derivative of the spectrum and identifying the point on the ascending slope where values equaled zero. No drift in fluorescent peak position was observed between replicate sample analyses.

Where possible, the fluorophores revealed in the spectra from John Evans Glacier, Outre Glacier and Victoria Upper Glacier were identified by comparison with spectra reported in the literature, for which accompanying fluorophore identification has been provided (e.g. Ferrari and Mingazzini, 1995). This information can potentially be used to better understand the characteristics of DOC variability in glacier systems.

2.3. Results and Discussion.

2.3.1. John Evans Glacier.

Meltwater samples taken from John Evans Glacier during the 2001 melt season (18 June-29 July, 2001) were analyzed for DOC concentration (Table 2.1, Fig. 2.1a) and fluorescence emission spectra (Fig. 1b). Supraglacial and subglacial meltwaters contained an average of 0.256 ppm (SD = 0.096, n = 35) and 0.225 ppm (SD = 0.075, n = 48) DOC, respectively (Table 2.1). These mean concentrations are lower than the 0.44 ppm reported by Lafreniere and Sharp (2004) for a glacial stream flowing from an alpine glacier in the Canadian Rocky Mountains, and considerably lower than the 4.4 ppm that has been reported as an average for river waters in North America (Aiken et

al., 1985). This is not unexpected because of the poorly developed soils and sparse vegetation (thus low abundance of OC) that characterize the arctic tundra biome.

The position of the emission fluorescence peak of DOC is less variable in samples from the supraglacial stream than in samples from the subglacial stream (Fig. 2.1b). In supraglacial samples, the peak position is typically located between 442 nm and 446 nm, values that are usually associated with microbially derived DOC (McKnight et al., 2001). DOC concentrations in the supraglacial stream rose noticeably above the mean concentration on three occasions (Fig. 2.1a). During the first of these (Days 183-187; maximum DOC concentration of 0.403 ppm), the fluorescence emission peak values were relatively low (437-438 nm) (Fig. 2.1b). On the second occasion (Day 199), DOC concentrations of 0.315 ppm were associated with an emission peak at 444 nm. On the final occasion (Days 206-207), the maximum DOC concentration was 0.466 ppm and the emission peak varied between 443 and 444 nm. These results indicate that supraglacially derived DOC is microbial in character (McKnight et al., 2001) and that periodic increases in the DOC concentration may be the result of flushing of microbially derived DOC from the snowpack and supraglacial cryoconite holes. Cryoconites are produced by the melting of wind-blown sediment into the surface of the glacier, and the resulting meltwater pool has been found to host microbial communities (Christner et al., 2003). DOC from cryoconite holes has an emission peak at ~443 nm (mean = 442.7 nm, SD = 0.339, n = 5) (data not shown). The similarity between the cryoconite fluorescence and the fluorescence during the second and third events indicates that these events result from the flushing of cryoconite holes, while the first event is likely the result of flushing of microbially derived DOV from the snowpack (mean = 436.3 nm, SD = 6.278, n = 5) (data not shown). This is consistent with the progressive removal of the seasonal snowpack and exposure of glacier ice surfaces that pockmarked by cryoconite holes over the course of the melt season.

The peak position for the subglacial stream DOC shifts from shorter wavelengths (~438 nm) to longer wavelengths (~458 nm) as the melt season progresses (Fig. 2.1b). This represents a statistically significant shift (t-test, $P<0.05$) from predominantly microbially derived DOC to predominantly terrestrially derived DOC (McKnight et al., 2001). There is no consistent relationship between concentration and fluorescence emission peak position for subglacial stream DOC. Increases in subglacial DOC are accompanied by shifts to longer fluorescence peak wavelengths on Day 180, but to shorter wavelengths on Day 207 (Figs. 2.1a and 2.1b). The

shortest (436 nm) and longest (462 nm) peak wavelengths in the subglacial stream record occur on Day 192 and 198, and correspond to DOC concentrations of 0.197 ppm and 0.144 ppm, respectively. While the fluorescence peak positions on these days are exceptional within the subglacial stream record, the corresponding DOC concentrations are not. This indicates that separate subglacial pools of microbial and terrestrial DOC can be accessed by the subglacial drainage system. The minimum and maximum peak positions of the DOC in subglacial water (e.g. Days 192 and 198, respectively) fall outside the range of peak values observed in the supraglacial meltwater at any time during the melt season, indicating that supraglacial meltwater is not the only source of DOC in subglacial meltwater. While these pools do not contribute enough DOC to increase DOC concentrations in the bulk subglacial meltwater flow significantly above background levels, their contribution is detected in the fluorescence record. The amount of variability in subglacial peak position also increases with time (Fig. 2.1b), suggesting that the predominant fluorescence characteristics of DOC in subglacial meltwater become more variable as the melt season progresses.

These results indicate that various pools of DOC with distinct microbial and terrestrial characteristics are accessed by the bulk subglacial flow during the melt season. This is most likely a consequence of seasonal development of the glacier drainage system coupled with discharge-related variations in the routing of meltwaters across the glacier bed (Bingham et al., 2005). The first subglacial meltwater to be released is extremely solute-rich, and the DOC within it has a strongly microbial fluorescence signature (Fig. 2.1b). This water has likely experienced prolonged storage in an environment where subglacial microbial communities are active. As the melt season progresses and the character of the subglacial drainage system evolves from distributed to more channelized in form (Bingham et al., 2005), a shift in fluorescent peak positions indicates that subglacially routed meltwaters gain access to a source of terrestrial DOC, such as vascular plant biopolymers (e.g. lignin) at the glacier bed. As the channelized system develops, intermittent hydrologic connections between the main conduits and the residual distributed system may permit the flushing of previously isolated pools of subglacially stored water, with microbial fluorescence characteristics, into the bulk flow.

2.3.2. Outre Glacier.

DOC concentrations in Outre Glacier runoff are low (subglacial mean = 0.1 ppm, n = 72) and stable (SD = 0.08) relative to those observed at John Evans Glacier (Table 2.1, Fig. 2.2a). Outre Glacier likely overran rainforest soils and vegetation during its Little Ice Age advance and so may have a large subglacial OC pool. The low DOC concentrations in the subglacial meltwater at Outre Glacier (Table 2.1, Fig. 2.2a), however, indicate that if such a pool exists it is not normally accessed by bulk subglacial meltwaters.

Ferrari and Mingazzini (1995) identified fluorophores with peaks at 270 nm and 370 nm in synchronous fluorescence spectra, which they interpreted as indicating the presence of proteins and fulvic material, respectively. Proteins are labile, and the presence of proteinaceous material in DOC has been interpreted as evidence of active microbial synthesis (De Souza Sierra et al., 1994). Fulvic material results from secondary abiotic humification reactions (Sylvia et al., 1999) and is recalcitrant. The ratio between the heights of the fluorescent peaks at 270 nm and 370 nm (270/370 nm) is therefore used here as a basis for discriminating between the contributions from primary material of recent origin and secondary altered material to the DOC in a sample.

The average synchronous spectra from the supraglacial and subglacial streams at Outre Glacier are the most similar in shape, and different from the spectra from the non-glacial stream and basal ice (which are also different from each other) (Figs. 2.2b and 2.2c). The range of relative emission intensities recorded in the synchronous spectra of the DOC from the subglacial stream encompasses the average supraglacial spectrum (Fig. 2.2d) suggesting that, on some occasions, the synchronous spectra of the subglacial meltwater may be identical to those of the supraglacial meltwater. There is, however, a difference in the mean 270/370 nm between supraglacial (1.87) and subglacial (1.58) streams (Fig. 2.2b), which suggests that the relative contribution from fulvic material is greater in the subglacial stream than in the supraglacial stream. The 270/370 nm in the average synchronous spectrum of DOC in the non-glacial stream (1.59) is similar to the value for the subglacial stream, while the spectrum from basal ice indicates an enrichment in proteinaceous material relative to fulvic material (270/370 nm = 3.66) (Fig. 2.2c). These results suggest that there is a subglacial source of fulvic DOC. DOC in supraglacial meltwater is proteinaceous in

character, which suggests active microbial DOC synthesis. Likewise, active microbial synthesis also appears to occur in basal ice.

The 270/370 nm of synchronous spectra from the DOC in the subglacial stream changes diurnally, with higher 270/370 nm occurring on the rising limb of the discharge hydrograph and lower 270/370 nm occurring during decreasing discharge (Figs. 2.3a and 2.3b). This indicates a more significant contribution by the proteinaceous fluorophore to the fluorescence spectra during periods of rising discharge in the subglacial stream than during periods of decreasing discharge. A higher resolution sampling of subglacial meltwater shows that this variation in 270/370 nm occurs throughout the day and that it follows the trend in the subglacial stream discharge (Fig. 2.3b).

Several subglacial meltwater channels are incised into bedrock (N-channels) in the proglacial area of Outre Glacier, and the current subglacial stream occupies an N-channel at the glacier terminus. It is therefore likely that much of the subglacial flow at Outre Glacier is confined to subglacial N-channels and that water passing through these channels is isolated from areas of the glacier bed where OC may still be found. The similarity between subglacial and supraglacial DOC concentrations at Outre Glacier (Table 2.1, Fig. 2.2a) supports this hypothesis and could be taken to indicate that under most flow conditions supraglacially derive DOC is transported directly through a subglacial N-channel network to the terminus. The similarity between the average subglacial and supraglacial fluorescence spectra (Figs. 2.2b and 2.2d) is also consistent with this suggestion. However, the diurnal change in the fluorescence spectra of DOC in the subglacial meltwater, as indicated by changes in the 270/370 nm (Figs. 2.2b, 2.3a and 2.3b), suggests that there is also a subglacial source of more recalcitrant DOC. The diurnal change in subglacial DOC 270/370 nm (Figs. 2.3a and 2.3b) suggests that water is diverted from the major channels into a distributed subglacial drainage system as discharge and channel water pressures rise, and returned to the major channels as discharge and channel water pressures fall (e.g. Hubbard et al., 1995). Under these circumstances, the distinctive spectra of DOC exported from the glacier during declining discharges may reflect an input of DOC from areas of the bed drained by a distributed drainage system that is isolated from the major drainage channels at times of high flow. During periods of surface melt, proteins produced supraglacially by microbes in the snowpack (e.g. algae) will be flushed and routed to the glacier bed through crevasses and moulins, and supraglacially derived meltwater will dominate subglacial flow. During declining

discharges, when water pressure in the main channels decreases and flow from the distributed system contributes to the bulk subglacial flow, fulvic material, which is likely derived from glacially overridden terrestrial organic matter, is detected. However, the DOC concentration in the bulk subglacial meltwater is relatively constant throughout the melt season. This suggests that the contribution of DOC form the distributed system to the bulk flow is small, though still identifiable by the change in the fluorophores found in the subglacial stream DOC.

The fact that the overall shape of the fluorescence spectra of the DOC flushed from Outre Glacier differs from that of the DOC in the adjacent non-glacial stream (Figs. 2.2b and 2.2c) indicates either that the source of DOC beneath Outre Glacier differs from that of the DOC in the non-glacial stream, of that biogeochemical processes acting on DOC in the subglacial environment are different from those occurring in proximal non-glacial environments. For example, the peaks at 270 nm and 370 nm are most prominent in the non-glacial stream fluorescence spectra, and 270/370 nm in the average non-glacial stream spectrum is very similar to that of the average subglacial stream spectrum. The peak at 320 nm (indicative of two condensed ring systems; Ferrari and Mingazzini, 1995) is more prominent in the subglacial stream fluorescence spectra than in the non-glacial stream spectra. This observation indicates that either the fluorescence peaks resulting from the production of proteins and fulvic acids in the non-glacial stream DOC overwhelms the peak at 320 nm, that the production of the fluorophore at 320 nm is the result of a supraglacial process, or that subglacial biogeochemical conditions favour the preservation of molecules that fluoresce in this region of the spectrum, relative to the non-glacial stream.

2.3.3. Victoria Upper Glacier.

Evidence of differences in the fluorescence characteristics of DOC in the distributed and channelized drainage systems beneath Outre Glacier and in the supraglacial and subglacial meltwater systems at John Evans Glacier suggests that DOC properties vary spatially within glacial environments. If this is true, spatial variations in the abundance and properties of DOC within and between glacier ice and basal ice might also be expected due to differences in DOC source. For example, subglacially accreted basal ice might be expected to incorporate DOC from subglacial sources, whereas meteorically derived glacier ice might be expected to incorporate DOC from supraglacial sources.

DOC concentrations vary along a vertical transect across the boundary between glacier ice and basal ice at Victoria Upper Glacier, with a zone of particularly high DOC concentrations located immediately above the glacier ice/basal ice contact (Fig. 2.4). The fluorescence spectra of the DOC also change though the profile (Fig. 2.5). The only consistent fluorescent peaks in DOC from glacier ice occur at 276 nm and 317 nm. The 317 nm peak becomes dominant as the basal ice contact is approached. Minor peaks at 370 nm and 526 nm appear sporadically throughout the glacier ice transect. The basal ice spectra also contain peaks at 276 nm and 317 nm, but show stronger peaks than the glacier ice spectra at 370 nm and 526 nm, and a unique peak at 417 nm. The peak at 317b nm does not feature as prominently in the basal ice spectra as it does in the glacier ice spectra from 0-8 cm above the basal ice contact.

The heterogeneity of DOC characteristics and concentrations observed in the ice of Victoria Upper Glacier could reflect a range of possible DOC sources and incorporation mechanisms including atmospheric deposition, overriding of lake ice or lake sediment during past advances, or basal freeze-on of DOC-rich lake water (e.g. Souchez et al., 2004). To resolve this uncertainty, one would need to characterize individual fluorophores as carbon functional groups.

The peak at 276 nm indicates proteins (Ferrari and Mingazzini, 1995) and suggests recent biological productivity (De Souza Sierra et al., 1994). The fact that the protein peak in Victoria Upper Glacier ice occurs at longer wavelengths than the protein peak in Outre Glacier subglacial meltwater suggests that the protein at Victoria Upper Glacier is more conjugated and/or contains condensed ring systems. The sporadic peaks at 417 nm and 526 nm indicate the presence of humic material in the ice (Ferrari and Mingazzini, 1995). Like fulvic material, humic material is formed by abiotic secondary condensation reactions and would be expected to be older and more recalcitrant than proteinaceous material. The most likely source of this humic material at Victoria Upper Glacier is overridden sediment, and the fact that the basal ice has stronger peaks at these wavelengths supports this hypothesis. The 276/370 nm (note that the ratio has been changed relative to that used for Outre Glacier to accommodate the protein peak position at Victoria Upper Glacier) through the transect at Victoria Upper Glacier indicates that, relative to protein, fulvic material contributes more to the fluorescence spectra in the basal ice than in the glacier ice (Fig.

2.6). The occasional detection of these peaks in the glacier ice may be the result of wind-blown deposition of sediment on the surface of the glacier.

The ubiquitous peak at 276 nm in the fluorescence spectra of both glacier and basal ice at Victoria Upper Glacier indicates the presence of proteinaceous material. The fact that the protein peak can occur in the absence of the fulvic (370 nm) of humic (>417 nm) peaks suggests that the presence of the protein is not a consequence of wind-blown sediment deposition (in the case of glacier ice) of the incorporation of overrun sediment (in the case of basal ice), but that it may indicate biological production within the ice itself.

The peak at 317 nm, which features so prominently near the glacier ice/basal ice contact, indicates the presence of two condensed ring systems (Ferrari and Mingazzini, 1995) which shift fluorescence to longer wavelengths. For example, the amino acid tryptophan, which contains a two condensed ring system as an indole substituent on the β carbon, fluoresces at 291 nm, while the amino acid tyrosine, which has only one condensed ring (as a phenol), fluoresces at 277 nm (Ferrari and Mingazzini, 1995). Given the provenance of proteinaceous fluorophores in the ice at Victoria Upper Glacier, and the evidence of protein conjugation, a possible explanation for the peak at 317 nm is the presence of a condensed ring system in association with proteinaceous material. Why this fluorophore becomes dominant at the glacier ice/basal ice interface is unclear.

2.4. Summary and Conclusions.

The concentration and fluorescence characteristics of DOC were measured in ice and meltwaters from three glaciers with different thermal and hydrological regimes, and with different potential sources of OC. The average DOC concentrations in subglacial and supraglacial meltwaters do not differ significantly at the sites investigated. This might be taken as evidence of a lack of subglacial OC sources. However, fluorescence analyses indicate that the fluorescence characteristics of the DOC in bulk subglacial meltwater can differ from those of the DOC that enters the glacier via its surface. The nature of these differences suggests that there are sources of DOC in the subglacial environment that have both microbial and terrestrial provenance. The mobilization and export of subglacial DOC in glacier meltwater is dependent on meltwater flow

routing. The results from analyses of DOC in ice at Victoria Upper Glacier indicate that DOC abundance and properties can vary spatially within the glacier itself.

Proteins and proteinaceous material, such as amino acids, fluoresce at different wavelengths depending on their molecular structure. The proteinaceous fluorophore in the ice at Victoria Upper Glacier fluoresces at wavelengths that have been attributed to the amino acid tyrosine (Ferrari and Mingazzini, 1995), whereas the proteinaceous fluorophore in the subglacial meltwater at Outre Glacier may be a tyrosine precursor, such as phenylalanine, which fluoresces at shorter wavelengths (Yamashita and Tanoue, 2003). The ubiquitous presence of tyrosine-like fluorescence within glacier and basal ice, independent of fulvic fluorescence, suggests *in situ* protein production.

While fluorescence spectroscopy is useful for detecting changes in DOC characteristics, one must currently rely on published reports to explain which fluorophores are responsible for the fluorescence response that is detected, or resort to techniques such as ^{13}C-NMR, FTIR, and EPR to identify the functional groups that are present in the sample. The overall form of the synchronous spectra reported here differs from that of spectra previously published for other environments (e.g. Parlanti et al., 2000). It is recognized that synchronous spectra from different environments are unique (for example soil vs. marine synchronous spectra; Lombardi and Jardim, 1999) due to the combination of unique DOC sources and unique biogeochemical processes that transform the characteristics of DOC in each environment. The unique fluorescence spectra reported here (e.g. Outre subglacial vs. non-glacial spectra) suggest that the dominant biogeochemical process responsible for the synchronous spectra of glacially derived DOC may differ from those in adjacent non-glacial environments. In order to identify the fluorophores and biogeochemical processes that occur in glacial environments, techniques that identify specific carbon functional groups in glacier samples will be needed. For example, FTIR analysis would be useful for characterizing the fluorophore that is associated with the 317 nm peak in the fluorescence spectra at Victoria Upper Glacier. Such information may provide insight into the biogeochemical processes that may be modifying the proteinaceous material in the ice and help to resolve the unanswered question of why the 317 nm peak is prominent at the glacier ice/basal ice transition at Victoria Upper Glacier.

2.5. References.

Aiken, G.R., D.M. McKnight, R.L. Wershaw, and P. MacCarthy. 1985. An introduction to humic substances in soil, sediment, and water. In Aiken, G.R., D.M. McKnight, R.L. Wershaw, and P. MacCarthy. *eds. Humic substances in soil, sediment, and water.* New York, John Wiley and Sons, 1-12.

Bingham, R.G., P.W. Nienow, M.J. Sharp, S. Boon. 2005. Subglacial drainage processes at a High Arctic polythermal valley glacier. *Journal of Glaciology* 51(172): 15-24.

Boon, S. and M. Sharp. 2003. The role of hydrologically-driven ice fracture in drainage system evolution on an Arctic glacier. *Geophysical Research Letters* 30(18).

Cabaniss, S.E. and M.S. Shuman. 1987. Synchronous fluorescence spectra of natural waters: tracing sources of dissolved organic matter. *Marine Chemistry* 21(1): 37-50.

Chen, J., E.J. LeBoeuf, S. Dai and B. Gu. 2003. Fluorescence spectroscopic studies of natural organic matter fractions. *Chemosphere* 50(5): 639-647.

Christner, B.C., B.H. Kvitko, and J.N. Reeve. 2003. Molecular identification of bacteria and eukarya inhabiting an Antarctic cryoconite hole. *Extremophiles* 7(3): 177-183.

Cuffey, K.M., H. Conway, B. Hallet, A.M. Gades and C.F. Raymond. 1999. Interfacial water in polar glaciers and glacier sliding at -17°C. *Geophysical Research Letters* 26(6): 751-754.

Dash, J.G., H. Fu and J.S. Wettlaufer. 1995. The premelting of ice and its environmental consequenses. *Reports on Progress in Physics* 58(1): 115-167.

De Souza Sierra, M.M., O.F.X. Donard, M. Lamotte, C. Belin and M. Ewald. 1994. Fluorescence spectroscopy of coastal and marine waters. *Marine Chemistry* 47(2): 127-144.

Donahue, W.F., D.W. Schindler, S.J. Page and M.P. Stainton. 1998. Acid-induced changes in DOC quality in an experimental whole-lake manipulation. *Environmental Science and Technology* 32(19): 2954-2960.

Ferrari, G.M. and M. Mingazzini. 1995. Synchronous fluorescence spectra of dissolved organic matter (DOM) of algal origin in marine coastal waters. *Marine Ecology Progress Series* 125: 305-315.

Fraser, C.J.D., N.T. Roulet and T.R. Moore. 2001. Hydrology and dissolved organic carbon biogeochemistry in an ombrotrophic bog. *Hydrological Processes* 15(16): 3151-3166.

Horowitz, N.H., R.E. Cameron and J.S. Hubbard. 1972. Microbiology of the Dry Valleys of Antarctica. *Science* 176: 242-245.

Hubbard, B.P., M.J. Sharp, I.C. Willis, M.K. Nielsen, and C.C. Smart. 1995. Borehole water-level variations and the structure of the subglacial hydrological system of Haut Glacier d'Arolla, Valais, Switzerland. *Journal of Glaciology* 41(139): 572-583.

Lafreniere, M.J. and M.J. Sharp. 2004. The concentration and fluorescence of dissolved organic carbon (DOC) in glacial and nonglacial catchments: interpreting hydrological flow routing and DOC sources. *Arctic, Antarctic and Alpine Research*, 36(2): 156-165.

Lombardi, A.T., and W.F. Jardim. 1999. Fluorescence spectroscopy of high performance liquid chromatography fractionated marine and terrestrial organic materials. *Water Research* 33(2): 512-520.

McKnight, D.M., G.R. Aiken and R.L. Smith. 1991. Aquatic fulvic acids in microbially based ecosystems: results from two desert lakes in Antarctica. *Limnology and Oceanography* 36(5): 998-1006.

McKnight, D.M., E.D. Andrews, S.A. Spaulding and G.R. Aiken. 1994. Aquatic fulvic acids in algal-rich Antarctic ponds. *Limnology Oceanography* 39(8): 1972-1979.

McKnight, D.M., E.W. Boyer, P.K. Westerhoff, P.T. Doran, T. Kulbe and D.T. Andersen. 2001. Spectrofluorometric characterization of dissolved organic matter for indication of precursor organic material and aromaticity. *Limnology Oceanography* 46(1): 38-48.

Miano, T.M., G. Sposito and J.P. Martin. 1988. Fluorescence spectroscopy of humic substances. *Soil Science Society of America Journal* 52: 1016-1019.

Miller, J.C. and J.N. Miller. 1988. *Statistics for analytical chemistry*. Ellis Horwood Limited, Chichester. 227 pp.

Mobed, J.J., S.L. Hemmingsen, J.L. Autry and L.B. McGown. 1996. Fluorescence characterization of IHSS humic substances: total luminescence spectra with absorbance correction. *Environmental Science and Technology* 30(10): 3061-3065.

Parlanti, E., K. Worz, L. Geoffroy and M. Lamotte. 2000. Dissolved organic matter fluorescence spectroscopy as a tool to estimate biological activity in a coastal zone submitted to anthropogenic inputs. *Organic Geochemistry* 31(12): 1765-1781.

Penzer, G. 1980. Molecular emission spectroscopy (fluorescence and phosphorescence). In Brown, S.B., *ed. An introduction to spectroscopy for biochemists*. Oxford, Alden Press, 70-114.

Price, P.B. 2000. A habitat for psychrophiles in deep Antarctic ice. *Proceedings of the National Academy of Sciences* 97(3): 1247-1251.

Skidmore, M.L. and M.J. Sharp. 1999. Drainage system behaviour of a high-arctic polythermal glacier. *Annals of Glaciology* 28: 209-215.

Souchez, R., D. Samyn, R. Lorrain, F. Pattyn and S. Fitzsimons. 2004. An isotopic model for basal freeze-on associated with subglacial upward flow of pore water. *Geophysical Research Letters* 31: L02401.

Stedmon, C.A., S. Markager and R. Bro. 2003. Tracing dissolved organic matter in aquatic environments using a new approach to fluorescence spectroscopy. *Marine Chemistry* 82(3-4): 239-254.

Sylvia, D.M., J.J. Fuhrmann, P.G. Hartel and D.A. Zuberer. 1999. *Principles and applications of soil microbiology*. New Jersey, Prentice Hall, 550pp.

Tranter, M., M. Skidmore, and J. Wadham. 2005. Hydrological controls on microbial communities in subglacial environments. *Hydrological Processes* 19(4): 995-998.

Yamashita, Y. and E. Tanoue. 2003. Chemical characterization of protein-like fluorophores in DOM in relation to aromatic amino acids. *Marine Chemistry* 82(3-4): 255-271.

Table 2.1: DOC abundance

Site	Location	Mean DOC (ppm)	DOC Range (ppm)	Sample Type	n	Sampling Duration
John Evans Glacier (subglacial)	79°49'N, 74°00'W	0.225	0.124-0.427	water	48	18 June-30 July 2001
John Evans Glacier (supraglacial)		0.252	0.114-0.471	water	35	
Outre Glacier (subglacial)	56°14'N, 130°01'W	0.100	0.057-0.175	water	72	6 July-25 August 2002
Outre Glacier (supraglacial)		0.188	0.328-0.111	water	3	
Outre Glacier (non-glacial)		0.151	0.099-0.211	water	5	
Outre Glacier (basal ice)		0.303	0.301-0.305	ice	2	
Victoria Upper Glacier	77°16'S, 161°29'E	5.897	1.783-46.66	ice		January 2003

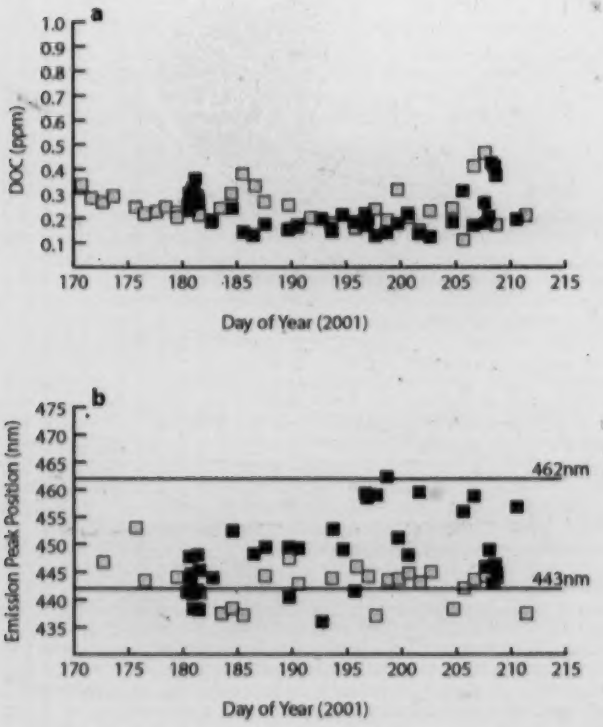

Fig. 2.1: a) Dissolved organic carbon concentrations, and b) emission fluorescence spectra peaks for ■ subglacial and □ supraglacial meltwater samples from John Evans Glacier, 2001.

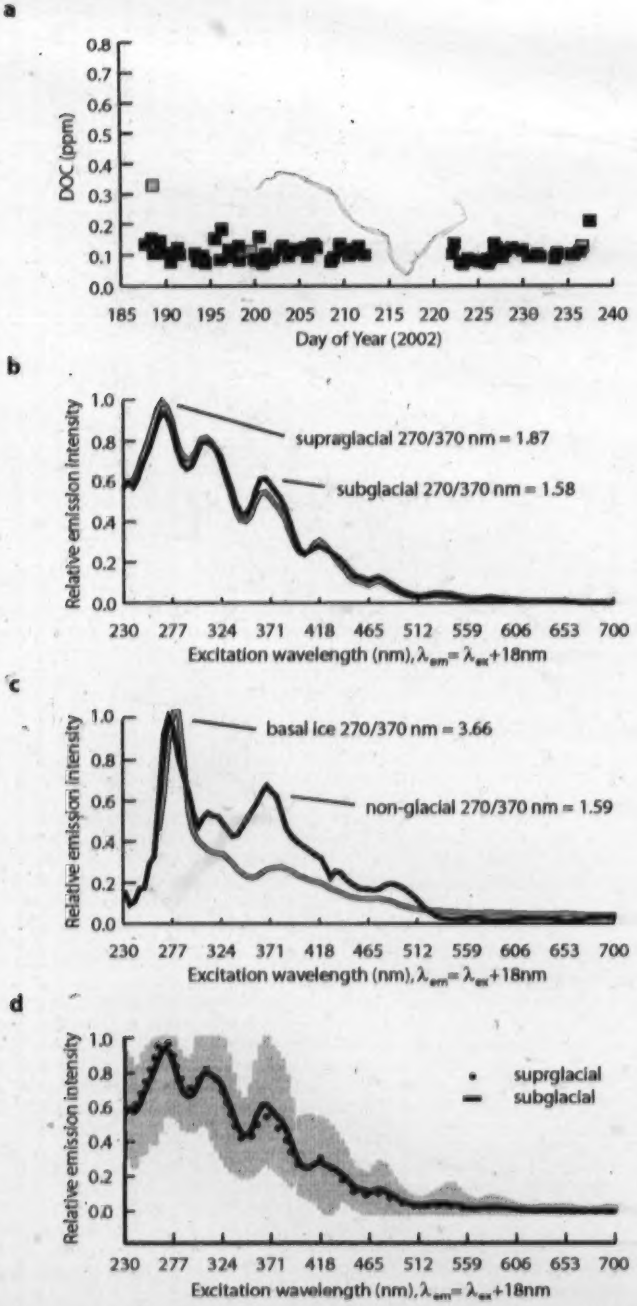

Fig. 2.2: a) Dissolved organic carbon concentrations for ■ subglacial, □ supraglacial and ■ non-glacial samples from Outre Glacier, 2002. b) Synchronous spectra for averaged subglacial, supraglacial and, c) basal ice and non-glacial stream samples from Outre Glacier, 2002. d) Average subglacial and supraglacial synchronous spectra. The shaded area indicates the range of relative emission intensities for each wavelength during the monitoring period for the subglacial stream. Note that the subglacial and non-glacial stream samples were taken from the same elevation.

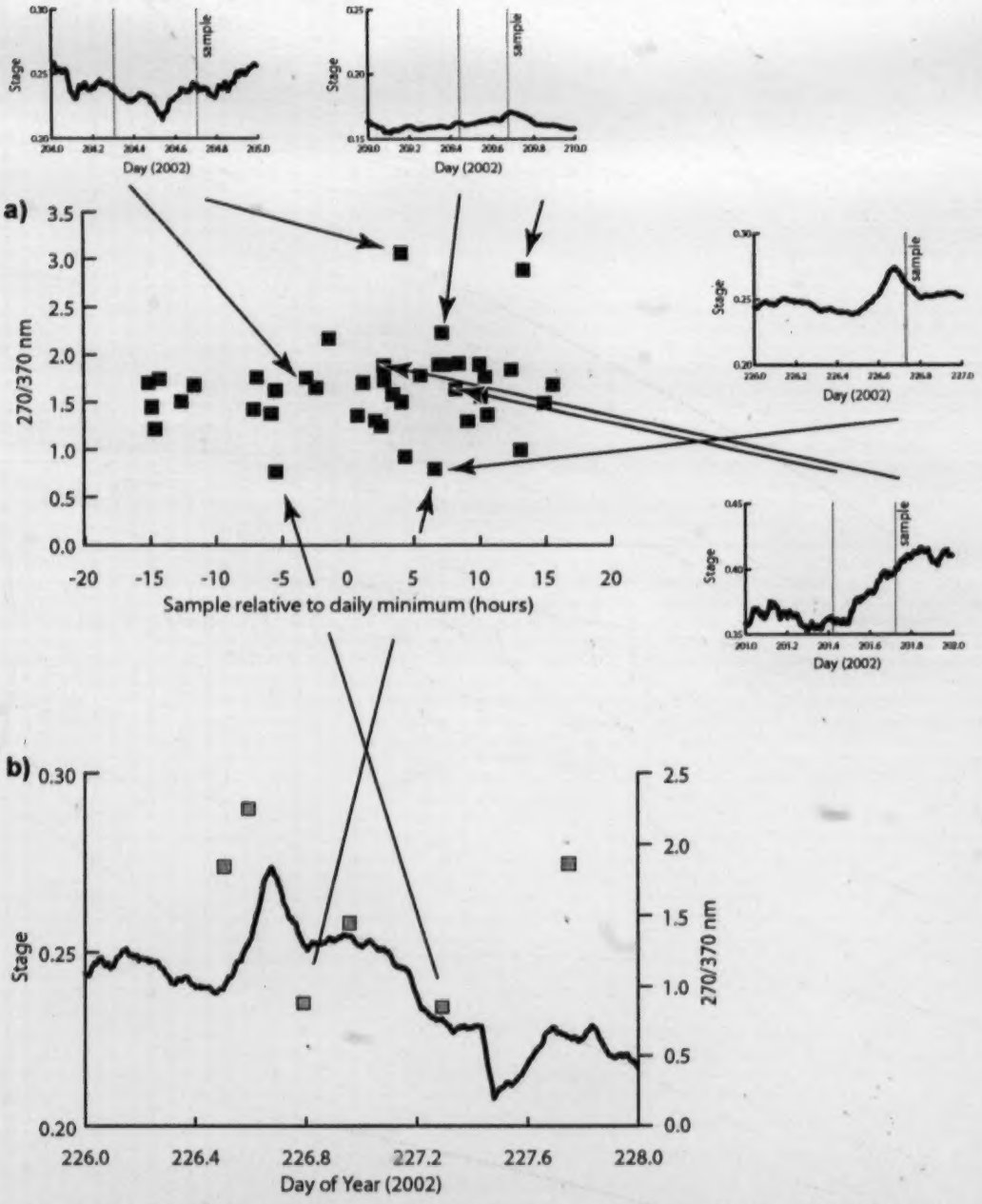

Fig. 2.3: **a)** Plot of 270/370 nm relative to the time of the daily minimum flow for the subglacial stream at Outre Glacier. Accompanying hydrographs show that higher 270/370 nm occur on ascending limbs of the subglacial stream discharge hydrograph, while lower 270/370 nm occur on descending limbs. **b)** A higher resolution plot of 270/370 nm over the associated subglacial stream discharge hydrograph.

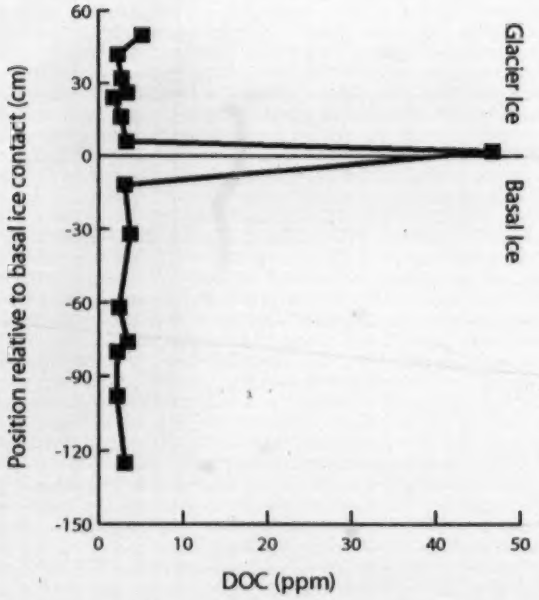

Fig. 2.4: Dissolved organic carbon concentrations in ice along a transect from glacier ice to basal ice at Victoria Upper Glacier.

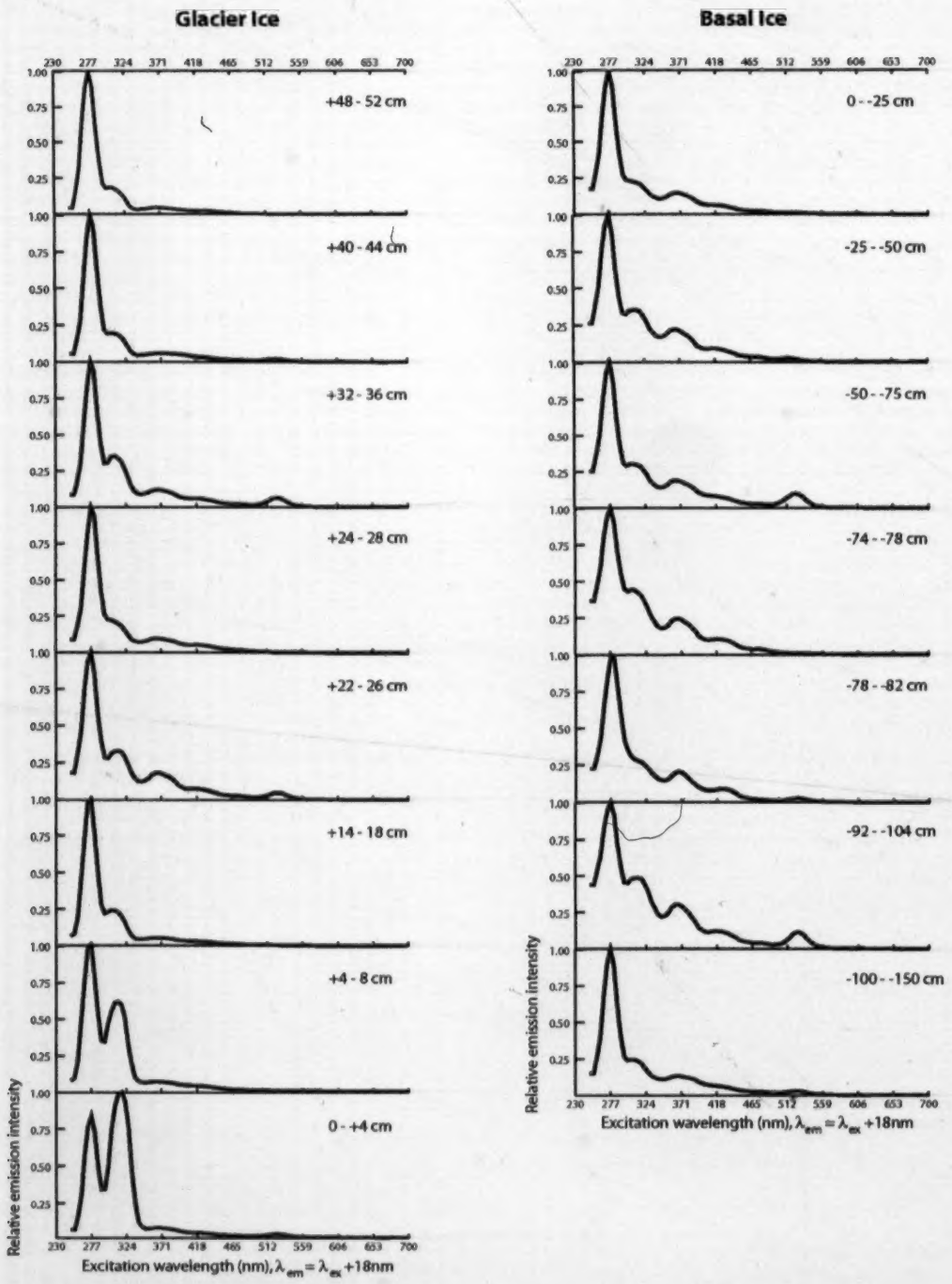

Figure 2.5: Synchronous spectra from ice samples at Victoria Upper Glacier. All distances are relative to the glacier ice/basal ice contact. Spectra have been corrected to represent intensity relative to the maximum intensity in the spectrum.

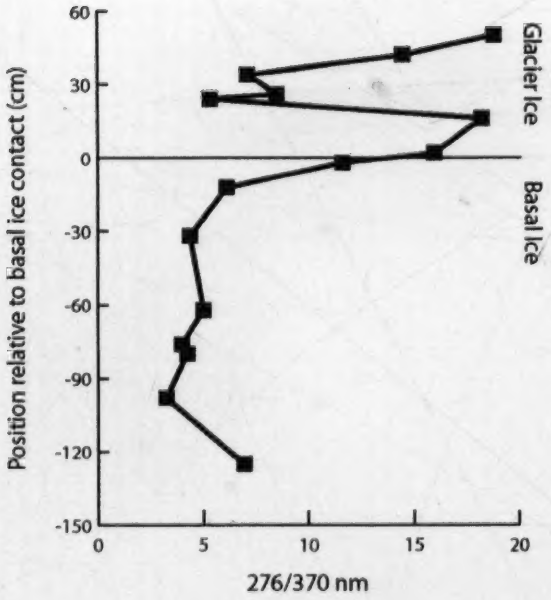

Fig. 2.6: The 276/370 nm ratio in ice along a transect from glacier ice to basal ice at Victoria Upper Glacier. The difference between the 276/370 nm in basal ice and glacier ice is statistically significant (*t*-test, $P < 0.05$).

Chapter 3: Using Synchronous Fluorescence Spectroscopy and Principal Components Analysis (PCA) to Monitor Dissolved Organic Matter (DOM) Dynamics in a Glacier System[1]

3.1. Introduction.

Dissolved organic matter (DOM) is a complex mixture of compounds of varying molecular weight and reactivity which plays a central role in the biogeochemistry and bioavailability of metals (e.g. Cabaniss, 1992), affects water column optical properties (e.g. Kowalczuk et al., 2005), and is a potential nutrient source for microbial communities in aquatic environments (e.g. Coffin, 1989). The ecological function of DOM depends on its molecular composition and characteristics (e.g. aromatic vs. aliphatic), which depend on its organic source material and biogeochemical history. In most freshwater and coastal aquatic environments, the primary source of DOM is plant matter (Stedmon et al., 2003), as indicated by the presence of aromatic biopolymers (e.g. lignin-derived, Lombardi and Jardim, 1999), as opposed to a microbial DOM source, as indicated by the presence of microbially produced biopolymers (e.g. amino acids or proteins, e.g. Coble, 1996). Organic matter degradation by biotic and abiotic processes during transport determines its ultimate molecular characteristics and ecological function.

In glacier systems, organic matter (OM) sources include OM in sediment, soil and vegetation that have been overrun during periods of glacier advance, and supraglacially-derived OM (which is derived from OM in eolian sediment and algal production in the supraglacial snowpack and/or cryoconite holes (e.g. Porazinska et al., 2004, Mueller et al., 2001) in ice at the glacier surface). This supraglacially-derived OM may be transported to the glacier bed by meltwater draining vertically via moulins and crevasses, and can supplement the subglacial (beneath the glacier) OM pool, which consists of overrun OM. The subglacial environment is largely inaccessible to direct observation, and specific DOM sources and evidence of the biogeochemical processes that alter DOM are not readily determined. However, because the molecular characteristics of DOM

---

[1] A version of this chapter has been submitted for publication: Barker, J.D., Sharp, M.J., Turner, R.J. Using Synchronous Fluorescence Spectroscopy and Principal Components Analysis (PCA) to Monitor Dissolved Organic Matter (DOM) Dynamics in a Glacier System. *Hydrological Processes*. (submitted February, 2007).

reflect both its source and biogeochemical history, the characteristics of DOM in meltwater issuing from beneath glaciers may provide an indication of OM sources and biogeochemical processes in both supraglacial and subglacial environments.

The compositional complexity of DOM presents challenges for DOM characterization. Several analytical techniques focus on characterizing specific components of DOM (e.g. fulvic acid) even though the target component may represent only a small portion of the bulk DOM (e.g. McKnight et al., 1991). As a result, the remainder of the bulk DOM remains uncharacterized. Fluorescence spectroscopy has emerged as a useful technique for characterizing the fluorescence properties, and thus the molecular characteristics, of bulk aquatic DOM (e.g. Yamashita and Tanoue, 2003; De Souza Sierra et al., 1994). Fluorescence techniques provide information on the chemical characteristics of bulk DOM as a function of its component fluorescing functional groups (fluorophores). Fluorophores exist as a broad range of chemical compounds that comprise DOM (e.g. aromatic amino acids, humic material). This makes fluorescence spectroscopy well suited for bulk DOM characterization. Specifically, synchronous fluorescence spectroscopy provides rapid, high resolution characterization of DOM in bulk solutions containing multiple fluorophores by identifying fluorophores as individual peaks in the fluorescence spectrum while minimizing the spectral overlap between them (Peuravuori et al., 2002; Ferrari and Mingazzini, 1995).

The complexity of a multi-peaked synchronous fluorescence spectrum makes the detection of subtle changes in spectral waveform from a large collection of spectra difficult. Statistical methods such as Principal Components Analysis (PCA) have been used to decompose complex multivariate signals into linearly independent components that characterize the variance in a given system (e.g. Bernat et al., 2005; Hannah et al., 2000). The purpose of this investigation is to use PCA to characterize the variance in a collection of synchronous fluorescence spectra of DOM from glacier meltwater samples that were collected over the course of a melt season from a single glacier system. The goals of this analysis are to a) identify DOM components and DOM sources, b) detect temporal changes in the characteristics of DOM in runoff and use this information to identify changes in either DOM source, or the extent and characteristics of biogeochemical alteration of a DOM source, in a glacial environment. DOM source and composition in glacier meltwater might be expected to change over the course of a melt season as the glacial drainage system evolves in response to changes in surface meltwater input (e.g. Nienow et al., 1998). In addition, there may be changes in the amounts of dissolved gases (O_2 and CO_2) in the meltwater delivered to the subglacial environment that will influence the range of biogeochemical processes occurring subglacially (Tranter et al., 2005).

3.2. Field Site and Methodology.

3.2.1. Outre Glacier.

Outre Glacier (56°14'N, 130°01'W) is a warm-based valley glacier (liquid water at the bed throughout the year) located in the Coast Mountains of north-western British Columbia, Canada (Fig. 3.1). Outre Glacier currently terminates below treeline (Fig. 3.2a) in a coastal-temperate rainforest and it likely overran rainforest soils and vegetation during its Little Ice Age (LIA) advance. It may therefore have a subglacial pool of overrun rainforest-derived OM. Relict subglacial meltwater drainage channels are incised into sedimentary bedrock (N-channels) within the glacier forefield, and the main subglacial meltwater stream (SUB) that emerges from beneath the glacier is confined within an N-channel (Fig. 3.2b).

Meltwater also drains from a second subglacial outlet (SUB2, Fig. 3.1), which is located at a slightly higher elevation (1161 m a.s.l.) than SUB (1153 m a.s.l.). SUB2 occupies a channel cut into the unconsolidated till (< 0.3 m thick) which is draped over underlying bedrock. The surface of Outre Glacier is heavily crevassed and supraglacial drainage (SUPRA) is routed via several small streams that flow for only short distances before descending into moulins and crevasses. Outre Glacier also has a small marginal stream (MARG, Fig. 3.1) that flows parallel to SUB, but is separated from it by a low drainage divide. MARG is supplied by supraglacial meltwater from the lower ablation zone that cascades off the glacier directly onto the proglacial bedrock surface. Discharge in MARG was very sensitive to changes in air temperature, which suggests that this stream is fed primarily by supraglacial melt from the lower ablation zone with minimal inputs from subglacial sources or seepage from surrounding areas.

A small alpine stream (Alpine Stream) drains a non-glacierized catchment to the south of Outre Glacier (Fig. 3.1). This stream originates as seepage from a moss-dominated alpine meadow and its discharge increases with distance towards the Betty Creek valley floor. An unnamed warm-based valley glacier (referred to here as South Glacier) is located to the south of Alpine Stream (Fig. 3.1). South Glacier currently terminates above treeline, but a well-defined trimline further down valley indicates that it overran temperate rainforest soils and vegetation during its LIA advance. Its current high terminal position however suggests that a significant pool of overrun OM is unlikely to exist beneath this glacier.

3.2.2. Sampling.

Meltwater from SUB and MARG was sampled at the approximate times of daily minimum and maximum discharge during July and August, 2002. SUB2 was also sampled after flow from this source was initiated on August 13. SUPRA meltwater was sampled from small supraglacial streams immediately below the snowline twice during the melt season, on July 18 and 19. The Alpine Stream and South Glacier stream were sampled opportunistically. On July 29, a series of samples was collected along the course of the Alpine Stream in order to sample DOM from different rainforest environments, as defined by differences in the dominant vegetation surrounding the stream (e.g. moss (*Lycopodium spp.*), Sitka willow (*Salix sitchensis*), Sitka alder (*Alnus sinuata*), Amabilis fir (*Abies amabilis*)).

All water samples were collected in 250 ml amber glass bottles. Each bottle was rinsed 3 times with sample water before the analytical sample was collected. DOM is commonly defined as that OM which passes through a glass fibre filter (GF/F; 0.7 μm) (e.g. Stedmon et al., 2003; Yamashita and Tanoue, 2003; De Souza Sierra et al., 1994). Samples were filtered on site using a glass filtration apparatus that had been rinsed with 2N HCl and deionized water and fitted with a pre-combusted GF/F filter paper. The sample chamber was rinsed three times with sample before 150 ml was decanted for filtration. The filtrate chamber was rinsed three times with filtrate before the remainder of the sample was filtered. The filtrate was then decanted in duplicate into acid washed and pre-combusted 40 ml amber glass vials. Filtered water samples were stored in the dark and kept cool (stored in shade near the glacier) until transport to the University of Alberta for analysis at the end of the field season.

Debris-rich basal ice (BASAL) was sampled from locations along the north margin of Outre Glacier where glacier flow had created cavities on the lee side of bedrock obstacles. All equipment used for basal ice sampling was ethanol washed and flame sterilized. Prior to sampling, the basal ice face was cleaned by removing the first 10 cm of ice from the surface. Basal ice was chipped away with a chisel and collected in an aluminum tray and transferred into sterile Whirlpak bags. The basal ice was then left to melt in a dark container at ambient temperatures and filtered and stored as described above for water samples.

3.2.3. Fluorescence Analysis.

After transport to the laboratory, meltwater samples were stored in the dark at 4°C until analysis. Synchronous fluorescence spectra were obtained using a SPEX Fluorolog-3 spectrofluorometer. The fluorometer was equipped with both excitation and emission monochromators with a Xenon lamp as an excitation source. Scans were performed on samples that had warmed to room temperature at 1 nm increments with a 0.1 s integration period using a 10 nm bandwidth and an 18 nm offset ($\Delta\lambda$ = 18 nm) between monochromators. Water samples were contained within a quartz glass cuvette with a 10 nm path length. All spectra were Raman corrected by subtracting the synchronous spectrum of deionized water derived under identical scanning conditions. All scans were dark corrected and internally corrected to compensate for variations in lamp performance. The shapes of synchronous spectra are a function of $\Delta\lambda$. Multiple synchronous scans were performed on several meltwater samples using different offsets and a $\Delta\lambda$ of 18 nm was found to provide the best resolution of the multiple fluorophores that were present in the samples (data not shown). Miano and Senesi (1992) also found that $\Delta\lambda$ = 18 nm is optimal for samples which contain multiple fluorophores, such as are found in fulvic and humic acid samples. Studies that use a different $\Delta\lambda$ will report a different spectral peak wavelength for identical fluorophores, and the magnitude of this difference will be proportional to the difference in $\Delta\lambda$ used. Because of this, care must be taken when comparing spectral peak wavelengths from different studies. However, even though peak positions may change, studies using similar $\Delta\lambda$ will report peak wavelengths within a "region", and this region can be used to compare spectral peaks between studies. Similarly, fluorophore spectral peak locations derived using different fluorescence spectroscopic techniques may occur over a similar range. For example, the emission wavelength for spectral peak locations cited for fluorophores identified using the total luminescence technique, from which excitation-emission matrices (EEMs) can be derived, can potentially be used to define a region on the synchronous fluorescence spectrum where similar fluorophores would be expected to be found, especially when relatively low $\Delta\lambda$ are used (e.g. Sierra et al., 2005). All of the synchronous spectra obtained here were smoothed using a centered 12 point running average and normalized to the highest peak within each individual spectrum to ensure that the PCA focused on identifying variations in spectral shape (fluorophore composition) rather than spectral intensity.

3.2.4. Principal Components Analysis (PCA).

PCA was performed using STATISTICA v.5 (StatSoft) statistical software. The rationale for using PCA is to identify principal components (PCs) that can be interpreted as "type" spectra that permit the identification of compounds that comprise, and account for the bulk of the variation in, the fluorescence spectra of DOM derived from the Outre Glacier region. The potential non-independence of the spectral data collected here, which is common in time series data, and which may invalidate the use of PCA where the goal is inferential in nature (Jolliffe, 1986, pg. 299), should not affect the descriptive nature of the analysis presented here.

Several PCAs were conducted on the fluorescence spectra from Outre Glacier and surrounding environments. The first PCA included all of the fluorescence spectra collected during the field season (referred to as TOTAL). A data matrix was constructed where spectra from each sample were arranged chronologically as variables (x-axis) with the synchronous scan wavelengths as cases (y-axis) within each glacier environment that was sampled (SUB, SUB2, MARG, Alpine Stream, South Glacier, BASAL, SUPRA). The input matrix consisted of 116 variables (spectra) and 101 cases (wavelengths). Subsequent PCAs were conducted for individual environments. The spectra for individual environments were arranged in chronological order as outlined above for the TOTAL PCA. In all PCAs the number of PCs retained was limited to those that represented at least 1% of the original variance (e.g. Kaiser, 1960). The matrix was rotated using the *Varimax Raw* algorithm (when more than one PC was retained) to maximize the variance between spectra (columns) and maximize the loading on individual PCs in the data matrix (StatSoft, 1995).

The data matrix was ill-conditioned for all of the PCAs. Ill-conditioning is a result of a high degree of inter-correlation among the variables. This is not unexpected with the dataset being analyzed here as minor changes in DOM source and biogeochemical history will result in subtle changes in spectral waveform over the time series from a single environment, and would be expected to result in a high degree of correlation. To correct for this, and to permit the PCA, STATISTICA artificially reduces the degree of inter-correlation between variables by adding a small constant to the diagonal of the matrix. The PC factor patterns are not affected by this procedure, but the estimates of the percentage of variance in the dataset accounted for by each PC

will not be exact (StatSoft, 1995). The relative magnitudes of the percentage of variance explained by each PC should be unchanged.

3.3. Results.

The average synchronous fluorescence spectrum for the DOM in all 116 water samples contains 4 main fluorophores, with several poorly resolved fluorophores at longer wavelengths (Fig. 3.3). The standard deviations associated with each spectral peak suggest that the relative contribution of each fluorophore to the bulk fluorescence varies between samples. The presence of a shoulder on the 420 nm peak and the asymmetry of the 365 nm peak suggest that additional fluorophores may be present, but they are ill defined in the average spectrum. PCA is used here to help resolve these complexities.

3.3.1. TOTAL PCA.

The TOTAL PCA yielded 4 PCs that account for 97.5% of the variance in the 116 synchronous spectra. The plots of factor scores (values of each case) vs. wavelength for each PC provide an indication of the spectral shape of individual PCs and therefore identify the fluorophores that contribute to the variance in the spectral signals (Fig. 3.4). A comparison between the fluorophores detected here and those that have previously been characterized as specific compounds (Table 3.1) allows a tentative identification of the fluorophores that make up the TOTAL spectra. TOTAL PC1 (91% of the variance) is associated with a single protein-like fluorophore at 273 nm (Table 3.1). TOTAL PC2 (3.9%) is associated with a primary fluorophore centered at 363 nm, which is indicative of humic material, specifically fulvic acid (Table 3.1). Humic material is a general term that is used to describe material formed by the abiotic condensation of degraded organic matter (Sylvia et al., 1999). It includes humic acid (soluble in water at pH>2), fulvic acid (soluble in water at any pH) and humin (insoluble in water). TOTAL PC2 also has fluorophores at 275 nm and 477 nm, which indicate the presence of protein-like and humic material (humic acid) respectively (Table 3.1). Peaks that appear as shoulders on the 363

nm peak are indicative of humic material (322 nm, 350 nm and 414 nm; Table 3.1). TOTAL PC3 (1.5%) has weak peaks at 332 nm, which is indicative of naphthalene, and at 360 nm and 383 nm, which are indicative of humic material (Table 3.1). Several small and ill-defined peaks exist in the spectral region between 414 nm and 477 nm. This spectral region is associated with humic material and lignin precursors (Table 3.1). TOTAL PC4 (1.1%) has a peak at 313 nm (humic material) and, like TOTAL PC3, displays ill-defined peaks between 414 nm and 477 nm (humic material and lignin precursors) (Table 3.1).

3.3.2. PCA by environment.

3.3.2.1. Subglacial.

The factor scores for SUB and SUB2 are perfectly correlated ($r^2 = 1$, Table 3.2) and account for 95.5% and 94.5% of the variance in the fluorescence spectra from their respective environments (data not shown). This indicates that the DOM in SUB and SUB2 is essentially identical in character. Therefore, a single PCA was performed on all spectra from SUB and SUB2 in order to characterize DOM from the subglacial environment (SUBGLACIAL). The SUBGLACIAL PCA yielded two PCs (SUBGLACIAL PC1 (95.2%) and SUBGLACIAL PC2 (1.6%) which account 96.8% of the overall variance (Fig. 3.5). The SUBGLACIAL PC1 spectral waveform indicates the prevalence of a fluorophore at 261 nm (protein-like) and a shoulder at 304 nm, which also indicates the presence of a protein-like fluorophore (Table 3.1). The spectral waveform for SUBGLACIAL PC2 indicates a main fluorophore at 363 nm (humic material) with secondary fluorophores at 269 nm (protein-like), 324 nm, 414 nm and 473 nm (humic material) (Table 3.1).

3.3.2.2. Marginal.

The MARG PCA yields two PCs (Fig. 3.5), which account for 93.9% of the variance in MARG fluorescence spectra (MARG PC1, 89.7%; MARG PC2, 4.3%). A fluorophore at 265 nm (protein-like) dominates the MARG PC1 spectra while a fluorophore at 324 nm (humic material)

dominates the MARG PC2 spectra. Furthermore, while MARG PC1 displays a secondary peak at 367 nm (humic material), MARG PC2 displays secondary peaks at longer wavelengths (418 nm and 477 nm (humic material), and at 540 nm (wavelength approaching pigment-like fluorescence) (Table 3.1).

3.3.2.3. Alpine Stream.

The PCA for the Alpine Stream environment yields a single PC that accounts for 90.6% of the variance in the fluorescence spectra (Fig. 3.5). This PC displays a primary peak at 273 nm (protein-like), and secondary peaks at 367 nm, 422 nm and 481 (humic material). A shoulder on the primary peak occurs at 312 nm (protein-like) (Table 3.1).

3.3.2.4. Basal.

The PCA for the basal ice samples from Outre Glacier and South Glacier yields a single PC that accounts for 95% of the variance in the fluorescence spectra (Fig. 3.5). The BASAL PC shows a primary peak at 367 nm (humic material) with secondary peaks at 277 nm (protein-like), 320 nm, 418 and 480 nm (humic material) and 532 nm (pigment). A shoulder occurs on the primary peak at 347 nm (humic material) (Table 3.1).

3.3.2.5. South Glacier.

The South Glacier PCA yields a single PC that accounts for 98.8% of the variance (Fig. 3.5) and its spectral waveform is very similar to that of the total averaged spectrum (Fig. 3.3). The South Glacier PCA was derived from only 3 synchronous spectra, and the fact that this PC explains a relatively high proportion of the variance indicates either that the DOM in South Glacier

subglacial meltwater is relatively homogeneous or that the sample size was insufficient to capture any variation in DOM composition over the course of the melt season.

3.3.2.6. Supra.

Only two spectra were collected from the supraglacial environment, which precludes the use of PCA because of an insufficient sample size. However, the plot of the SUPRA average spectrum (Fig. 3.5) shows a primary peak at 273 nm (protein-like), with a shoulder at 313 nm and two ill defined peaks at 367 nm and 383 nm and a small peak at 477 (humic material).

3.3.3. PC shape interpretation.

Plots of the PCA factor scores vs. wavelength provide a representation of the spectral waveform of each PC. Peaks that are centered in the range from 255-295 nm indicate the presence of a protein-like fluorophore that has been interpreted as indicating aromatic amino acids (Table 3.1). The most common amino acid peak encountered during this investigation occurs at 273 nm (± 5 nm), which is in the spectral region associated with tyrosine. This peak is present in the factor score plots for each environment at Outre Glacier and is the dominant peak in the SUBGLACIAL PC1, MARG PC1, Alpine Stream, South Glacier PCs and the SUPRA average plot (Fig. 3.5). It is also the dominant peak in TOTAL PC1 and a secondary peak in TOTAL PC2 (Fig. 3.4).

Tyrosine biosynthesis occurs in both plants and microorganisms. Tyrosine is derived from chorismate, a product of the shikimate pathway (Schmid and Amrhein, 1999). Microbial tyrosine biosynthesis occurs in the cytoplasm where 90% of chorismate is used for amino acid synthesis (Schmid and Amrhein, 1999). Tyrosine biosynthesis in plants is believed to occur in the chloroplasts, is less efficient than microbial tyrosine biosynthesis, and produces secondary products such as lignin precursors and quinones (Schmid and Amrhein, 1999). Due to a tendency to transfer energy to other functional groups, tyrosine typically only fluoresces in the absence of associated tryptophan (Creighton, 1993) or humic substances (Yamashita and Tanoue, 2003).

This suggests that the tyrosine represented by TOTAL PC1 is indicative of freshly produced amino acid that has not undergone molecular condensation and humification or bonded to existing humic material. Furthermore, the existence of the prominent tyrosine fluorophore in TOTAL PC1, MARG PC1 and SUBGLACIAL PC1, and the absence of strong tryptophan, pigment, or free quinone peaks suggests that the production of tyrosine is a product of a microbial metabolic pathway. These two lines of evidence suggest that a microbial source is responsible for the observed tyrosine rather than the decay of plant material.

The tyrosine peak in TOTAL PC1 (273 nm) appears as a shoulder on a peak in the spectral region that is associated with phenylalanine (an amino acid which is biosynthesized by both plants and microbes) in SUBGLACIAL PC1. A second shoulder (304 nm) also appears on the phenylalanine peak in SUBGLACIAL PC1. This coincides with the spectral range that is cited for the amino acid tryptophan (Table 3.1). The presence of this fluorophore could result from either the presence of tryptophan or tyrosine metabolites (e.g. catechol) in the DOM (e.g. Determann et al., 1998). The presence of the phenylalanine peak at 261 nm suggests the latter because phenylalanine fluorescence is transferred to tryptophan if both amino acids are present (Yamashita and Tanoue, 2003). The expression of the phenylalanine fluorophore suggests that such an energy transfer is not occurring and that tryptophan is not present.

A similar phenomenon is observed in MARG PC2 where the main aromatic amino acid peak (265 nm) is slightly blue-shifted relative to TOTAL PC1 (273 nm), but is still indicative of the presence of tyrosine (Table 3.1). A shoulder on the tyrosine peak at 275 nm may be taken as evidence of the presence of tryptophan. Tryptophan is photo-oxidized to produce N-formyl-kynurenine (e.g. VanderMeulen and Judy, 1988) so, as with the SUBGLACIAL PC1 waveform, the shoulder is interpreted here as evidence of the presence of tyrosine metabolites or small amounts of non-degraded tryptophan.

The dominant peak in the TOTAL PC2, SUBGLACIAL PC2 and BASAL spectral waveforms is located at 365 nm (Figs. 3.4 and 3.5) and is indicative of the presence of humic material (Table 3.1). Secondary peaks at 414 nm and 479 nm are also indicative of the presence of humic material. The weakly developed peak at 532 nm approaches the spectral region cited for pigments. The two shoulders on the main humic material peak at 322 nm and 347 nm (TOTAL PC2 and BASAL only) fall within the spectral range of fulvic acid. The fact that these two shoulders bracket the naphthalene spectral region (330 nm) suggests that the humic material indicated by these two shoulders is derived from a refractory, possibly vascular plant-derived,

source of OM. This, and the abundance of vegetation in the environment surrounding Outre Glacier suggest that the pigment-like fluorophore is likely derived from pigments found in plant material. The presence of multiple fluorophores suggests a multiple source contribution to the DOM represented by TOTAL PC2, SUBGLACIAL PC2 and BASAL. This is similar to the spectral waveform characteristic of soil humic material (e.g. Miano and Senesi, 1992). Soil humic material is a product of the abiotic molecular condensation of a wide range of organic compounds that are derived from the surrounding environment (Sylvia et al., 1999). In the case of TOTAL PC2, SUBGLACIAL PC2, and BASAL, a combination of both labile (amino acid) and recalcitrant (humic material) OM sources contribute to the PC waveform. Furthermore, the presence of both tyrosine and humic material fluorescence suggests that the amino acid is not closely associated with the humic material because complete energy transfer from tyrosine to humic material has not occurred. The presence of an amino acid that is not associated with humic material would be expected in soil where both biotic and abiotic processes are occurring simultaneously and fresh amino acids are produced.

TOTAL PC3 and TOTAL PC4 are poorly correlated with all other PCs (Table 3.2). TOTAL PC3 is unique because it is the only PC that displays a spectral peak at 332 nm (Fig. 3.4), which is indicative of naphthalene. This, and the presence of other spectral peaks at 359 nm (fulvic acid) and 528 nm (pigment-like) and several small and ill-defined peaks in the region between 400–475 nm (humic material and lignin descriptors), suggests that the TOTAL PC3 waveform is indicative of DOM which is derived from humic sources. TOTAL PC3 is also the only PC to show a primary fluorophore at <260 nm, which may be indicative of phenylalanine (Table 3.1). Phenylalanine is produced by microbes and plants using the same metabolic pathway as is used for the biosynthesis of tyrosine (Schmid and Amrhein, 1999). The general blue shift of fluorophores in TOTAL PC3 relative to TOTAL PC2 (Fig. 3.4) may be indicative of a less-condensed molecular structure, and thus possibly humic material that is derived from microbial (aliphatic) organic residues or less-developed or younger vascular plant-derived humic material. Phenylalanine that is not associated with humic material is considered to be a labile compound that is mineralized rapidly by microbes (Keil and Kirchman, 1993). The presence of non-mineralized phenylalanine and the abundance of vascular plants in the Outre Glacier environment support the hypothesis that TOTAL PC3 may represent poorly developed humic material of both vascular plant and microbial provenance that has not undergone extensive mineralization of labile compounds.

TOTAL PC4 displays a main fluorophore at 313 nm that is indicative of fulvic acid. Similar to TOTAL PC3, TOTAL PC4 displays a possible phenylalanine fluorophore (<260 nm) and a weak fluorescence between 400 - 475 nm (humic material and lignin descriptors), and may also indicate weakly developed microbial- and vascular plant-derived humic material.

In summary (Table 3.3), TOTAL PC1, SUBGLACIAL PC1, MARG PC1 and the Alpine Stream PC are correlated (Table 3.2) and show a dominant fluorophore at 273 nm that is indicative of a protein-like fluorophore, likely tyrosine. The SUPRA average spectrum also has its dominant fluorophore at 273 nm. The existence of the prominent tyrosine-like fluorophore and the absence of fluorophores which are indicative of tryptophan, pigment or quinone peaks suggests that the tyrosine which is detected in TOTAL PC1, SUBGLACIAL PC1, MARG PC1, the Alpine Stream PC and the SUPRA average spectrum is derived from a microbial source which is found in the supraglacial environment. TOTAL PC2, SUBGLACIAL PC2, MARG PC2 and BASAL are correlated (Table 3.2) and show fluorophores at longer wavelengths that are indicative of humic material. The dominant fluorophore in these PCs is located at 365 nm (humic material) with secondary peaks in the fulvic and humic acid range (322 – 479 nm) of the spectrum. Of note is that two fluorophores that occur as shoulders on the main fluorophore at 322 nm and 347 nm, bracket the spectral region which is cited for naphthalene (330 nm) and suggest that the humic material in the spectra which are associated with TOTAL PC2, SUBGLACIAL PC2, MARG PC2 and BASAL may be derived from a refractory vascular plant source. TOTAL PCs 3 and 4 are poorly correlated with any other PC and each other. However, the presence of the phenylalanine fluorophore in TOTAL PC 3 and 4 suggests that the DOM represented by these PCs is weakly developed microbial and vascular plant-derived humic material.

3.3.4. PC Loadings.

The loading of each individual spectrum on each PC provides an indication of how well each PC correlates with an individual synchronous fluorescence spectrum. Only the loadings for the TOTAL PCs are considered here to facilitate the comparison of factor loadings between environments and the detection of similarities and differences in DOM source and/or biogeochemical processes between environments.

Figure 3.6 displays the relationships between PCs and raw spectra by comparing the TOTAL PC spectral waveforms with synchronous spectra from samples that were highly loaded on each of the four TOTAL PCs. Note that the higher the PC loading, the stronger the similarity between the PC and the synchronous spectrum.

The loadings of individual spectra in the time series on each TOTAL PC are displayed in Figure 3.7. All PCs show variation with respect to loading over the course of the melt season and trends in PC loadings can be discerned. TOTAL PC1 and PC2 are typically the most strongly loaded PCs. This is not surprising as these PCs account for the largest fractions of the variance in the overall signal (91% and 3.9% respectively).

In SUB, a significant change in the molecular characteristics of DOM in meltwater occurred on August 14 and coincides with the initiation of meltwater discharge from SUB2. TOTAL PC1 shows an increase in loading (and TOTAL PC2 shows a decrease in loading) to values observed in MARG (~0.7) until spectrum 37 (August 14), the day after flow in SUB2 was initiated (Fig. 3.7a). TOTAL PC1 and TOTAL PC2 loadings are similar in SUB and SUB2 after August 14 and TOTAL PC1 loadings in SUB after August 14 are significantly lower (t-test, $P < 0.05$) than TOTAL PC1 loadings prior to August 14. This indicates that a significant change in the molecular characteristics of the subglacial OM has occurred, from a predominantly microbially-derived, protein-like source to a humic-like source. This change coincides with the onset of subglacial discharge from SUB2. Of note is a sharp increase in TOTAL PC1 loadings on August 13 (spectrum 34) that precedes the change in TOTAL PC1 loading on August 14 (Fig. 3.7a). This increase in TOTAL PC1 loading is indicative of an increase in the microbially derived component of the DOM, as indicated by the dominance of the tyrosine fluorophore (TOTAL PC1) in the bulk DOM spectral waveform (Fig. 3.4, Table 3.3).

Although TOTAL PC1 accounts for the majority of the variance (91%) in the spectra from all 116 samples, there are some spectra that load more heavily on the other TOTAL PCs. This is indicative of a change in the dominant fluorophores that contribute to the spectral properties of the DOM. For the purposes of comparison, the loadings for TOTAL PC1 are plotted against to those for TOTAL PC2, PC3 and PC4 (Fig. 3.8a-c). Although the spectrum which corresponds to the August 14 SUB sample (spectrum 34) does not fall outside 2 standard deviations of the mean, it is loaded the most strongly on TOTAL PC1 and most weakly on TOTAL PC2 of any of the SUB samples (Fig. 3.8a). This suggests that the SUB DOM has a predominantly microbial character on August 14. Other spectra that load significantly on TOTAL PC1 (microbial),

relative to TOTAL PC2 (humic) are the spectra from the lower reaches of the Alpine Stream (spectra 105 - 107, Fig. 3.8a).

Conversely, all of the BASAL spectra (spectra 112 - 114) load more strongly on TOTAL PC2 than on TOTAL PC1 (Fig. 3.8a). While some of the BASAL spectra also load more heavily on TOTAL PC3 and PC4 than on TOTAL PC1 (Fig. 3.8b, c), their loading on all three of these PCs is low. Other spectra that load more heavily on TOTAL PCs other than TOTAL PC1 include spectrum 70 (MARG July 20) which loads more heavily on TOTAL PC2, spectrum 96 (MARG August 19) which loads more heavily on TOTAL PC2 and PC4, and spectrum 47 (SUB August 20) which loads more heavily on TOTAL PC3. This suggests that the DOM from the Outre Glacier basal ice samples is significantly different from that in the majority of the subglacial meltwater samples, and that significant changes from a microbial source to a humic-like source for the DOM occur periodically in both the subglacial and supraglacial environments.

Similar to the decrease in SUB spectral loading on TOTAL PC1 on August 14, the MARG spectral loading on TOTAL PC1 decreases to levels that are similar to TOTAL PC2 loading on August 15 (spectrum 92; Fig. 3.7a). This similarity between MARG TOTAL PC1 and PC2 loading persists until August 20 (spectrum 97), when TOTAL PC1 and PC2 loadings return to pre-August 15 levels. MARG spectral loadings on TOTAL PC3 and TOTAL PC4 increase from August 13-15 (spectra 80 - 91; Fig. 3.7b) and from August 15-19 (spectra 92 - 96; Fig. 3.7b) respectively. This indicates that the molecular characteristics of the DOM in supraglacial meltwater, including that from the lower ablation zone, change from August 13-20.

3.4. Interpretation.

The PCA of synchronous fluorescence spectra from Outre Glacier and surrounding environments yields 4 PCs that pick out several distinct fluorophores. Together, these account for 97.5% of the overall variance in the original spectra. The spectral shape of each PC permits the identification of spectral "types" which, depending on the fluorophores present in each PC and the relative loading of individual spectra on each PC, provide useful information concerning DOM composition and the relative contributions of different DOM sources to the original fluorescence spectra.

The most significant PC is associated with a set of fluorophores that includes one which is indicative of a fresh microbial source of a "protein-like" (tyrosine) material (TOTAL PC1). This PC accounts for 91% of the variance in the full set of 116 fluorescence spectra, 95.2% of the variance in the subglacial samples (SUBGLACIAL PC1), 89.7% in spectra from the lower supraglacial environment (MARG PC1), 98.8% in subglacial meltwater from South Glacier and 90.6% in spectra from the Alpine Stream. It also features strongly in the SUPRA average plot. A second PC (TOTAL PC2) is characterized by fluorophores that correspond to humic material. It accounts for 3.9% of the variance in the full set of spectra, 1.6% of the variance in subglacial meltwater samples (SUBGLACIAL PC2), 4.3% of the variance in supraglacial meltwater from the lower ablation zone (MARG PC2) and 95% of the variance in basal ice spectra (BASAL). There is a decrease in TOTAL PC1 loading and a corresponding increase in TOTAL PC2 loading on August 14, a day after flow from SUB2 was initiated in subglacial meltwater samples. This suggests that there is a hydrological control on the molecular characteristics of DOM in subglacial meltwater.

The subglacial drainage system is generally viewed as having channelized and distributed components (Hubbard and Nienow, 1997). A network of linked cavities that covers a large area of the bed typically characterizes the distributed system. Basal meltwater flows more slowly through this system than through the major subglacial channels. The distributed system is more likely to drain meltwater and material which is derived from basal ice melt while the main channels drain supraglacially-derived meltwater and dissolved material that are delivered to the glacier bed via moulins and crevasses. When the supraglacial meltwater flux into basal channels exceeds channel capacity, overflow from the main channels to the distributed system occurs. As the volume of water in a channelized system decreases, or the channel volume increases to accommodate an increase in water flux (for example channel enlargement by melting of the ice that forms the roof of the N-channels), the hydraulic gradient reverses and flow from the distributed system to the channelized system occurs.

The initiation of meltwater discharge from SUB2 on August 13 suggests that the capacity of the main channel has increased. An increase in water depth in the main proglacial channel (Fig 3.9a) on August 13 supports the hypothesis that an increased volume of meltwater was flowing through the subglacial drainage system.

During periods of high supraglacial meltwater input to the channelized component of the drainage system, subglacial meltwater flows to the distributed system and supraglacially-derived DOM

dominates the subglacial DOM spectrum. The initiation of discharge from SUB2 coincided with a sharp increase in the loading of the SUB spectrum on TOTAL PC1 (spectrum 34, August 13; Fig. 3.7a and 3.8a), suggesting that the "protein-like" fluorophore was more prominent in subglacial DOM when the meltwater flux to the subglacial channelized system was high. The fact that the tyrosine fluorophore is prominent in the supraglacial spectra (SUPRA and MARG PC1) supports the hypothesis that the "protein-like" fluorophore is derived from tyrosine production in supraglacial snow and ice melt.

During periods of decreasing subglacial meltwater discharge, flow occurs from the distributed drainage system component to the channelized component and DOM derived from overridden soils and vegetation becomes a more prominent component of subglacial DOM spectra. TOTAL PC1 loadings in SUB were significantly lower after August 14, indicating that the molecular characteristics of the subglacial DOM were different from earlier in the season. The similarity between post August 14 SUB and SUB2 TOTAL PC1 and TOTAL PC2 loadings (Fig. 3.7a) suggests that a hydraulic connection between the main channel and channel-marginal areas had been established and that transport of subglacial DOM from the channelized system to the distributed system was occurring. Flow in the proglacial stream on August 13 was relatively high and corresponded to high daily temperatures (Fig. 3.9a, b). Proglacial stream flow was lower and daily average and overnight temperatures were cold after August 13 (Fig. 3.9a, b). This suggests that the hydraulic pressure in the channelized system was low, promoting flow from the distributed system to the channelized system. The DOM that is represented by TOTAL PC2 is similar to SUBGLACIAL PC2 (Table 3.2). These PCs are highly loaded on the BASAL spectra (112-114) (Fig. 3.7 and Fig. 3.8a). They reflect a humic source of OM (Table 3.3) and are most similar to the PC of stream flow from a moss-covered alpine meadow, as indicated by relatively high TOTAL PC2 loadings on spectra 103 and 104 (Fig. 3.7). The increase in TOTAL PC2 loading relative to TOTAL PC1 loading in subglacial spectra suggests that meltwater draining through the distributed system could access an OM pool, either in melting basal ice or in overrun soils or vegetation, that is similar to that found in a moss-covered soil environment. The establishment of a more efficient hydrological connection between the distributed and channelized systems on August 13, as indicated by the similarity between the TOTAL PC1 and PC2 loadings in SUB and SUB2 after August 15, permitted the detection of the distributed system OM in the bulk subglacial meltwater. TOTAL PC3 and PC 4 show no trend throughout the monitoring period, and account for relatively little variance (1.5% and 1.1% respectively). This suggests that the mechanism responsible for the introduction of "weakly developed" humic

material to the bulk subglacial meltwater was relatively minor. An exception occurs on August 20 (spectrum 47), when the SUB spectrum was most highly loaded on TOTAL PC3 (Fig. 3.8b).

Hydrological conditions also governed the mobilization of DOM in the supraglacial environment. While the majority of the DOM that is mobilized supraglacially appears to be derived from microbial populations in the supraglacial snowpack, periods of exceptional melt stimulated the flow of water through cryoconite holes and/or lowered the glacier ice surface, promoting the mobilization of DOM from cryoconite holes. DOM in supraglacial meltwater from the ablation zone was also influenced by a secondary OM source, represented by MARG PC2, but the differences in spectral waveform between MARG PC2 and SUBGLACIAL PC2 (Fig. 3.5) suggest that the molecular characteristics of the secondary OM source are different in the two environments. For example, while both MARG PC2 and SUBGLACIAL PC2 have primary peaks that are indicative of humic material, those in MARG PC2 are indicative of a less condensed form of humic material than those in SUBGLACIAL PC2, as indicated by the shorter wavelength of the primary peak. Additionally, tyrosine is present as a well-defined fluorophore in SUBGLACIAL PC2, while it appears as a shoulder on the humic peak in MARG PC2. In addition to these spectral shape differences, the MARG spectral loadings on TOTAL PC1 and TOTAL PC2 suggest that the source of this secondary OM differed between the MARG and SUBGLACIAL environments. The sharp decrease in TOTAL PC1 loading occurred on August 15 (spectrum 92) in MARG, a day later than it did in SUB (August 14). In SUB, this decrease in loading on TOTAL PC1 persisted until the end of the monitoring period due to the establishment of a hydrological connection between the subglacial channelized and distributed systems. The TOTAL PC2 increase in MARG persisted for only 5 days, until August 20 (spectrum 97). These lines of evidence indicate that while the secondary source of OM in the subglacial environment may be overrun soil, most likely from a moss-covered environment, the secondary source of OM in MARG is different, though also derived from a soil-related environment. The most likely source of soil-related OM to the supraglacial environment is wind-blown sediment that has been deposited on the glacier surface and/or accumulated in cryoconite holes. Cryoconite holes are cylindrical depressions that result from the melting of dark wind-blown sediment into the glacier surface (Porazinska et al., 2004). Microbial communities are known to exist in cryoconite holes (Porazinska et al., 2004; Mueller et al., 2001), so cryoconite OM may have both microbial and terrestrial characteristics, as is observed in the MARG PC2 spectral waveform. The event that stimulated the flux of microbially derived DOM from the supraglacial snowpack to the subglacial environment on August 13 (likely melt induced flushing) also stimulated a mobilization of a

secondary source of OM in the lower ablation zone. It should be noted that air temperatures rose between August 12-15, after a cooler period (August 7-11) and that minimum air temperatures were the highest recorded during the observation period (Fig. 3.9b). The time lag between the subglacial change in OM properties in response to the melt event and the response in MARG may reflect the amount of time required to mobilize the DOM characterized by TOTAL PC2 and MARG PC2. Such a situation could be envisaged if the MARG PC2 OM is derived from cryoconite holes. At Outre Glacier, most of the cryoconite holes are located at higher elevations on the glacier (~1250 m a.s.l.), where the glacier surface slope is gentle enough to permit the accumulation of supraglacial sediment. Cryoconite holes are generally partially filled with water and the mobilization of the cryoconite DOM pool requires either a lowering of the glacier surface to below the cryoconite water level (e.g. Boon and Sharp, 2003) or supraglacial water flow through the cryoconite.

The spectra from the forested reaches of the Alpine Stream load most highly on TOTAL PC1 (mean = 0.94, Fig. 3.7). This is an unexpected result because a higher proportion of fluorophores that are associated with vascular plant material (e.g. lignin biopolymers) or soil (e.g. humic material), which is represented by the fluorophores characteristic of TOTAL PC2, would be expected in the DOM from the mature forest reaches of the Alpine Stream because of its proximity to mature forest vegetation and developed soils. A possible explanation for this result is that the physically larger fraction of OM (POM (particulate organic matter), >0.7 μm) may be vascular-plant derived while the finer fraction (DOM, <0.7 μm), which is considered here, may derived from microbes in the water column (e.g. McKnight et al., 1997). Spectra from the upper reaches of the Alpine Stream (waters draining from an alpine moss-covered soil environment) load heavily on TOTAL PC2, which suggests that vascular plant biopolymers and/or humic material are sufficiently small to be detected as DOM. This would be expected where vascular plants are sparse and/or degraded into smaller biopolymers or where environmental conditions are conducive to the formation of humic material. The upper Alpine Stream samples were taken from seepage flow that drains a moss covered meadow above tree line in the non-glacierized catchment. This suggests that the soil in this area have high pore water content and that organic matter input to the soil is most likely derived from the moss cover rather than tree and/or root material. These wet conditions, in association with a largely non-vascular plant OM input favour the abiotic condensation of recalcitrant OM (non-microbial) to form humic material (Sylvia et al., 1999).

3.5. Summary and Conclusions.

PCA has been shown to be an effective technique for identifying the constituent components of synchronous fluorescence spectra of DOM from Outre Glacier. The DOM in water and basal ice at Outre Glacier and surrounding environments is composed of several fluorophores. These contribute to varying degrees to the bulk DOM fluorescence in different environments and at different times over the course of the melt season. PCA identifies 4 "type" fluorescence spectra (PCs), which account for 97.5% of the total variation in the spectral signal. The waveforms of each of these PCs indicate that a tyrosine fluorophore, which may be derived from microbial biosynthesis in the supraglacial snowpack (TOTAL PC1) accounts for 91% of the variance in the overall spectral signal. This fluorophore also features prominently in the spectra from the Outre Glacier subglacial (SUBGLACIAL PC1), South Glacier subglacial (South Glacier PC), ice marginal (MARG PC1) and supraglacial (SUPRA) streams. The remaining 3 PCs display spectral waveforms consisting of fluorophores which are indicative of a humic or a vascular plant/soil-derived source of DOM (TOTAL PCs 2, 3 and 4). These fluorophores are also prominent in the lower order PCs from the individual environments (SUBGLACIAL PC2, MARG PC2) and in the basal ice spectra (BASAL PC).

As the supraglacial snowpack at Outre Glacier is flushed either by melting or by precipitation, "microbial" DOM is flushed from the snowpack and transported through moulins and crevasses to the subglacial environment. Microbial DOM from supraglacial snowmelt dominates the DOM spectra in the supraglacial meltwater, but a second DOM pool, possibly resulting from the drainage of supraglacial cryoconite holes, which displays fluorophores indicative of humic material, contributes to the supraglacial DOM flux. A second "humic" source of DOM is expressed more strongly in basal ice and in meltwater that has flowed through the distributed component of the subglacial drainage system. The existence of this DOM source suggests that a subglacial pool of OM, which may be derived from overrun moss and soil, exists beneath Outre Glacier in basal ice and/or in the area drained by the distributed drainage system. Hydrological conditions govern the mobilization of DOM in both the subglacial and supraglacial environments. An increased flux of supraglacial meltwater to the subglacial channelized system enhances meltwater flow into the distributed drainage system. By contrast, a decrease in flow through the channelized system promotes the flow of subglacial meltwater (and DOM) from the distributed

system to the channelized system. A similar process has been described for subglacial dissolved solute transport (e.g. Tranter et al., 1997).

While no clear indication of specific biogeochemical alteration of OM is evident from the analyses reported here, the presence of amino-acid fluorophores and humic fluorophores in the same PC (e.g. TOTAL PC 3 and PC4) suggests that the amino acid is recently produced and have not bound to humic material. This may be indicative of recent microbial biosynthesis. The lower order PCs (e.g. TOTAL PC3 and PC4) may be indicative of intermediate products resulting from microbial activity or early stages of humification.

3.6. References.

Barker, J.D., M.J. Sharp, S.J. Fitzsimons, R.J. Turner. 2006. Abundance and dynamics of dissolved organic carbon in glacier systems. *Arctic, Antarctic and Alpine Research* 38(2): 163-172.

Bernat, E.M., W.J. Williams, W.J. Gehring. 2005. Decomposing ERP time-frequency energy using PCA. *Clinical Neurophysiology* 116(5): 1314-1334.

Boon, S., M.J. Sharp, P.W. Nienow. 2003. Impact of an extreme melt event on the hydrology and runoff of a high Arctic glacier. *Hydrological Processes* 17(6): 1051-1072.

Cabaniss, S.E. 1992. Synchronous fluorescence spectra of metal-fulvic acid complexes. *Environmental Science and Technology* 26(6): 1133-1139.

Coble, P.G. 1996. Characterization of marine and terrestrial DOM in seawater using excitation-emission matrix spectroscopy. *Marine Chemistry* 51(4): 325-346.

Coffin, R.B. 1989. Bacterial uptake of dissolved free and combined amino acids in estuarine waters. *Limnology and Oceanography* 34(3): 531-542.

Creighton, T.E. 1993. *Proteins: Structure and molecular properties*. W.H. Freeman: New York; 512.

De Souza Sierra, M.M., O.F.X. Donard, M. Lamotte, C. Belin, M. Ewald. 1994. Fluorescence spectroscopy of coastal and marine waters. *Marine Chemistry* 47(2): 127-144.

Determann, S., J.M. Lobbes, R. Reuter, J. Rullkotter. 1998. Ultraviolet fluorescence excitation and emission spectroscopy of marine algae and bacteria. *Marine Chemistry* 62(1-2): 137-156.

Ferrari, G.M., M. Mingazzini. 1995. Synchronous fluorescence spectra of dissolved organic matter (DOM) of algal origin in marine coastal waters. *Marine Ecology Progress Series* 125: 305-315.

Hannah, D.M., B.P.G. Smith, A.M. Gurnell, G.R. McGregor. 2000. An approach to hydrograph classification. *Hydrological Processes* 14(2): 317-338.

Hubbard, B., Nienow, P. 1997. Alpine subglacial hydrology. *Quaternary Science Reviews* 16(9): 939-955.

Jolliffe, I.T. 1986. *Principal Components Analysis*. Springer-Verlag: New York; 271.

Kaiser, H.F. 1960. The application of electronic computers to factor analysis. *Educational and Psychological Measurement* 20: 141-151.

Keil, R.G., D.L. Kirchman. 1993. Dissolved combined amino acids: chemical form and utilization by marine bacteria. *Limnology and Oceanography* 38(6): 1256-1270.

Kowalczuk, P., J. Ston-Egiert, W.J. Cooper, R.F. Whitehead, M.J. Durako. 2005. Characterization of chromophoric dissolved organic matter (CDOM) in the Baltic Sea by excitation emission matrix fluorescence spectroscopy. *Marine Chemistry* 96(3-4): 273-292.

Lombardi, A.T., W.F. Jardim. 1999. Fluorescence spectroscopy of high performance liquid chromatography fractionated marine and terrestrial organic material. *Water Research* 33(2): 512-520.

McKnight, D.M., R. Harnish, R.L. Wershaw, J.S. Baron, S. Schiff. 1997. Chemical characteristics of particulate, colloidal, and dissolved organic material in Loch Vale Watershed, Rocky Mountain National Park. *Biogeochemistry* 36(1): 99-124.

McKnight, D.M., G.R. Aiken, R.L. Smith. 1991. Aquatic fulvic acids in microbially based ecosystems: results from two desert lakes in Antarctica. *Limnology and Oceanography* 36(5): 998-1006.

Miano, T.M., N. Senesi. 1992. Synchronous excitation fluorescence spectroscopy applied to soil humic substance chemistry. *The Science of the Total Environment* 117/118: 41-51.

Mueller, D.R., W.F. Vincent, W.H. Pollard, C.H. Fritsen. 2001. Glacial cryoconite ecosystems: a bipolar comparison of algal communities and habitats. *Nova Hedwigia* 123: 171-195.

Nienow, P., Sharp, M., Willis, I. 1998. Seasonal changes in the morphology of the subglacial drainage system, Haut Glacier d'Arolla, Switzerland. *Earth Surface Processes and Landforms* 23(9): 825-843.

Peuravuori, J., R. Koivikko, K. Pihlaja. 2002. Characterization, differentiation and classification of aquatic humic matter separated with different sorbents: synchronous scanning fluorescence spectroscopy. *Water Research* 36(18): 4552-4562.

Porazinska, D.L., A.G. Fountain, T.H. Nylen, M. Tranter, R.A. Virginia, D.H. Wall. 2004. The biodiversity and biogeochemistry of cryoconite holes from McMurdo Dry Valley glaciers, Antarctica. *Arctic, Antarctic and Alpine Research* 36(1): 84-91.

Schmid, J., N. Amrhein. 1999. The shikimate pathway. In. *Plant Amino Acids: Biochemistry and Biotechnology*, Singh, B.K. (ed). Marcel Dekker: New York; 147-169.

Sierra, M.M.D., M. Giovanela, E. Parlanti, E.J. Soriano-Sierra. 2005. Fluorescence fingerprint of fulvic and humic acids from varied origins as viewed by single-scan and excitation/emission matrix techniques. *Chemosphere* 58(6): 715-733.

Sylvia, D.M., Fuhrmann, J.J., Hartel, P.G., Zuberer, D.A. 1999. *Principles and applications of soil microbiology*. Prentice Hall: New Jersey; 550.

StatSoft, Inc. 1995. *STATISTICA, Volume III, Statistics II*: 3201-3231.

Stedmon, C.A., S. Markager, R. Bro. 2003. Tracing dissolved organic matter in aquatic environments using a new approach to fluorescence spectroscopy. *Marine Chemistry* 82(3-4): 239-254.

Tranter, M., M. Skidmore, J. Wadham. 2005. Hydrological controls on microbial communities in subglacial environments. *Hydrological Processes* 19(4): 995-998.

Tranter, M., M.J. Sharp, G.H. Brown, I.C. Willis, B.P. Hubbard, M.K. Nielsen, C.C. Smart, S. Gordon, M. Tulley, H.R. Lamb. 1997. Variability in the chemical composition of in situ subglacial meltwaters. *Hydrological Processes* 11(1): 59-77.

VanderMeulen, D.L., M.M. Judy. 1988. Photooxidative changes of lysozyme with 337.1 nm laser radiation. *Radiation and Environmental Biophysics* 27(4): 307-316.

Yamashita, Y., E. Tanoue. 2003. Chemical characterization of protein-like fluorophores in DOM in relation to aromatic amino acids. *Marine Chemistry* 82(3-4): 255-271.

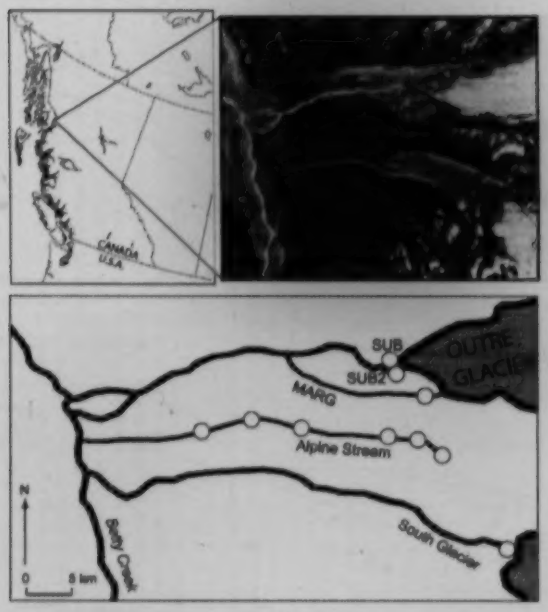

Fig. 3.1.: Location of the Outre Glacier field site. Open circles indicate sampling areas

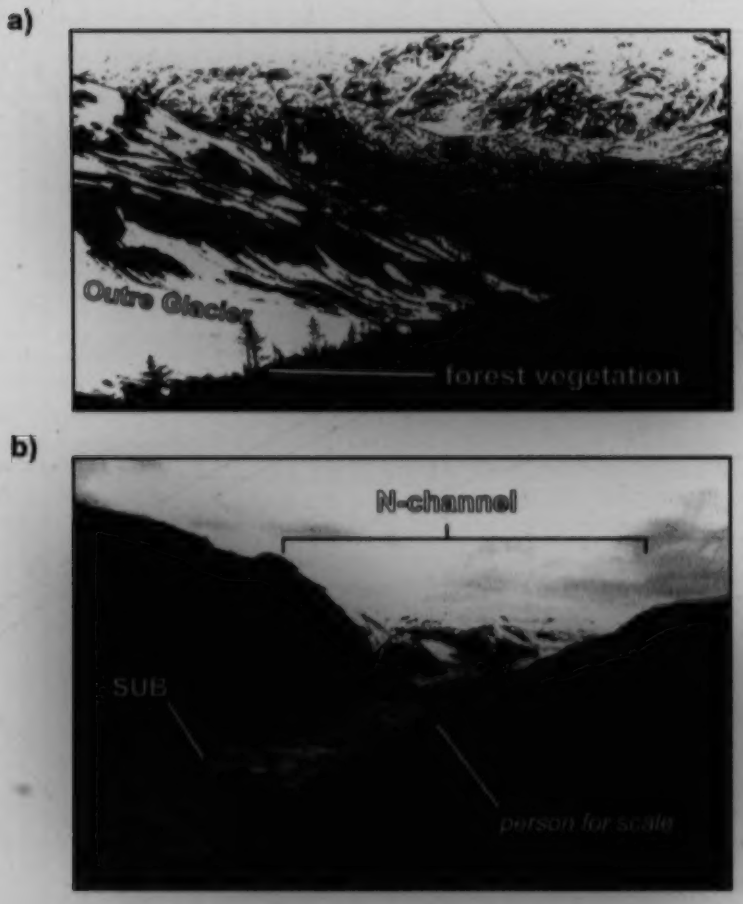

Fig. 3.2.: Photographs showing that a) Outre Glacier terminates below, and is surrounded by forest vegetation; b) the main subglcial meltwater stream (SUB) is confined by an incised bedrock channel (N-channel) at the Outre Glacier terminus.

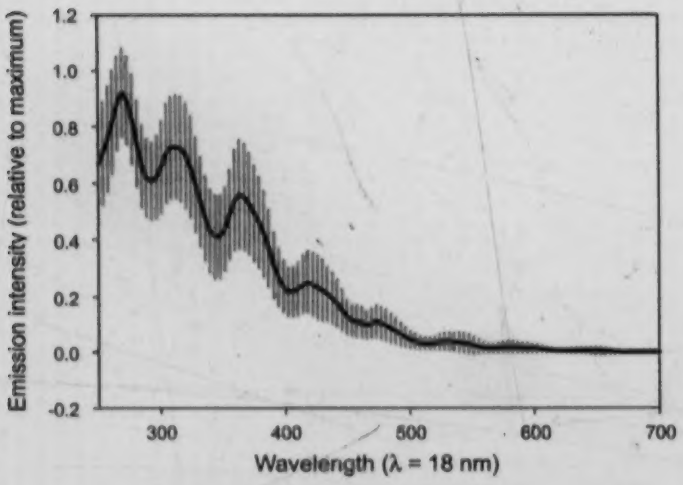

Fig. 3.3.: The average synchronous fluorescence spectrum from Outre Glacier (n=116). The shaded area indicates one standard deviation from the mean.

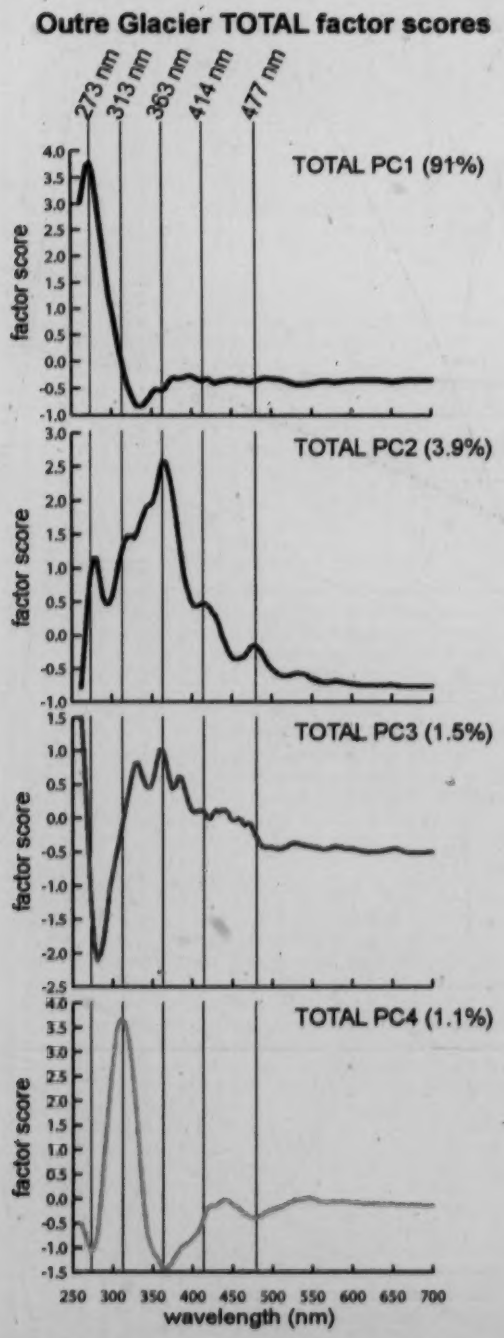

Fig. 3.4.: TOTAL PCA factor scores vs. spectral wavelength. These plots indicate which spectral shapes are associated with the variance in the overall signal, which is used to identify the fluorophores that contribute to the variance in the Outre Glacier DOM. The bracketed values indicate the percent of the overall variance that each PC represents.

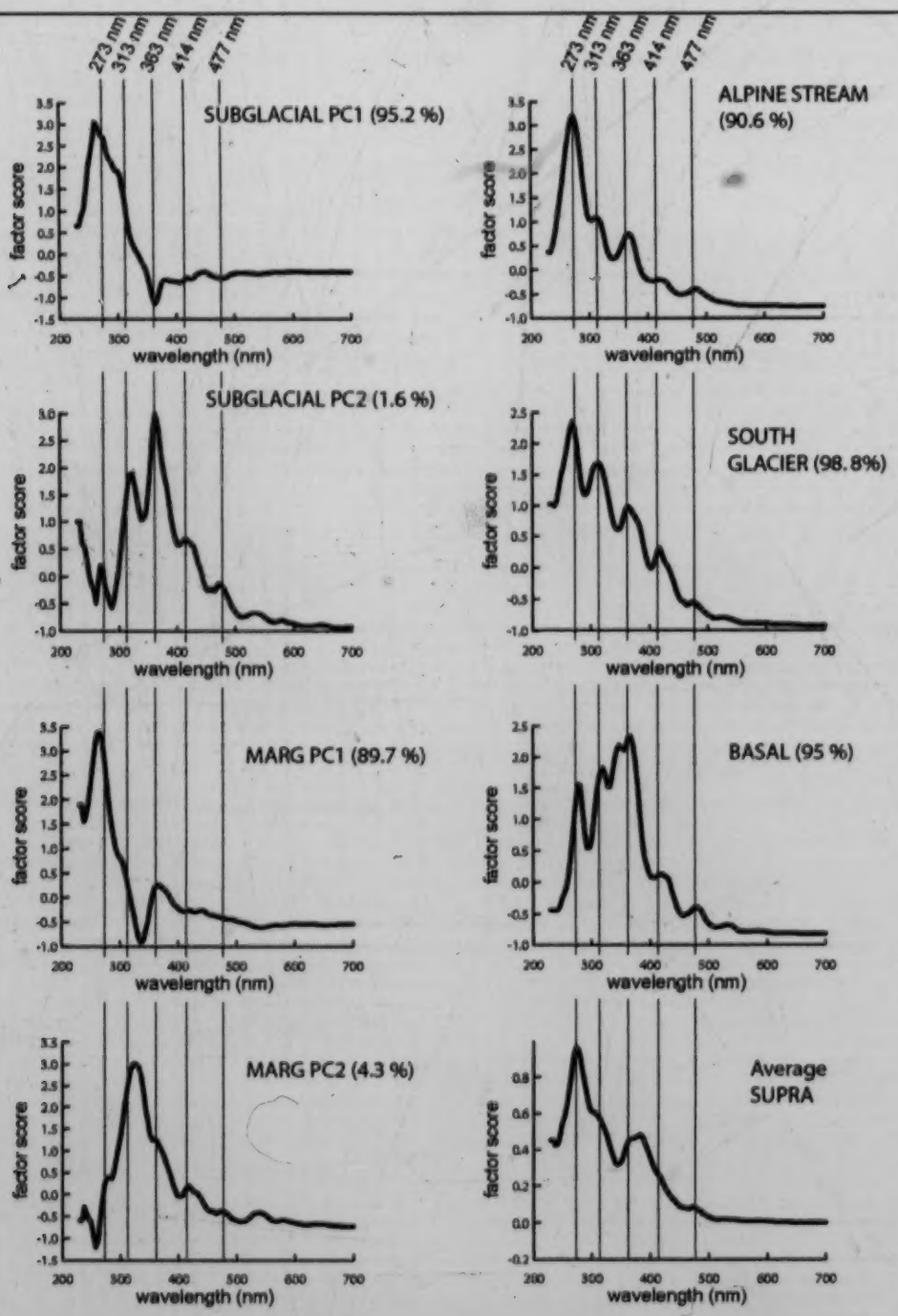

Fig. 3.5.: The spectral waveform for the PCs from each environment. The bracketed values indicate the percent of the variation that each PC represents. Note that the sample size for SUPRA was insufficient for PCA (n = 2) so the average spectrum is plotted here.

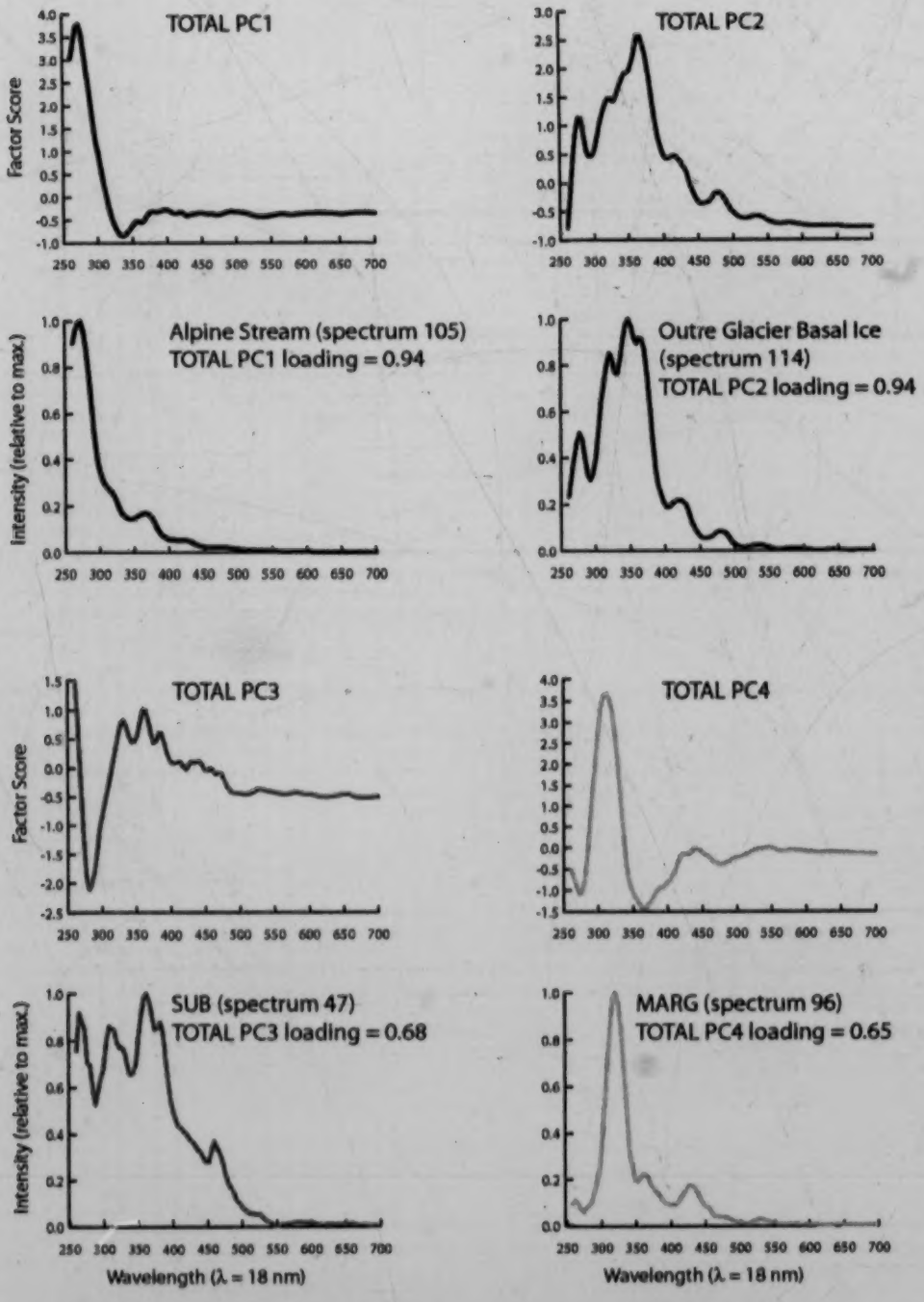

Fig. 3.6.: A plot showing the relationship between the shape of each TOTAL PC and the shape of individual spectra that load strongly on them. Note that strong loadings indicate a similarity between spectral shapes of the TOTAL PCs and the individual spectra.

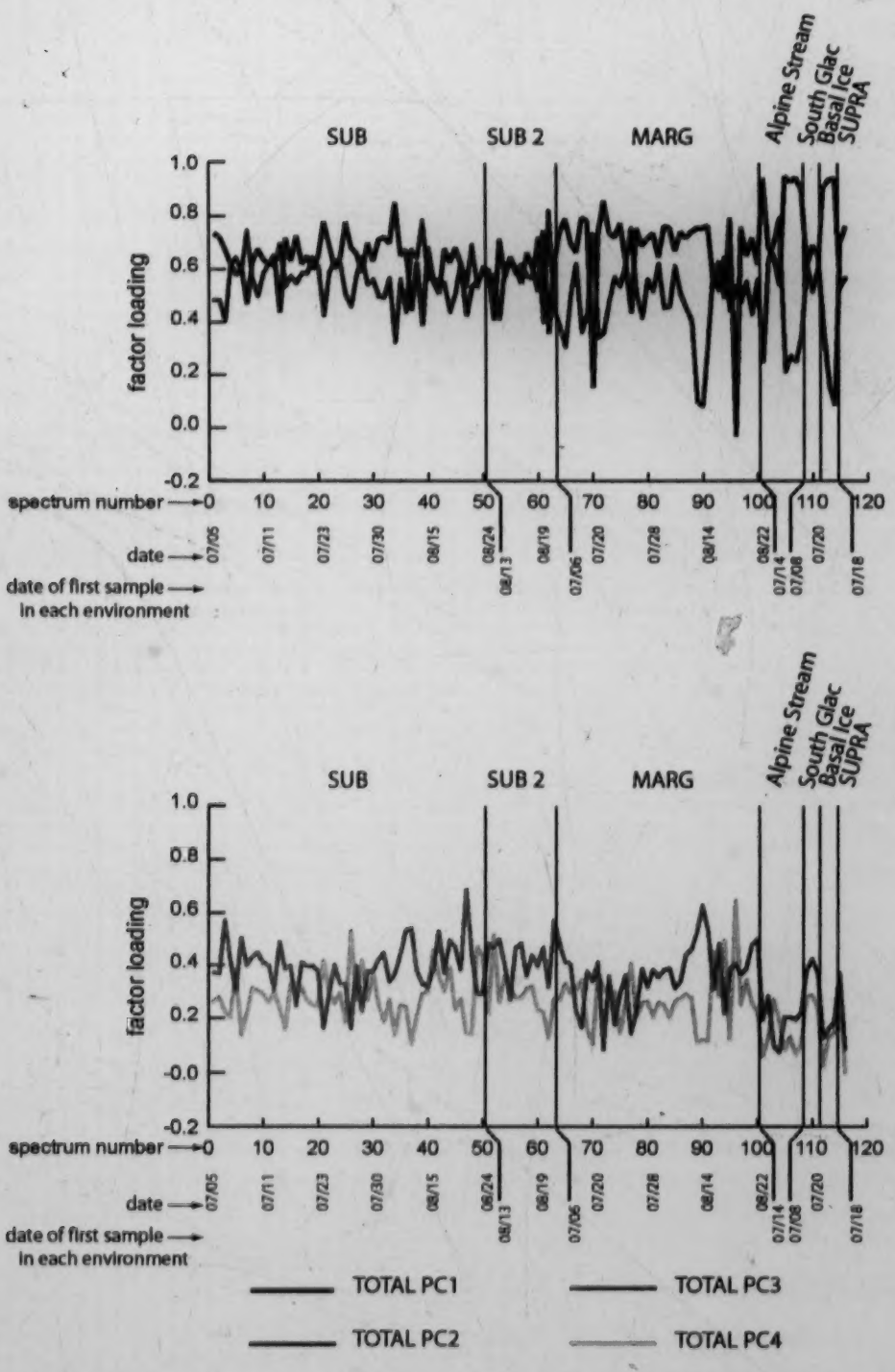

Fig. 3.7.: TOTAL PC factor loadings. The spectra are arranged chronologically within each environment.

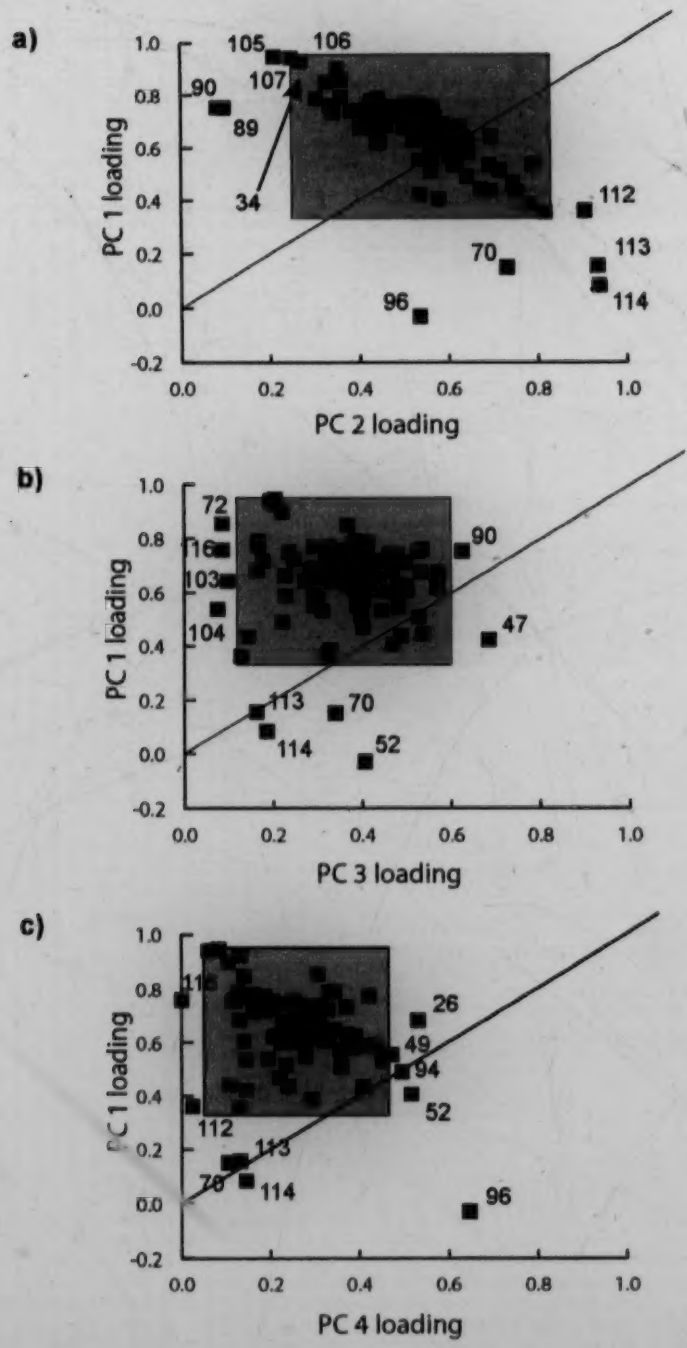

Fig. 3.8.: Synchronous spectra loading on a) TOTAL PC2, b) TOTAL PC3, c) TOTAL PC4 relative to TOTAL PC 1. The grey box indicates two standard deviations from the mean on each loading.

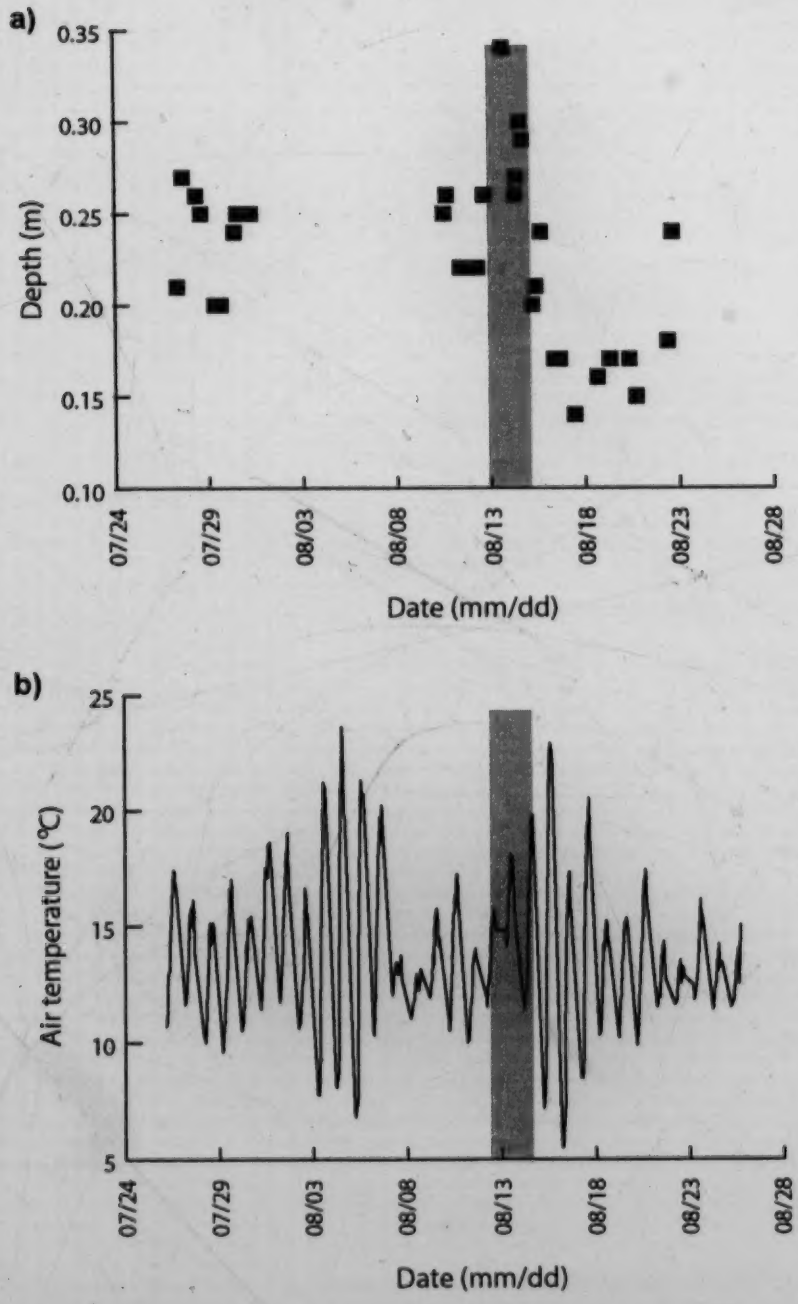

Fig. 3.9.: a) a plot of the manually recorded water depth at a fixed point in the proglacial stream channel; b) the air temperature record at Stewart, B.C., which is located at sea level ~30 km from Outre Glacier. The shaded area indicates the period of time when the TOTAL PC loadings shift in the subglacial and marginal streams. Note that the shift corresponds with a period of anomalously high daily minimum temperatures.

TABLE 3.1: Fluorescence peak designation.

compound	peak wavelength (nm)	source
phenylalanine standard (EEM)	255-265	Yamashika and Tanoue, 2003
phenylalanine ($\Delta\lambda$ = 10nm)	263	Sikorska et al., 2004
tyrosine-like (EEM)	265-280	Yamashika and Tanoue, 2003
tyrosine standard (EEM)	270-275	Yamashika and Tanoue, 2003
monoaromatics ($\Delta\lambda$ = 25 nm)	270-300	Ferrari and Mingazzini, 1995
protein- and/or phenol-like ($\Delta\lambda$ = 20 nm)	275	Sierra et al., 2005
aromatic amono acids ($\Delta\lambda$ = 18 nm)	280	Peuravuori et al., 2002
tyrosine ($\Delta\lambda$ = 10 nm)	283	Sikorska et al., 2004
tyrosine-like (EEM)	275	Coble, 1996
tryptophan-like (EEM)	275	Coble, 1996
tryptophan-like (EEM)	275-285	Yamashika and Tanoue, 2003
tyrosine ($\Delta\lambda$ = 25 nm)	277	Ferrari and Mingazzini, 1995
tryptophan standard (EEM)	280	Yamashika and Tanoue, 2003
tryptophan ($\Delta\lambda$ = 10 nm)	296	Sikorska et al., 2004
tryptophan ($\Delta\lambda$ = 25 nm)	291	Ferrari and Mingazzini, 1995
marine humic (EEM)	300-330	Yamashika and Tanoue, 2003
protein-like ($\Delta\lambda$ = 18 nm)	307	Lombardi and Jardim, 1999
2 condensed ring systems ($\Delta\lambda$ = 25 nm)	310-370	Ferrari and Mingazzini, 1995
marine humic-like (EEM)	312	Coble, 1996
fulvic acid (soil extract) (EEM)	315	Yamashika and Tanoue, 2003
soil fulvic acid ($\Delta\lambda$ = 18 nm)	317	Lombardi and Jardim, 1999
naphthalene ($\Delta\lambda$ = 18 nm)	330	Peuravuori et al., 2002
humic-like (EEM)	350	Coble, 1996
humic (EEM)	350-365	Yamashika and Tanoue, 2003
fulvic acid ($\Delta\lambda$ = 18 nm)	357-457	Miano and Senesi, 1992
marine DOM ($\Delta\lambda$ = 18 nm)	352	Lombardi and Jardim, 1999
polycyclic aromatics (4 benzene) ($\Delta\lambda$ = 18 nm)	355	Peuravuori et al., 2002
fulvic acid ($\Delta\lambda$ = 25 nm)	370-400	Ferrari and Mingazzini, 1995
Suwannee River fulvic acid (standard) ($\Delta\lambda$ = 20 nm)	400	Chen et al., 2003
polycyclic aromatics (5 benzene) ($\Delta\lambda$ = 18 nm)	400	Peuravuori et al., 2002
fulvic acid ($\Delta\lambda$ = 18 nm)	400-520	Miano et al., 1988
humic acid ($\Delta\lambda$ = 18 nm)	405-495	Miano and Senesi, 1992
polycyclic aromatics (7 benzene) ($\Delta\lambda$= 18 nm)	460	Peuravuori et al., 2002
lignin descriptors ($\Delta\lambda$ = 18 nm)	460	Peuravuori et al., 2002
humic acid ($\Delta\lambda$ = 20 nm)	470	Chen et al., 2003
humic acid ($\Delta\lambda$ = 25 nm)	470 and above	Ferrari and Mingazzini, 1995
humic acid ($\Delta\lambda$ = 18 nm)	475-480	Miano et al., 1988
humic acid standard ($\Delta\lambda$ = 25 nm)	475	Ferrari and Mingazzini, 1995
soil fulvic acid ($\Delta\lambda$ = 18 nm)	486	Lombardi and Jardim, 1999
phycoerithine (algal pigment) ($\Delta\lambda$ = 18 nm)	566	Lombardi and Jardim, 1999

TABLE 3.2: Correlation matrix for PC scores.

	TOTAL PC1	TOTAL PC2	TOTAL PC3	TOTAL PC4	SUB	SUB2	SUBGLACIAL PC1	SUBGLACIAL PC2	MARG PC1	MARG PC2	Alpine Stream	South Glacier	BASAL
TOTAL PC1	1	0	0	0	0.65	0.60	0.92	-0.70	0.91	-0.06	0.86	0.65	0.20
TOTAL PC2		1	0	0	0.58	0.59	0.02	0.85	0.04	0.84	0.44	0.58	0.95
TOTAL PC3			1	0	0.40	0.44	0.11	0.48	0.40	0.08	0.20	0.40	0.16
TOTAL PC4				1	0.29	0.30	0.34	0.05	0.02	0.48	0.14	0.27	0.10
SUB					1	1	0.75	0.66	0.78	0.62	0.93	1	0.78
SUB2						1	0.71	0.70	0.76	0.64	0.91	1	0.79
SUBGLACIAL PC1							1	0	0.88	0.15	0.87	0.75	0.27
SUBGLACIAL PC2								1	0.19	0.76	0.42	0.66	0.86
MARG PC1									1	0	0.88	0.78	0.29
MARG PC2										1	0.41	0.61	0.86
Alpine Stream											1	0.93	0.65
South Glacier												1	0.77
BASAL													1

TABLE 3.3: Proposed source of each PC.

Component	Source
TOTAL PC1	microbial
SUBGLACIAL PC1	
MARG PC1	
Alpine Stream	
South Glacier	
SUPRA average	
TOTAL PC2	soil-derived humic material
SUBGLACIAL PC2	
BASAL	
TOTAL PC3	poorly developed humic material
TOTAL PC4	

Chapter 4: An investigation of particulate and dissolved organic matter in basal ice.

4.1. Introduction.

Glaciers overrun organic matter (OM) in soil, sediment and vegetation during their advance and this may be incorporated during the formation of basal ice. Evidence for the presence of microbial communities and microbial activity in basal ice indicates that there is a microbial component to basal ice. For example Barker et al. (2006; Chapter 2) present evidence for recent microbial activity in the basal ice of an Antarctic glacier. Their conclusions are based on the presence of a fluorophore that is indicative of proteinaceous material in dissolved organic carbon (DOC) samples from basal ice samples at Victoria Upper Glacier (VUG), McMurdo Dry Valleys. Skidmore et al. (2000) cultured psychrophilic aerobic and anaerobic bacteria from basal ice at John Evans Glacier (JEG), Nunavut, Canada. Similarly, Bhatia et al. (2006) report evidence for the presence of bacterial communities that are unique to the subglacial environment in basal ice from JEG based on a terminal restriction fragment length polymorphism analysis of bacterial 16S rRna genes from samples taken in the subglacial, supraglacial and proglacial environments. A terrestrial OM component (that OM which is derived from overrun soil and plant matter) would also be expected to exist in the basal ice that has overrun terrestrially-derived OM due to the mechanisms by which basal ice is formed. Basal ice accretes subglacial material onto the glacier sole and differs from meteorically derived glacier ice because while glacier ice is a product of snow firnification, and exhibits many of the characteristics of the source snow (Knight, 1997), basal ice is formed by processes, and exhibits characteristics of, conditions at the bed (Knight, 1997; Hubbard and Sharp, 1989). Terrestrially-derived OM is generally thought to be less labile than microbially-derived OM (Repeta et al., 2002). OM lability is a result of its molecular structure and composition. The molecular characteristics of terrestrially-derived biopolymers tend to be more aromatic, relatively poor in alkoxyl carbon, less linear and less open in structure, and possess a higher C/N ratio than microbially-derived biopolymers (Repeta et al., 2002). Labile organic compounds are mineralized by heterotrophic microorganisms while less labile compounds are metabolized more slowly, or accumulate in the environment (Kaplan and Newbold, 2003).

Studies that characterize OM differentiate between dissolved OM (DOM) and particulate OM (POM) with DOM being that fraction which passes through a 0.7 μm glass fiber filter (GF/F) and POM being the filter retinate (e.g. Whitehead and Vernet, 2000, Wetzel and Likens, 1991). In

most aquatic systems, the majority of OM is in the dissolved phase (e.g. Findlay and Sinsabaugh, 2003, Dawson et al., 2002, McKnight et al., 1997) and DOM is likely to be the more significant form of OM for microbial metabolism because it may be directly available to microorganisms. POM typically requires extracellular enzymatic breakdown before it can be transferred across the microbial cell membrane (Arnosti et al., 2005). Consequently, POM represents a relatively unaltered form of OM and is more likely to resemble the organic parent material more than does DOM.

Little is known about OM in basal ice. Evidence for the presence of unique microbial populations and of recent microbial activity in basal ice indicates that there is a microbial component to basal ice OM. The purpose of this investigation is to describe the molecular characteristics of DOM and POM in basal ice from glaciers exhibiting potentially different types of organic parent material, with the goal of determining a) the relative contribution of microbial and terrestrial OM in basal ice and b) whether the OM source (terrestrial vs. microbial) is different for DOM and POM. To accomplish these goals, we use micro-Fourier Transform infrared spectroscopy (micro-FTIR) to describe the molecular characteristics of non-polar (e.g. fatty acids and lipids) compounds in POM and fluorescence spectroscopy to describe the molecular characteristics of DOM.

4.2. Field Sites.

Basal ice samples were collected from John Evans Glacier and Victoria Upper Glacier.

John Evans Glacier (79°49′N, 74°00′W) is a polythermal valley glacier located on the east coast of Ellesmere Island, Canada (Copland and Sharp, 2001). JEG overlies, and is surrounded by, carbonate bedrock and sediments and is situated in the high arctic biome (World Wildlife Fund, 2006) which is characterized by sparse low lying vascular plants (e.g. Dwarf Willow (*Salix herbacea*)) and moss). DNA from vascular plants (from the family Salicaceae and *Saxifraga spp.*) has been isolated from JEG basal ice samples that were obtained during this investigation (Willerslev et al., in review). This indicates that vascular plants have been entrained in the JEG basal ice. Outflow of subglacial meltwater from JEG is confined to the period between late June and early August, coincident with the penetration of supraglacial meltwater to the glacier bed via crevasses and moulins (Boon and Sharp, 2003). Basal ice sampling at JEG was conducted in early May, 2003, before the onset of supraglacial snowmelt.

Victoria Upper Glacier (VUG, 77°16′S, 161°29′E) is a cold-based valley glacier which overlies predominantly silicate sand and terminates adjacent to a permanently ice-covered proglacial lake (referred to here as Lake Upper Victoria). VUG is located in the Antarctic desert biome (World Wildlife Fund, 2006), which is devoid of vascular plants. Generally, the highest concentrations of OM in the McMurdo Dry Valleys are found in permanently ice-covered lakes that host algal communities (McKnight et al., 1991). The proximity of VUG to Lake Upper Victoria, and the existence of Victoria drift on the opposite side of Lake Upper Victoria from VUG, suggests that VUG may have overrun, and may currently overlie, sediment and algae derived from Glacial Lake Victoria or Lake Upper Victoria (e.g. Kelly et al., 2002, Hall et al., 2002).

4.3. Sampling and Methods.

4.3.1. Basal Ice Sampling.

4.3.1.1. JEG.

A tunnel was excavated a distance of 12 m into the JEG terminus in May, 2003. Ice samples were collected from roof to floor along 2 m high vertical sections on the tunnel wall at 10 m and 12 m from the entrance. A sterile chisel (ethanol bathed and flame sterilized) was used to remove 10 cm of ice from the surface of each 2 m section. The chisel was then re-sterilized and ice samples were chiseled at 20 cm intervals into an ethanol bathed and flame sterilized aluminum tray and transferred into sterile Whirlpak bags. All samples were stored frozen and in the dark.

Basal ice is typically sediment rich (Hubbard and Sharp, 1989), but there was little sediment in the ice exposed along the tunnel walls at JEG. To determine if this ice was basal ice formed by refreezing of subglacial water, as opposed to glacier ice, ice samples from the section at 10 m were analyzed for their hydrogen (δD) and oxygen ($\delta^{18}O$) stable isotope composition by mass spectrometry. Results are expressed relative to Standard Mean Oceanic Water (SMOW) using the δ notation (e.g. Faure and Mensing, 2005). A co-isotopic plot of δD vs. $\delta^{18}O$ was used to determine whether the ice along the JEG tunnel wall was formed from re-frozen meltwater (e.g. Jouzel and Souchez, 1982). Ice which is derived from the firnification of snow (glacier ice) will plot along a line with a slope of ~8 (local meteoric water line) resulting from the isotopic fractionation of water which occurs during condensation (Craig et al., 1963). However, basal ice will plot along a line with a lower slope (the freezing slope, Souchez and Jouzel (1984)) due to

kinetic isotopic effects that occur during refreezing. Ice from the tunnel at JEG plots along a line with a slope of 4.8 ($\delta D = 4.8\ \delta^{18}O - 75.5$ ($r^2 = 0.8$, $n = 19$)). This is less steep than the slope of the local meteoric water line ($\delta D = 8.2\ \delta^{18}O + 17.9$ ($r^2 = 0.9$, $n = 10$; Fig. 4.1)) that was determined by the isotopic analysis of snow samples from a longitudinal profile that extended from the terminus (100 m a.s.l.) to a location near the JEG ice divide (1520 m a.s.l.). The JEG basal ice freezing slope (4.8) is different from the theoretical freezing slope of 5.5, that would be expected in a closed system and 5.6, that would be expected in an open system using the δD and $\delta^{18}O$ values at the intersect of the two lines as the parent water (e.g. Souchez and Jouzel, 1984). This indicates that the ice along the tunnel walls at JEG does not conform to the Souchez and Jouzel (1984) model for basal ice formation. This suggests that the basal ice at JEG may have a complicated freezing history and that the isotopic composition of the parent water identified here is not an accurate representation of the actual water source. However, the ice along the tunnel walls at JEG is different from the meteoric water line and thus has experienced refreezing. Consequently, we consider it to be basal ice.

4.3.1.2. VUG.

Two vertical sections were excavated across the glacier ice/basal ice transition at the VUG terminus (~ 25 m above ground). This transition was easily identified because the basal ice is sediment-rich relative to the overlying glacier ice (Fig. 4.2). The basal ice at VUG is characterized by thin bands of sand-sized particles forming horizontal laminae. The first vertical section (Trench 1) was excavated, as outlined above for JEG, to a depth of 75 cm into the ice face while the second section (Trench 2) was excavated to a depth of 25 cm. Trench 2 was located 50 m to the south of Trench 1 and Trench 1 was located 1 m to the south of the trench that was excavated by Barker et al., (2006) (Chapter 2). Basal ice was sampled at 10 cm intervals from the basal ice contact to 300 cm below the basal ice contact in Trench 1 and at 50 cm intervals from the basal ice contact to 200 cm below the basal ice contact in Trench 2.

4.3.2. Sample Preparation and Analysis

4.3.2.1. Micro-FTIR.

All samples were transported frozen to the University of Alberta for preparation and analysis. No sample melting occurred during transport and the frozen samples were melted in the dark at room temperature. Meltwater leakage from several of the Whirlpak bags indicated that those bags had been punctured during transport. These samples are excluded from this study. Melted samples (150 ml) were filtered under vacuum through pre-combusted (480 °C for 8 hours) glass fiber filter papers (GF/F, 0.7 μm) using an acid washed (HCl) and combusted (480 °C for 8 hours) glass filtration unit. The filter paper was then removed from the filtration unit using sterile (autoclaved) forceps, then folded in half, placed in a sterile Whirlpak bag and frozen. The frozen filter papers were freeze-dried in reduced light to remove water from the sample. The presence of water causes a broad absorption at 3800-3000 cm^{-1} due to O-H stretching and 1750-1520 cm^{-1} due to O-H bending (Shriner et al., 2004) which potentially masks absorption bands that are indicative of organic functional groups that may be of interest (e.g. O-H stretch of alcohols, C=O stretch of esters, respectively). The freeze-dried filter papers were then weighed and cut in half using a sterile scalpel and each section was weighed. One half of the filter paper was used for micro-FTIR analysis while the other half was archived at the University of Alberta.

The freeze-dried filter paper was held at an angle (to direct solute runoff) with sterile forceps and approximately 2 ml of reagent grade dichloromethane (DCM) was dripped onto the filter paper surface to elute the POM. DCM was chosen for use as a solvent because it is polar aprotic and it does not have a carbonyl group that might appear in the FTIR spectra as an artifact. DCM is a common solvent that is used for the extraction of non-polar organics such as fatty acids (e.g. Staccioli et al., 1998). Lipids and/or fatty acids are ubiquitous in biological systems and their molecular structure reflects their source OM. For example, terrestrially-derived fatty acids (e.g. cholesterol) have a more aromatic structure than many bacterially-derived lipids, which are more aliphatic and display a greater degree of aliphtatic chain branching. The DCM that ran off of the filter paper was collected in a glass vial and evaporated under a filtered stream of air. Immediately prior to micro-FTIR analysis, approximately 1 ml of DCM was added to the glass vial and an aliquot was withdrawn with a DCM-washed capillary tube, placed on a NaCl disk and left to evaporate. The NaCl disk was then placed on the stage of a Thermo-Nicolet FTIR

spectrometer fitted with a Continuum infrared (IR) microscope and KBr beam splitter. The stage was purged with a continuous stream of dry nitrogen-oxygen mixed gas to maintain a stable atmosphere and limit the effect of atmospheric water vapour on the FTIR spectrum. OM was identified (using the IR microscope) as a "waxy" mass on the NaCl slide in the area where the DCM drop had evaporated (Fig. 4.3). Interferograms were acquired in transmission mode over the 4000-600 cm^{-1} range at a spectral resolution of 4 cm^{-1}. Two hundrede fifty interferograms were collected per spectrum to decrease signal noise and all spectra were baseline corrected by subtracting a blank spectrum. All spectra were normalized to the most intense absorption in each spectrum. Organic functional groups were assigned to spectral bands (Table 4.1) using references found in the literature (e.g. Silverstein and Webster, 1998). The assignment of absorbance bands to mineral species was not considered in the interpretation of the FTIR spectra because the use of the IR microscope permitted the visual targeting of OM and the exclusion of mineral particles from the interferogram acquisition.

FTIR spectra indicate the presence of functional groups as bands of absorbance. The presence of functional groups in an FTIR spectrum does not imply that they exist as a single molecule, but rather that they exist in the sample being analyzed. Thus, the specific functional groups that are identified here are discussed as components (moieties) of the bulk POM. FTIR spectra of OM from natural systems are difficult to interpret because of the abundance of absorbance bands, which are the result of potentially numerous organic functional groups in the sample. The fact that a single absorbance band may correspond to multiple molecular absorbencies complicates the interpretation further. To help mitigate these difficulties, where possible, corresponding bands are identified in the spectra. For example, an absorbance at 1600 cm^{-1} may be indicative of N-H bend, C-O stretch, C=O stretch and C=C stretch. However, a corresponding band at 900 cm^{-1} (N-H wag) would indicate that the band at 1600 cm^{-1} results from the N-H stretch (Table 4.1), which would be indicative of nitrogen-containing moieties (e.g. amides) in the sample.

4.3.2.2. Fluorescence Analysis.

The basal ice meltwater filtrate (above) for each sample was decanted into acid washed (HCl) and pre-combused (480 °C for 8 hours) amber glass vials and stored in the dark at 4°C until synchronous fluorescence analysis. Synchronous fluorescence spectra were obtained using

protocol described by Barker et al. (2006) (Chapter 2 and 3). Briefly, a SPEX Fluorolog-3 spectrofluorometer was used to obtain synchronous fluorescence scans. Scans were performed on basal ice meltwater at 1 nm increments with a 0.1 s integration period using a 10 nm bandwidth and an 18 nm offset ($\Delta\lambda$ = 18 nm) between monochromators. Water samples were allowed to warm to room temperature to eliminate temperature differences between samples. Samples were contained within a quartz glass cuvette with a 10 nm pathlength. All spectra were Raman corrected by subtracting the synchronous spectrum of deionized water derived under identical scanning conditions. All scans were dark corrected and internally corrected to compensate for variations in lamp performance. All of the synchronous spectra were smoothed using a centered 12 point running average and normalized to the highest peak within each individual spectrum. Fluorescence peak assignments were given according to published reports (e.g. Ferrari and Mingazinni, 1995).

4.4. Results and Interpretation.

4.4.1. Micro-FTIR.

Infrared absorbance is generated when energy is applied to a sample at infrared wavelengths. The infrared energy will be absorbed at frequencies that correlate to the vibration of specific chemical bonds within the molecule (Coates, 2000). The distribution of absorbance across the range of infrared energy that is applied to a sample (in this case 4000-600 cm^{-1}) is output as a spectrum, and absorbance bands are represented as peaks at the wavenumbers that energy absorbance occurs. Therefore, absorbance bands indicate the energy required to cause different types of molecular bond vibrations in a molecule. The identification of the absorbance bands in an FTIR spectrum provides information about the bond characteristics of the molecule and the functional groups that are present in the sample.

POM could be readily identified on the NaCl plates after elution with DCM (Fig. 4.3). Figure 4.4 shows the average FTIR spectrum of all the basal ice samples analyzed during this study. DCM absorbs at 3100 cm^{-1}, so the absence of absorption at this wave number in the FTIR spectra indicates that the solvent had evaporated and that the spectra result from the POM rather than from residual solvent. The average basal ice spectrum is characterized by several sharp and well

resolved bands and by multiple less resolved bands. This indicates spectral overlap between absorbance bands (e.g. in the 1274 cm^{-1} region), and suggests that the POM in the basal ice samples is composed of numerous functional groups. The most prominent absorption in the average basal ice spectrum occurs in the 3000-2800 cm^{-1} region and is characterized by strong absorbance bands at 2957 cm^{-1} (methyl C-H stretch), 2925 cm^{-1} and 2854 cm^{-1} (methylene C-H stretch) which are indicative of aliphatic molecular structure.

In addition to the 3000-2800 cm^{-1} absorption band, the average spectrum also displays less intense absorbance bands in the region 1750-700 cm^{-1}. The strongest absorbance bands in this region occur at 1729, 1462 and 1274 cm^{-1} (Fig. 4.4). The strong absorbance at 1729 cm^{-1} (C=O stretch) is indicative of relatively abundant ketone moieties, and in combination with the band at 1274 cm^{-1} (C-O stretch) indicates the presence of relatively abundant ester moieties in the basal ice POM. The band at 1462 cm^{-1} (C-H bend) corresponds to the strong absorption in the 3000-2800 cm^{-1} region, which is indicative of a strong aliphatic alkane component to the basal ice POM. Other minor absorption bands (fine structure) in the FTIR spectra are indicative of the presence of alkene, alkane, alcohol (polysaccharide (~1000 cm^{-1}, Chefetz et al., 1998)), ether and carboxylic acid moieties in the basal ice POM. The abundance of absorbance bands indicative of aliphatic structure, functional groups which are characterized by double-bonded oxygen (e.g. ketones, esters, carboxylic acids) and the lack of absorbance bands which would indicate an aromatic structure suggest that lipid or lipid-like compounds are present in the basal ice spectra and that these lipids may be microbially-derived (as opposed to vascular plant-derived; e.g. Melin et al., 2004, Tazaki et al., 1994). The overall spectral structure of the average micro-FTIR spectrum is similar to that reported by Tazaki et al. (1994) for fatty acids that were extracted from the interior of snow algae cells (*Chlamydomonas nivalis*).

As discussed above, the presence of multiple functional groups in an FTIR spectrum complicates its interpretation. As such, it is useful to use indices that target specific wave numbers to reveal structural information about the compound being investigated (e.g. Marshall et al., 2005, Lin and Ritz, 1993). The abundance of CH_2 relative to CH_3 decreases as the aliphatic chain branching increases and/or aliphatic chain length decreases, and previous investigations have used the ratio between ~2920 cm^{-1} and ~2955 cm^{-1} (CH_2/CH_3) in FTIR spectra as an indication of the degree of aliphatic chain branching and/or aliphatic chain length (Marshall et al., 2005, Lin and Ritz, 1993). The CH_2/CH_3 index has also been used to differentiate between sulphate and thiosulphate

reducing bacteria in cultures based on differences in acyl chain length or lipid content in the cell membrane (Melin et al., 2004) between different genera (e.g. Rubio et al., 2006).

Figure 4.5 shows the CH_2/CH_3 index for VUG and JEG basal ice FTIR spectra. VUG Trench 1 displays a CH_2/CH_3 index which ranges from 0.81 - 0.98 (average = 0.94, n = 22) and the CH_2/CH_3 in Trench 2 ranges from 0.92 - 0.96 (average = 0.94, n = 4). The CH_2/CH_3 at JEG varies between 0.91 - 0.95 (average = 0.93, n = 3) in the 10 m section and between 0.92 - 0.98 (average = 0.96, n = 6) in the 12 m section. The basal ice CH_2/CH_3 index at both JEG and VUG is similar to that reported for marine thiosulphate reducing bacteria (CH_2/CH_3 = 0.9, Rubio et al., 2006) and lower than that reported for olefinic acritarchs (CH_2/CH_3 = 1.9-2.5, Marshall et al., 2005) and algaenan-derived acritarchs (CH_2/CH_3 = 11.1, Marshall et al., 2005) and indicates a microbial origin for the DCM-extractable component of POM in both VUG and JEG.

The relatively strong absorbance intensity between 3000-2800 cm^{-1}, and the CH_2/CH_3 index values in basal ice at VUG and JEG indicate that the basal ice POM at both sites is highly aliphatic and similar to unaltered microbially-derived lipid compounds (with respect to aliphatic chain length and/or degree of aliphatic chain length branching), as opposed to aromatic in structure which would be expected with a vascular plant OM source. The similarity between VUG and JEG POM is unexpected given the difference in potential OM source (terrestrial vs. microbial) at each site. A more detailed examination of the FTIR spectra may provide an indication of differences in the DCM-extractable component of POM at VUG and JEG.

The micro-FTIR spectral composition changes through the basal ice profiles at VUG (Figs. 4.6, 4.7) and JEG (Figs. 4.8, 4.9). The most noticeable variation occurs in the 1000 cm^{-1} region, (e.g. Trench 1 200-210 cm vs. Trench 1 230-240 cm) which is indicative of the presence of polysaccharide moieties in the POM (Chefetz et al., 1998). Polysaccharide absorption occurs in both VUG and JEG FTIR spectra but is not ubiquitous in the basal ice POM at either site. The combination of sharp absorbance bands at 1729 cm^{-1} and ~3400 cm^{-1} are indicative of amides (e.g. Trench 1: 0-10 cm, 70-80 cm, 280-290 cm; Trench 2 100-150 cm) which appear to be more common in VUG POM spectra. The combination of strong absorption ~1500 cm^{-1} and broad absorption above 3125 cm^{-1} in the JEG 12 m 180-200 cm spectrum is indicative of aromatic moieties in the JEG POM in basal ice just above the glacier/bed interface. The JEG 12 m 180-200 cm sampling interval is the only spectrum to exhibit aromatic absorbance at either site.

4.4.2. Synchronous Fluorescence.

Figures 4.6 and 4.7 show the synchronous fluorescence spectra for VUG basal ice samples. The spectral composition of the synchronous spectra for VUG Trench 1 and Trench 2 samples are similar to those that were reported by Barker et al. (2006) (Chapter 2) for VUG basal ice. Similar to the FTIR spectra, the fluorescence spectra change through the profile. However, a peak at 276 nm is the most intense fluorescence peak in all of the spectra. Fluorescence at 276 nm is indicative of the presence of the amino acid tyrosine (Ferrari and Mingazzini, 1995) and is indicative of recent biological activity (De Souza Sierra et al., 1994). A secondary peak at 317 nm, which appears as a shoulder on the 276 nm peak and indicates the presence of two condensed ring systems (Ferrari and Minazzini, 1995), is also present in each basal ice synchronous spectrum. Relatively minor peaks at 370 nm, 417 nm and 526 nm indicate the presence of humic material in the basal ice (Ferrari and Mingazzini, 1995). Humic material is formed by abiotic secondary condensation reactions and is considered to be a terrestrial form of OM because it is highly aromatic and generally considered to be recalcitrant (Repeta et al., 2002).

Similarly, the synchronous spectra for JEG basal ice samples change through the 10 m and 12 m profiles, and the most intense fluorescence is associated with a fluorophore at 276 nm which is indicative of tyrosine and recent microbial activity. Similar to VUG basal ice spectra, a secondary peak at 317 nm is present in all samples as a shoulder on the 276 nm peak, and secondary peaks at 370 nm and 526 nm also appear sporadically. Interestingly, the fluorescence intensity of the humic material fluorophores in JEG DOM is less, relative to the tyrosine fluorophore, than is seen in VUG DOM. This suggests that the concentration of tyrosine in JEG basal ice is greater than in VUG basal ice, or that there is relatively less humic material in JEG basal ice than there is in VUG basal ice. JEG overlies sparsely distributed soils and vegetation, and there is a subglacial pool of terrestrial DOC at JEG (Barker et al., 2006) (Chapter 2). This suggests that the basal ice DOM at JEG should have a high abundance of fluorophores that are indicative of humic material, relative to VUG, and that the lack of fluorescence intensity of the humic material fluorophores at JEG, relative to the tyrosine fluorophore, is the result of high tyrosine concentrations in JEG basal ice DOM.

The tyrosine fluorophore at 276 nm in both JEG and VUG basal ice occurs in the absence of fluorophores that are indicative of humic material (370 nm, 417 nm, 526 nm) (e.g. JEG 12m 140-

160 cm, Trench 1 240-250 cm) which suggests that the presence of tyrosine is not derived from of overrun sediment but may indicate in situ biological production (Barker et al., 2006) (Chapter 2). If the biological production of amino acids occurs in basal ice, then a correlation between changes in the molecular characteristics of the DCM-extractable component of POM and the fluorescence characteristics of DOM might be expected as POM is degraded by active microbes. The absence of aromatic moieties in the basal ice FTIR spectra suggests that the DCM-extractable component is lipid-like in composition, exhibits significant polysaccharide moieties in some locations, and so may be a labile source of organic matter to microbes. There is no noticeable correlation between the changes in the structure of the synchronous spectra and the FTIR spectra at either site. This suggests that changes in the POM are occurring independently of changes in the DOM.

4.5. Discussion

Three general conclusions about OM in basal ice can be drawn from these results; 1) POM has a highly aliphatic component, 2) DOM in VUG and JEG basal ice is proteinaceous, 3) POM and DOM in VUG and JEG basal ice is similar.

1) *POM has a highly aliphatic component:*

The strong absorption between 3000-2800 cm^{-1} in all of the FTIR spectra collected during this investigation indicates that all of the POM contains abundant aliphatic moieties. A strongly absorbing feature at these wave numbers is not common in FTIR spectra of bulk OM from natural environments. Typically, FTIR investigations of OM composition in freshwater (e.g. Howe et al., 2002), soil (e.g. Kister and Pieri, 1996) and marine (e.g. Kovac et al., 2002) environments indicate a higher abundance of compounds such as ethers, amides, alcohols and/or polysaccharides, relative to methyl and methylene groups. A notable exception to this generalization is those investigations that examine the molecular structure of microbes (e.g. Kansiz et al., 1999) and kerogen (e.g. Derenne et al., 1992). The aliphatic characteristics of FTIR spectra from both microbial samples and marine kerogen and coal macerals are believed to be the result of organic moieties inside the cell itself (e.g. Tazaki et al., 1994) or cell membrane (Melin et al., 2004; Derenne et al., 1992).

Algaenans are fatty acid-derived, nonhydrolyzable and highly aliphatic biomacromolecules that comprise the outer cell wall of some species of microalgae (Gelin et al., 1999). Cross polarization/magic angle sample ^{13}C nuclear magnetic resonance (CP/MAS ^{13}C-NMR) investigations have revealed that the molecular structure of algaenans reflects a tridimensional network that is comprised of ether-linked polymethylenic (up to 30) chains (de Leeuw and Largeau, 1993). This network contains ester and hydroxyl groups that are sterically protected from microbial and chemical degradation. The ester groups are generally only vulnerable to pyrolysis, which is why algaenans comprise a major component of marine kerogen. In algae, the trilaminar sheath that characterizes algaenan structure is thought to provide protection against fungal parasitism (Honegger and Brunner, 1981) and/or desiccation (Good and Chapman, 1978).

Another class of highly aliphatic molecules that is found in environmental samples is lipids (Moran and Hodson, 1994). Lipids are water-insoluble and are major components of cells and cell membranes. Lipids are typically comprised of long chain fatty acid moieties that are bound to glycerol through ester linkages (Moran et al., 1994). In contrast to the trilayer observed in algaenans, lipids form a bilayer to form the biological membrane. Proteins are often embedded within, or attached to these bilayers (Moran et al., 1994).

The high aliphaticity of the OM in this investigation may be the result of two possible artifacts. The first artifact may arise from the melting of ice samples in Whirlpak bags. Previous investigations report the leaching of phthalate into liquid samples as "plasticizers" leach from plastic tubing and containers and increase absorption in the 3000-2800 cm^{-1} region (e.g. Lumsdon and Fraser, 2005). The polyethylene Whirlpak bags that were used in this investigation may contain plasticizers as phthalate, and it is possible that some phthalate leached from the bags into the meltwater during sample melting. To test for the influence of phthalate leaching during sample melting, a Whirlpak bag was filled with deionized and UV sterilized water, left to incubate with the melting samples, and processed as a procedural blank. No OM was eluted from the blank sample with DCM, which suggests that the effect of phthalate leaching on the overall structure of the FTIR spectra of the samples in this study is negligible. The second possible artifact may result from the use of DCM as a solvent to elute the OM from the filter paper. DCM is a polar aprotic solvent and was chosen so that non-polar organic substances, such as fatty acids, would be eluted for examination. It was thought that an examination of these types of substances would accentuate the difference between potential source OM (e.g. cutin in vascular plants vs. fatty acids in algae) in basal ice, thus permitting the assessment of the importance of source OM to the overall POM. While this artifact will under-represent the non-aliphatic components of the

bulk OM in the samples, the structure of the FTIR spectra presented here reflects substances that comprise the POM and that are present in the samples. Variation in the DCM-extracted POM represents variation in a component of the POM and permits OM inter-comparison between field sites and sub-environments at each site.

Even though the degree of aliphaticity in the FTIR spectra in this investigation may be influenced by the use of DCM as a solvent, the fact that the characteristics of absorption between 3000-2800 cm^{-1} (CH_2/CH_3) change between samples suggests that the aliphatic character of POM changes. The combination of a highly aliphatic component to the FTIR spectra, and the ubiquitous presence of ester and ketone moieties suggests that the material that was isolated in the samples during this investigation may be algaenan- or lipid-like in structure and composition. While algaenans are produced by specific classes of microalgae (e.g. Versteegh and Blokker, 2004), lipids are produced ubiquitously. As such there is a greater probability that the compounds identified here are lipid-like in structure and/or are derived from lipids. The fact that the FTIR spectra from different environments with different source material are similar with respect to their aliphatic character and abundance of ester, ketone and polysaccharide moieties supports the hypothesis that the DCM extraction has yielded lipid-like compounds and that these compounds exist in basal ice at both sites and the similarity between the CH_2/CH_3 index values reported here and those reported for microbes supports the hypothesis that the DCM-extractible POM at VUG and JEG is microbially-derived.

Bacteria are generally less than 0.7 μm in diameter and investigations that isolate bacteria from liquid use 0.2 μm membranes as a filter (e.g. Bhatia et al., 2006). Thus it seems unlikely that the microbially-derived POM that has been eluted from the GF/F filters (0.7 μm) is exclusively bacterial biomass. Instead it is possible that the observed microbially-derived DCM-extractable POM is comprised of extracellular polymeric substances (EPS) or bacterial biomass in EPS. EPS is the substance that "glues" microbial aggregates together. It is comprised of polysaccharides, proteins and lipids (Flemming et al., 2000) and is a major component of biofilms. The formation of biofilms permits microorganisms to remain stationary which is condusive to the formation of synergistic relationships because bacteria can live in close proximity inside a stable biofilm. DOC concentrations in basal ice are generally low relative to other aqueous environments (Barker et al., 2006, Chapter 2 and 3). The formation of synergistic relationships by microbes is advantageous in oligotrophic environments (Sylvia et al., 1999) because one microorganism may rely on another's metabolic byproduct as a nutrient source. Thus, the production of EPS to

facilitate the formation of synergistic relationships would be beneficial to microbes in basal ice. EPSs are larger than individual bacteria and can occur at lengths up to 5 μm, and so may be retained on the GF/F filters. Thus, it is possible that the DCM-extractable POM that is detected at JEG and VUG is lipid or lipid-like compounds, polysaccharides and proteins that is associated microbially-derived EPS and/or microbial biomass in EPS.

2) *DOM in VUG and JEG basal ice is proteinaceous:*

As reported by Barker et al. (2006) (Chapter 2), a fluorophore at 276 nm is present in basal ice synchronous spectra at VUG. Fluorescence at 276 nm is attributed to the amino acid tyrosine and its presence in the fluorescence spectra, regardless of the presence of fluorophores that are indicative of humic material, suggests that the amino acid is not a consequence OM incorporation from overrun soil, but may instead may indicate biological production within the basal ice (Barker et al., 2006) (Chapter 2).

The amino acid fluorophore is also a prominent feature in JEG basal ice synchronous spectra. Similar to VUG basal ice, the tyrosine fluorophore occurs independent of the presence of fluorophores which are indicative of humic material, which suggests that tyrosine production may be occurring within the basal ice.

3) *OM in VUG and JEG basal ice are similar:*

The micro-FTIR spectra from basal ice samples at JEG and VUG are similar. This is a surprising result given the difference in potential source material at JEG (terrestrial) and VUG (algae) and indicates a common source for POM in basal ice. The presence of vascular plants and soils at JEG would be expected to be reflected by the presence of aromatic moieties in JEG basal ice POM. The only basal ice sample that contained aromatic moieties was located at and immediately above the glacier/bed interface (JEG 12 m 180-200 cm; Fig. 4.9). The presence of aromatic moieties in the FTIR spectrum from this sampling interval suggests that either terrestrial POM is heterogeneously distributed and was sampled by chance, or that terrestrial POM has been degraded in the overlying basal ice and only microbially-derived OM exists. The heterogeneity in the fine structure of basal ice FTIR spectra at JEG suggests that the molecular characteristics of POM varies spatially. This line of evidence supports the hypothesis of a heterogeneous distribution of terrestrial POM and that the sampling resolution was insufficient to detect terrestrial moieties in the overlying basal ice. However, of note is that even in the JEG 12 m 180-200 cm spectrum, the overall characteristic of the POM was indicative of microbially produced

lipid and lipid-like moieties and the aromatic moiety was a relatively minor feature in the spectrum. Thus the microbially-derived POM appears to be ubiquitous while the terrestrially-derived POM appears to be heterogeneously distributed.

As was observed in the POM FTIR spectra, the synchronous spectra of DOM samples from JEG and VUG are similar in spectral composition. The ubiquitous presence of a fluorophore that indicates the presence of tyrosine suggests a common microbially-derived DOM source in basal ice environments. No evidence for a relationship between changes in the FTIR spectra and the fluorescence spectra was observed. This suggests that the DOM pool and the POM pool are biogeochemically separate. However, the synchronous fluorescence and FTIR techniques employed here likely only characterize a fraction of the bulk OM in basal ice (fluorescing compounds and DCM-extractable compounds, respectively). It is possible that a correlation between changes in the DOM and POM, which might be indicative of in situ biogeochemical activity linking the DOM and POM pools, could be detected by characterizing a larger fraction of the basal ice OM.

4.6. Summary and Conclusions.

Basal ice was collected from two polar glacier systems that are characterized by potential OM sources which exhibit different molecular characteristics. The vegetation at the JEG site includes vascular plants which contain a high abundance of lignin and cellulose, relative to non-vascular plants and microbes, and evidence for the incorporation of plant-derived OM into JEG basal ice is indicated by DNA analysis of basal ice samples obtained during this study (Willerslev et al., in review). The McMurdo Dry Valleys are largely devoid of vegetation due to the cold and dry conditions. Where vegetation does exist, it consists largely of algal communities in lakes and streams and there is evidence that VUG overran, and may currently rest on lake sediment (e.g. Hall et al., 2002; Kelly et al., 2002). This difference in potential source material would be expected to be reflected in the molecular characteristics of OM which each glacier may have overrun during periods of advance. Incorporation of OM into the subglacial OM pool would be expected to be reflected by the molecular characteristics of POM and DOM in the basal ice.

The FTIR spectra indicate that the basal ice POM is strongly aliphatic, regardless of the glacier from which it is sampled. The use of DCM as a solvent for eluting POM from the GF/F filter papers discriminated for non-polar moieties such as lipids and lipid-like compounds which are present in plants and microorganisms. While the degree to which the DCM extract represents the bulk POM in the samples is unknown, changes in the molecular characteristics of the isolated POM permit the identification of the composition of the DCM-extractable component of POM in basal ice.

The DCM-extractible POM at VUG and JEG is similar. Although changes in the fine structure of the FTIR spectra occur within and between basal ice sampling locations, the overall structure of all of the FTIR spectra indicates the existence of microbially-derived lipid and polysaccharide-rich POM, possibly associated with EPS. The production of EPS, as it relates to biofilm formation, is common in soils and aquatic environments and provides an ecological advantage for microbes in oligotrophic systems (such as basal ice) by facilitating the formation of synergistic relationships between microbes. Aromatic moieties, possibly resulting from terrestrially-derived POM, were detected in the sampling interval above the glacier/bed interface at JEG. This suggests that while there is a ubiquitous microbially-derived component to OM in basal ice, that is common to basal ice environments regardless of the characteristics of the potential source OM. Source OM may also be incorporated into basal ice but its distribution is heterogeneous.

Similarly, the ubiquitous presence of the tyrosine fluorophore in basal ice at JEG and VUG infers that a common microbial process influences the composition of basal ice DOM regardless of the characteristics of the potential source organic material.

While EPS itself is not considered to be a labile substrate for microbial metabolism (Sutherland et al., 1999), the lipids, proteins and microbial biomass that is associated with EPS are labile (Repeta et al., 2002). Likewise, the tyrosine component in basal ice DOM is also considered to be labile (De Souza Sierra, 1994). Thus, regardless of the quality of potential source organic material, basal ice contains a common labile OM, both in the dissolved phase and the particulate phase, that could serve as a metabolic substrate for microbes in basal ice or in downstream aquatic environments following basal ice melt.

4.7. References.

Arnosti, C., Durkin, S., Jeffrey, W.H., 2005. Patterns of extracellular enzyme activities among pelagic marine microbial communities: implications for cycling of dissolved organic carbon. *Aquatic Microbial Ecology* 38(2): 135-145.

Barker, J.D., Sharp, M.J., Fitzsimons, S.J., Turner, R.J., 2006. Abundance and dynamics of dissolved organic carbon in glacier systems. *Arctic, Antarctic and Alpine Research* 38(2): 163-172.

Bhatia, M., Sharp, M., Foght, J., 2006. Distinct bacterial communities exist beneath a high Arctic polythermal glacier. *Applied and Environmental Microbiology* 72(9): 5838-5845.

Boon, S., Sharp, M., 2003. The role of hydrologically-driven ice fracture in drainage system evolution of an Arctic glacier. *Geophysical Research Letters* 30(18): 1916.

Chefetz, B., Hadar, Y., Chen, T., 1998. Dissolved organic carbon fractions formed during composting of municipal solid waste: properties and significance. *Acta Hydrochimica Hydrobiologica* 26(3): 172-179.

Coates, J. 2000. Interpretation of infrared spectra, a practical approach. In Meyers, R.A. (ed). Encyclopedia of Analytical Chemistry. John Wiley and Sons, Chichester: 1-23.

Copland, L., Sharp, M., 2001. Mapping thermal and hydrological conditions beneath a polythermal glacier with radio-echo sounding. *Journal of Glaciology* 47(157): 232-242.

Craig, H., Gordon, L.I., Horibe, Y., 1963. Isotopic exchange effects in the evaporation of water. *Journal of Geophysical Research* 68(: 5079-5087.

Dawson, J.J.C., Billett, M.F., Neal, C., Hill, S., 2002. A comparison of particulate, dissolved and gaseous carbon in two contrasting upland streams in the UK. *Journal of Hydrology* 257(1-4): 226-246.

de Leeuw, J.W., Largeau, C., 1993. A review of macromolecular organic compounds that comprise living organisms and their role in kerogen, coal, and petroleum formation. In: Engel, M.H., Macko, S.A. (Eds.), Organic Geochemistry. Plenum Press, New York, pp. 23-72.

De Souza Sierra, M.M., O.F.X. Donard, M. Lamotte, C. Belin and M. Ewald. 1994. Fluorescence spectroscopy of coastal and marine waters. *Marine Chemistry* 47(2): 127-144.

Derenne, S., Le Berre, F., Largeau, C., Hatcher, P., Connan, J., Raynaud, J.F., 1992. Formation of ultralaminae in marine kerogens via selective preservation of thin resistant outer walls of microalgae. *Organic Geochemistry* 19(4-6): 345-350.

Faure, G., Mensing, T.M., 2005. Isotopes: principles and applications, 3rd Edition. John Wiley & Sons, New Jersey.

Ferrari, G.M., Mingazzini, M. 1995. Synchronous fluorescence spectra of dissolved organic matter (DOM) of algal origin in marine coastal waters. *Marine Ecology Progress Series* 125: 305-315.

Findlay, S.E.G., Sinsabaugh, R.L., 2003. Supply of dissolved organic matter to aquatic ecosystems: autochthonous sources. In: Findlay, S.E.G., Sinsabaugh, R.L. (Eds.), Aquatic Ecosystems: Interactivity of Dissolved Organic Matter. Academic Press, New York, pp. 1-24.

Flemming, H.-C., Wingender, J., Mayer, C., Korstgens, V., Borchard, W. 2000. Cohesiveness in biofilm matrix polymers. In Lappin-Scott, H.M., Gilbert, P., Wilson, M., Allison, D. (eds). Community Structure and Co-operation in Biofilms. Cambridge University Press, Cambridge: 87-105.

Gelin, F., Volkman, J.K., Largeay, C., Derenne, S., Sinninghe Damste, J.S., De Leeuw, J.W., 1999. Distribution of aliphatic, nonhydrolyzable biopolymers in marine microalgae. *Organic Geochemistry* 30(2-3): 147-159.

Good, B.H., Chapman, R.L., 1978. The ultrastructure of *Phycopeltis* (Chroolepidaceae: Chlorophyta). I. Sporopollenin in cell walls. *American Journal of Botany* 65(1): 27-33.

Hall, B.L., Denton, G.H., Overturf, B., Hendy, C.H. 2002. Glacial Lake Victoria, a high-level Antarctic lake inferred from lacustrine deposits in Victoria Valley. *Journal of Quaternary Science* 17(7): 697-706.

Honnegger, R., Brunner, U., 1981. Sporopollenin in the cell walls of *Coccomyxa* and *Myrmecia* phyobionts of various lichens: An ultrastructrual and chemical investigation. *Canadian Journal of Botany* 59(12): 2713-2734.

Howe, K.J., Ishida, K.P., Clark, M.M., 2002. Use of ATR/FTIR spectrometry to study fouling of microfiltration membranes by natural waters. *Desalination* 147(1-3): 251-255.

Hubbard, B., Sharp, M., 1989. Basal ice formation and deformation: a review. *Progress in Physical Geography* 13: 529-558.

Jouzel, J., Souchez, R.A., 1982. Melting-refreezing at the glacier sole and the isotopic composition of the ice. *Journal of Glaciology* 28(98): 35-42.

Kansiz, M., Heraud, P., Wood, B., Burden, F., Beardall, J., McNaughton, D., 1999. Fourier Transform Infrared microspectroscopy and chemometrics as a tool for the discrimination of cyanobacterial strains. *Phytochemistry* 52(3): 407-417.

Kaplan, A., Newbold, J.D., 2003. The role of monomers in stream ecosystem metabolism. In Findlay, S.E.G., Sinsabaugh, R.L. (eds). Aquatic Ecosystems: Interactivity of Dissolved Organic Matter. Academc Press, New York: 97-119.

Kelly, M.A., Denton, G.H., Hall, B.L., 2002. Late Cenozoic paleoenvironment in southern Vitoria Land, Antarctica, based on a polar glaciolacustrine deposit in western Victoria Valley. *Geological Society of America Bulletin* 114(5): 605-618.

Kister, J., Pieri, N., 1996. Effects of preheating and oxidation on two bituminous coals assessed by synchronous UV fluorescence and FTIR spectroscopy. *Energy and Fuels* 10: 948-957.

Knight, P.G. 1997. The basal ice layer of glaciers and ice sheets. *Quaternary Science Reviews* 16: 975-993.

Kovac, N., Bajt, O., Faganeli, J., Sket, B., Orel, B., 2002. Study of macroaggregate composition using FT-IR and ^{1}H-NMR spectroscopy. *Marine Chemistry* 78(2-3): 205-215.

Lin, R., Ritz, G.P., 1993. Studying individual macerals using i.r. microspectroscopy, and implications on oil versus gas/condensate proneness and "low rank" generation. *Organic Geochemistry* 20(6): 695-706.

Lumsdon, D.G., Fraser, A.R., 2005. Infrared spectroscopic evidence supporting heterogeneous site binding models for humic substances. *Environmental Science and Technology* 39(17): 6624-6631.

Mashall, C.P., Javaux, E.J., Knoll, A.H., Walter, M.R., 2005. Combined micro-Fourier transform infrared (FTIR) spectroscopy and micro-Raman spectroscopy of Proterozoic acritarchs: A new approach to Palaeobiology. *Precambrian Research* 138(3-4): 208-224.

McKnight, D.M., Aiken, G.R., Smith, R.L., 1991. Aquatic fulvic acids in microbially based ecosystems: Results from two desert lakes in Antarctica. *Limnology and Oceanography* 36(5): 998-1006.

McKnight, D.M., Harnish, R., Wershaw, R.L., Baron, J.S., Schiff, S., 1997. Chemical characteristics of particulate, colloidal, and dissolved organic material in Loch Vale Watershed, Rocky Mountain National Park. *Biogeochemistry* 36(1): 99-124.

Melin, A-M., Allery, A., Perromat, A., Bebear, C., Deleris, G., de Barbeyrac, B., 2004. Fourier transform infrared spectroscopy as a new tool for characterization of mollicutes. *Journal of Microbiological Methods* 56(1): 73-82.

Moran, M.A., Hodson, R.E., 1994. Dissolved humic substances of vascular plant origin in a coastal marine environment. *Limnology and Oceanography* 39(4): 762-771.

Moran, L.A., Scrimgeour, K.G., Horton, H.R., Ochs, R.S., Rawn, J.D., 1994. Biogeochemistry, 2nd Edition. Prentice Hall, New Jersey.

Repeta, D.J., Quan, T.M., Aluwihare, L.I., Accardi, A.-M. 2002. Chemical characterization of high molecular weight dissolved organic matter in fresh and marine waters. *Geochimica et Cosmochimica Acta* 66(: 955-962.

Rubio, C., Ott, C., Amiel, C., Dupont-Moral, I., Travert, J., Mariey, L., 2006. Sulfato/thiosulfato reducing bacteria characterization by FT-IR spectroscopy: a new approach to biocorrosion control. *Journal of Microbiological Methods*, 64(3): 287-296.

Shriner, R.L., Hermann, C.K.F., Morrill, T.C., Curtin, D.Y., Fuson, R.C., 2004. The Systematic Identification of Organic Compounds, 8 Edition. John Wiley & Sons, New Jersey.

Silverstein, R.M., Webster, F.X. 1998. Spectrometric Identification of Organic Compouds, 6 Edition. John Wiley & Sons, New Jersey.

Skidmore, M.L., Foght, J.M., Sharp, M., 2000. Microbial life beneath a high Arctic glacier. *Applied and Environmental Microbiology* 66(8): 3214-3220.

Souchez, R., Jouzel, J., 1984. On the isotopic composition in δD and $\delta^{18}O$ of water and ice during freezing. *Journal of Glaciology* 30(106): 369-372.

Staccioli, G., Sturaro, A., Parvoli, G. 1998. Investigation on the DCM extractives of Canadian Arctic fossil woods: the Resolute sample. *Wood Science and Technolog* 32(6): 375-380.

Sutherland, I.W. 1999. Polysaccharases for microbial exopolysaccharides. *Carbohydrate Polymers* 38(4): 319-328.

Sylvia, D.M., Fuhrnamm, J.J., Hartel, P.G., Zuberer, D.A., 1999. Principles and Applications of Soil Microbiology. Prentice Hall, New Jersey.

Tazaki, K., Fyfe, W.S., Iizumi, S., Sampel, Y., Watanabe, H., Goto, M., Miyake, Y., Noda, S. 1994. Clay aerosols and arctic ice algae. *Clay and Clay Minerals* 42: 402-408.

Versteegh, G.J.M., Blokker, P. 2004. Resistant macromolecules of extant and fossil microalgae. *Phycological Research* 52(4): 325-339.

Wetzel, R.G., Likens, G.E., 1991. Limnological Analysis, 2nd Edition. Springer Verlag, New York.

Whitehead, K., Vernet, M., 2000. Influence of mycosporine-like amino acids (MAAs) on UV absorption and dissolved organic matter in La Jolla Bay. *Limnology and Oceanography* 45(8): 1788-1796.

Willerslev, E., Cappellini, E., Boomsma, W., Nielsen, R., Hebsgaard, M.B., Brand, T.B., Hofreiter, M., Bunce, M., Poinar, H.N., Dahl-Jensen, D., Johnsen, S., Peder Steffensen, J., Benikke, O., Schwenninger, J-L., Nathan, R., Armitage, S., de Hoog, C.-J., Alfimov, V., Christl, M., Beer, J., Muscheler, R. Barker, J., Sharp, M., Penkman, K.E.H., Haile, J., Taberlet, Brochmann, C., P., Gilbert, M.T.P., Casoli, A., Campani, E., Collins, M.J., *in review*. Ancient biomolecules from deep ice cores reveal a forested southern Greenland more than 450 thousand years before present. *Science*.

World Wildlife Fund, 2006. http://worldwildlife.org/science/ecoregions/nearctic.cfm.

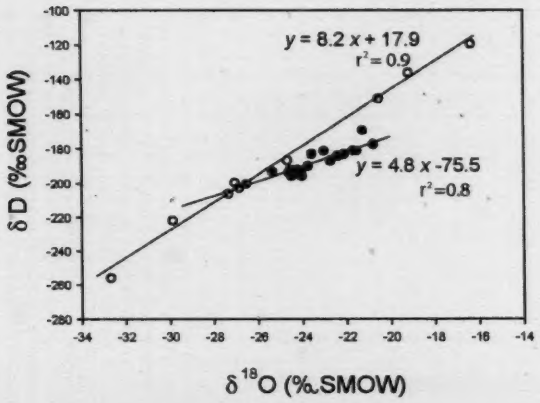

Fig. 4.1.: The co-isotope plot for JEG tunnel ice samples. The open circles are from supraglacial snow samples which are used to define the local meteoric water line and the closed circles are from tunnel wall ice samples.

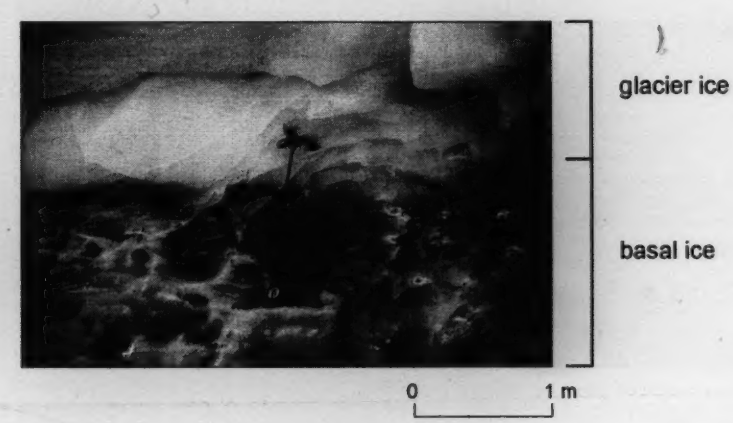

Fig. 4.2.: The glacier ice/basal ice transition at VUG Trench 1.

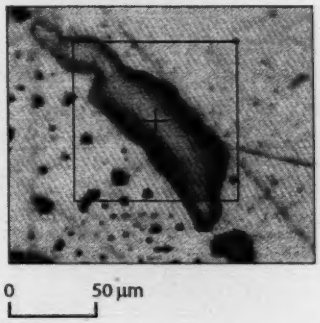

Fig. 4.3.: OM that has been eluted from the freeze-dried GF/F filter paper with DCM (JEG 10 m, 0-20 cm).

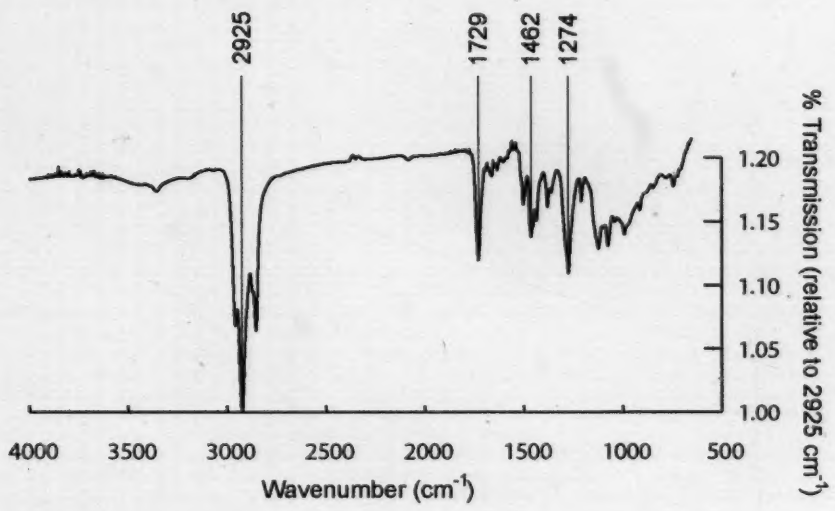

Fig. 4.4.: The average FTIR spectrum for all of the basal ice samples that were analyzed during this investigation. The absence of absorption at 3100 cm^{-1} in any of the spectra indicates that the DCM has evaporated completely.

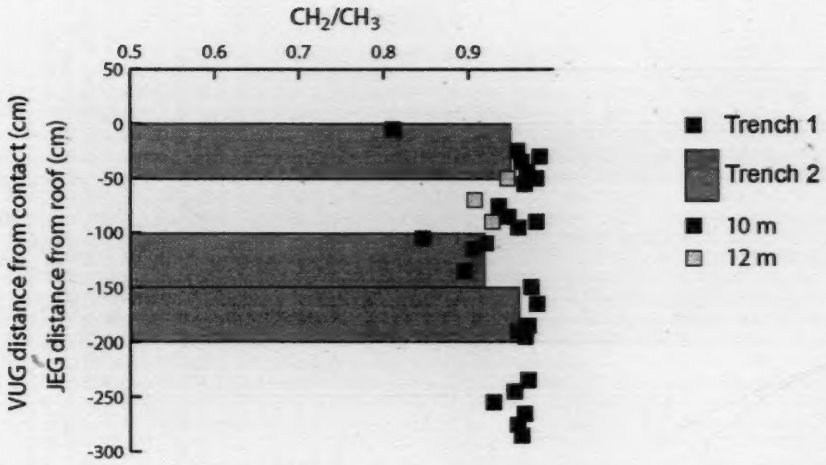

Fig. 4.5.: The CH_2/CH_3 ratio for VUG and JEG POM samples.

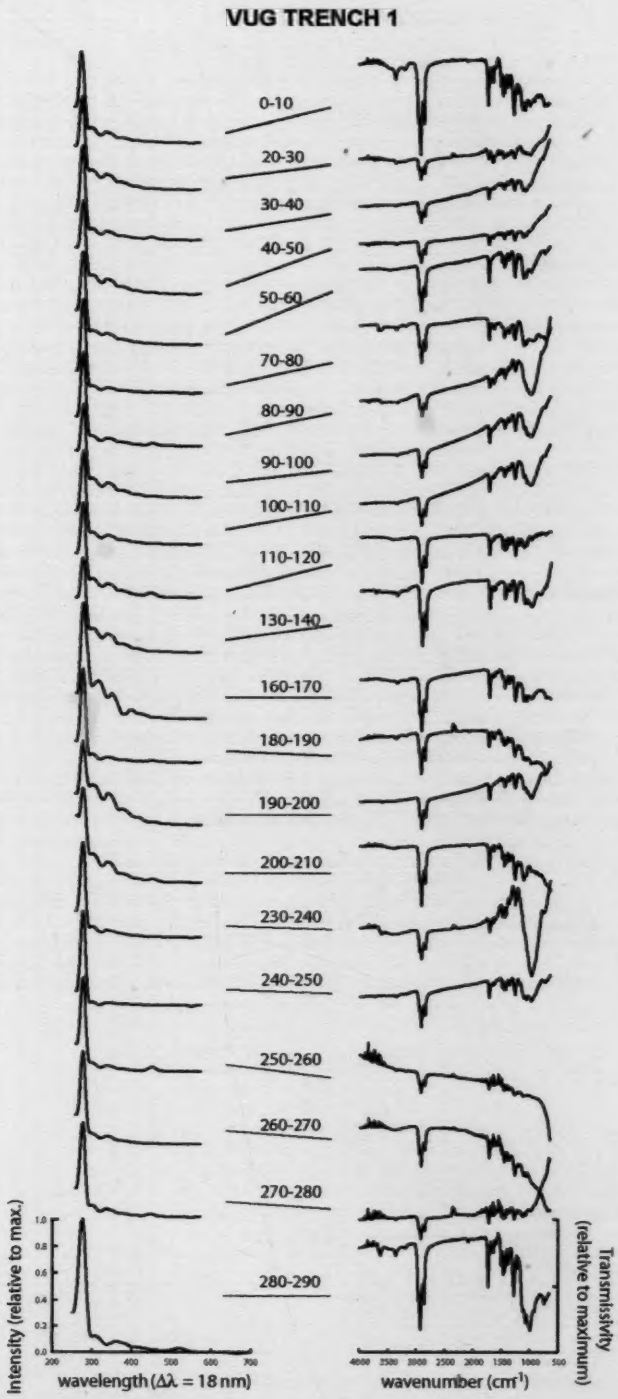

Fig. 4.6.: the synchronous spectra (left) and FTIR spectra (right) for basal ice samples from Trench 1 at VUG. Sample increment in centimeters below glacier ice/basal ice contact.

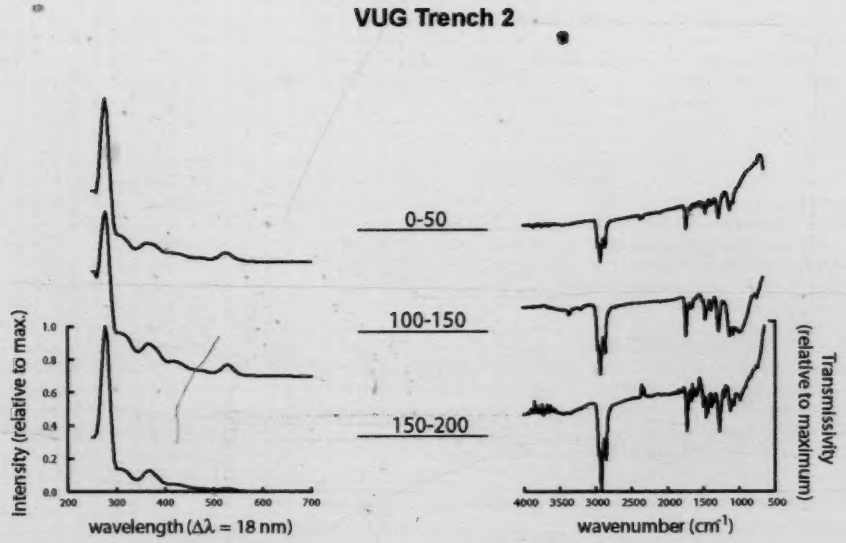

Fig. 4.7.: the synchronous spectra (left) and FTIR spectra (right) for basal ice samples from Trench 2 at VUG. Sample increment in centimeters below glacier ice/basal ice contact.

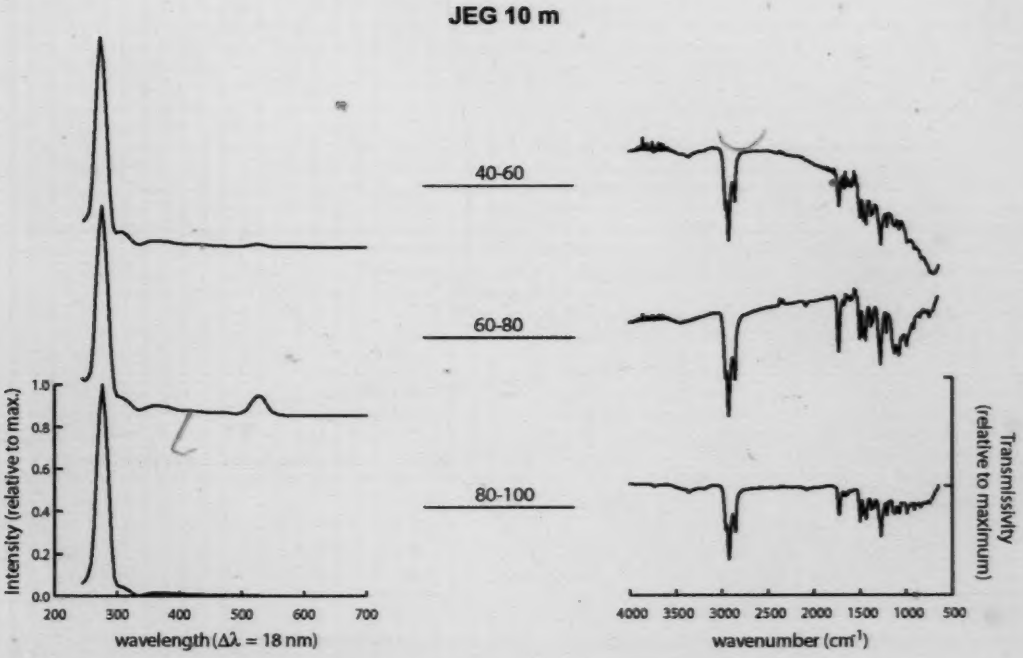

Fig. 4.8.: the synchronous spectra (left) and FTIR spectra (right) for basal ice samples from the 10 m section at JEG. Sample increment in centimeters below the tunnel roof.

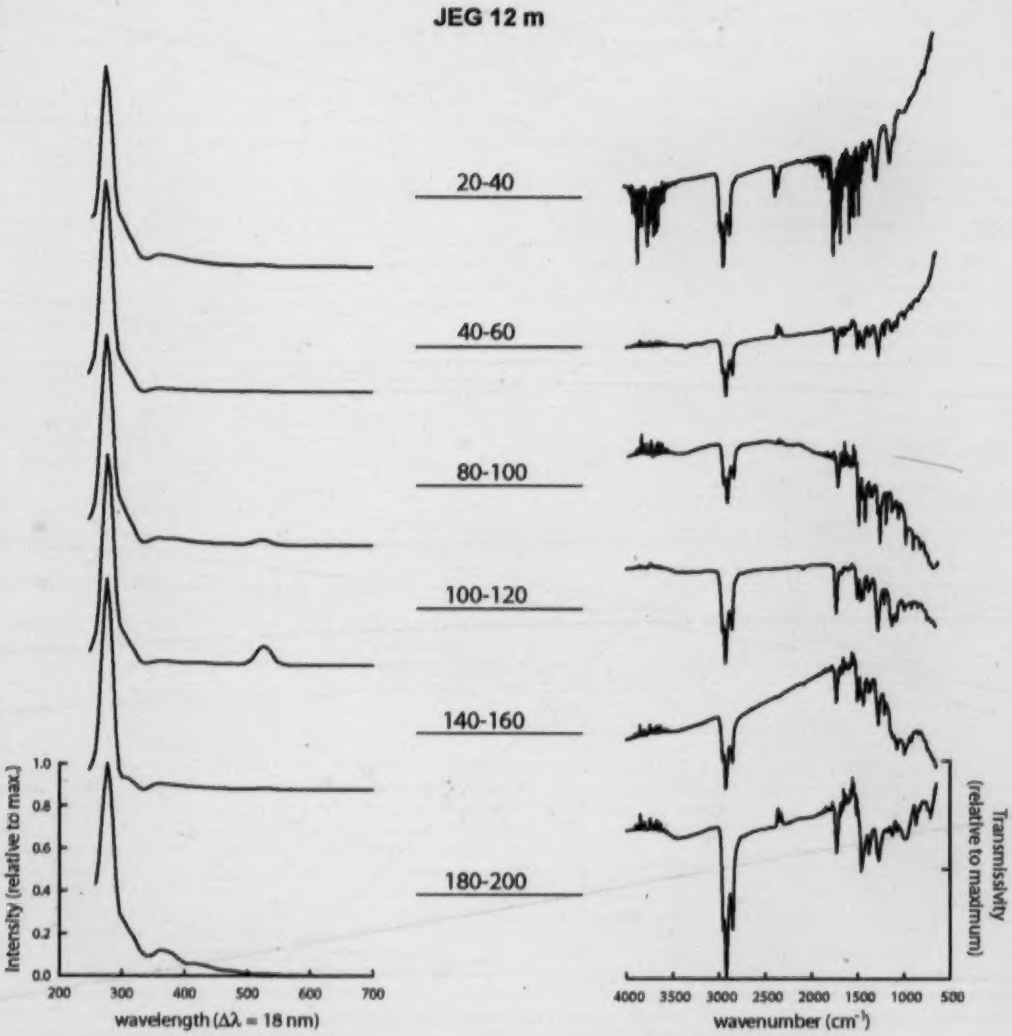

Fig. 4.9.: the synchronous spectra (left) and FTIR spectra (right) for basal ice samples from the 12 m section at JEG. Sample increment in centimeters below the tunnel roof.

Table 4.1. Absorbance band assignments (Shriner et al., 2004)

Functional Group	Corresponding Bands	Band Assignment
alkane	3000-2810	C-H stretch
	1480-1450	C-H bend
	1410-1370	C-H bend
	1220-770	C-H bend
alkene	3225-3000	=C-H stretch
	1670-1575	C=C stretch
	1120-775	=C-H bend
alcohol	4000-3110	O-H stretch
	1425-1325	O-H bend
	1255-1000	C-O stretch
amide	3520-3020	N-H stretch
	1650-1510	C-O stretch and N-H bend
	1425-1400	C-N stretch
	800-600	C-N stretch
amine	3650-3215	N-H stretch
	1675-1575	N-H bend
	1250-1010	C-N stretch
	920-600	N-H wag
benzene	3275-3125	≡C-H stretch
	2000-1425	C=C stretch (overtone)
	1210-1000	=C-H bend
	910-600	=C-H bend
carboxylic acid	3340-2510	O-H stretch
	1730-1600	C=O stretch
	1330-1140	O-H stretch
ester	1780-1700	C=O stretch
	1300-1000	C-O stretch
ether	1270-1000	C-O stretch
ketone	1870-1530	C=O stretch

Chapter 5: Synthesis and Discussion.

In the following sections, the major findings of this study are discussed within the context of the research goals that were outlined in the introduction.

5.1. OM abundance in glacier systems.

OM exists in detectable quantities in all of the glacier systems investigated here. While POC was not quantified micro-FTIR permitted the detection and characterization of the DCM-extractable component of the POC in basal ice from JEG and VUG.

5.1.1. Meltwater.

DOC was measured in subglacial meltwater at JEG and Outre Glacier. Subglacial DOC meltwater concentrations did not differ significantly from those in supraglacial meltwater. However, variations in supraglacial and subglacial meltwater DOC concentrations at JEG were not coupled, which suggests that the OM source for DOC in the supraglacial stream may be different than the OM source in the subglacial stream. The number of supraglacial samples collected at Outre Glacier was insufficient to characterize variability in supraglacial meltwater DOC concentrations. The lack of variability of the DOC concentration in Outre Glacier subglacial meltwater suggests that the subglacial drainage system is supplied with a consistent source of OM.

The mean DOC concentration in subglacial meltwater from both sites was low (JEG = 0.225 ppm, Outre = 0.1 ppm) compared to those reported for streams in arctic and alpine environments (2 ppm, Thurman; 1985, pg. 30). This result was not surprising for JEG meltwater because of the scarcity of organic source material at the JEG site. However, at the Outre Glacier site, which is located in a temperate rainforest ecosystem, subglacial meltwater concentrations were low, suggesting that there was no significant subglacial OM pool from overridden soils and vegetation, or that it was not accessed by the subglacial drainage system. The fact that Outre Glacier basal ice was found to have high DOC concentrations (relative to subglacial meltwater) and that the main subglacial meltwater stream was confined to a deeply incised N-channel at the terminus supports the latter hypothesis.

5.1.2. Ice.

DOC concentration varies spatially within glacier and basal ice at VUG. Bhatia et al. (2006) report a similar heterogeneity in the quantity of DOC in basal ice at JEG. The highest concentrations of DOC documented in this study occurred in basal ice, which suggests that OM is sequestered beneath glaciers and that basal ice represents a subglacial OM reservoir. The average DOC concentration in basal ice at Outre Glacier (0.303 ppm, n = 2) was higher than in supraglacial (0.188 ppm, n = 3) and subglacial (0.100, SD = 0.08, n = 72) meltwater, indicating that a subglacial pool of OM exists at Outre Glacier. At VUG, there was a zone of exceptionally high DOC concentration just above the basal glacier ice/basal ice interface. The DOC concentration of 46.66 ppm from 0-4 cm above the interface is higher than is reported in Dry Valley soils (0.3 mg C/gram soil; Barrett et al., 2005), and streams (1.4-5.6 ppm; Downes et al., 1986), and is within the range of concentrations that are reported for Dry Valley Lakes (0.6-63.8 ppm; Matsumoto, 1989). Excluding this zone of elevated DOC concentration, VUG basal ice DOC concentrations (mean = 2.91 ppm, SD = 0.63, n = 7) were more similar to Dry Valley stream and lake DOC concentrations than to soil concentrations, and similar to glacier ice DOC concentrations at VUG (mean = 3.05 ppm, SD = 1.09, n = 7). These results indicate that glaciers in the Dry Valleys may be significant reservoirs of OM. While the argument could be made that the DOC in VUG ice is derived from nearby Lake Upper Victoria and is thus atypical, the fact that several Dry Valley lakes are in close proximity to permanently ice covered lakes (e.g. Lake Fryxell, Lake Hoare, Lake Chad, Lake Bonney, Lake Brownsworth) suggests that the incorporation of lacustrine OM into basal ice may be common in the McMurdo Dry Valleys.

The finding that VUG glacier ice contains DOC suggests that glacier meltwater may be a source of OM to Dry Valley streams. Previous reports have attributed DOC in Dry Valley streams to autochthonous production by algal communities (McKnight and Tate, 1997) but the results reported here suggest that some OM may be glacially-derived and thus may have different characteristics from autochthonous algal-derived OM. As the Dry Valley climate continues to warm (Bomblies et al., 2001) and the export of glacier meltwater to Dry Valley streams and lakes increases, the release of OM from glacier systems to streams and lakes will also increase.

Prior to this study, the export of OM from glacier systems has not been considered. The results of this investigation show that detectable quantities of OM are exported from glacier systems in supraglacial and subglacial meltwater. Furthermore, this study shows that measurable quantities

of OM are sequestered in meteorically-derived glacier ice and basal ice. As glaciers melt, this OM will be released in glacier meltwater and exported to downstream aquatic ecosystems.

5.2. OM characteristics.

Generally, OM source influences the molecular characteristics of the DOM that was characterized at JEG, VUG and Outre Glacier. OM components which are indicative of microbially-derived DOM (e.g. tyrosine) and DOM which is derived from terrestrial sources (e.g. humic material) can be identified in bulk supraglacial and subglacial meltwater, glacier, and basal ice, and in stream flow from non-glacier-fed streams.

5.2.1. Meltwater.

OM in glacier meltwater has a significant microbial component. The presence of microbially-derived organic compounds (such as amino acids and proteins), as revealed by fluorescence analysis, in supraglacial meltwater at JEG and Outre Glacier suggests that microbial activity in the supraglacial snowpack and cryoconite holes produces DOC. This observation is similar to that reported by Lafreniere and Sharp (2004) that snow and/or ice melt exhibited "microbial" fluorescence characteristics. Microbially-derived DOC appears to be produced subglacially as well. Variations in the fluorescence characteristics of DOC at JEG indicate that pools of microbially produced OM, that are associated with the mobilization of meltwater with a long subglacial residence time (as indicated by high dissolved solute concentrations), are exported in subglacial meltwater.

Similarly, OM with characteristics that are indicative of a terrestrial organic source is also present in glacier meltwater. Terrestrial sources of OM include OM from terrestrial plants and soils that is characterized by the presence of vascular plant biopolymers and humic substances. Supraglacially, OM with terrestrial characteristics would be found in wind-blown sediment that is deposited on the glacier surface and that accumulates in cryoconite holes. Subglacially, OM with terrestrial characteristics is derived from overrun sediment, soils and vegetation. At JEG, supraglacial DOC did not display terrestrial characteristics, which is not surprising because of the sparse distribution of plants and developed soil in the surrounding environment. However, there is a pool of terrestrial OM in the subglacial environment, likely from overrun sediment and vegetation, which is exported to proglacial environments in subglacial meltwater as the subglacial

drainage system evolves from a predominantly distributed configuration to a channelized configuration (Bingham et al., 2005). At Outre Glacier, the majority of the subglacially exported DOM was microbially derived. However, occasional increases in the terrestrial component of DOM in subglacial meltwater, as indicated by the PCA of the synchronous fluorescence spectra of meltwater samples, occurred throughout the season. Similar to at JEG, this change of OM components in subglacial meltwater is the consequence of the seasonal development of the subglacial meltwater drainage system and the establishment of hydraulic connections between the main channels and the distributed system. The establishment of these hydraulic connections permits the flushing of a pool of subglacial OM, which exhibits terrestrial characteristics, into the bulk subglacial meltwater.

The molecular characteristics of DOM in glacier meltwater changes with time at both JEG and Outre Glacier. Interestingly, while the major fraction of DOM in rivers and lakes is derived from terrestrial sources (Stedmon et al., 2003, Repeta et al., 2002), a significant fraction of the total DOM exported in glacier meltwater is microbially-derived. Microbially-derived OM is generally considered to be more biologically labile than terrestrial OM. Microbial OM has a low C/N ratio (15-20), characteristically exhibits a more open and linear aliphatic molecular structure, and is rich in alkoxyl carbon. Conversely terrestrial OM has a high C/N ratio (40-50) and has a characteristically aromatic and highly condensed molecular structure (Repeta et al., 2002). At the initiation of subglacial meltwater discharge at JEG, the DOC displayed a microbial character. This suggests that the initial subglacial meltwater that emerges from JEG is the most labile to downstream communities. Over time, the terrestrial, and presumably more recalcitrant OM, becomes a more prominent fraction of the exported DOC. At Outre Glacier, microbially-derived, and presumably labile, DOM is the dominant fraction of subglacially exported OM early in the melt season, but the terrestrial DOM component becomes more prominent later in the season, following the establishment of a hydraulic connection between the subglacial distributed and channelized meltwater drainage systems. This trend is opposite to that reported by Lafreniere and Sharp (2004) where DOC in glacier meltwater from an alpine glacier was "terrestrial" at the beginning of the melt season and became more "microbial" as the melt season progressed. However, Lafreniere and Sharp (2004) did not sample meltwater at the glacier terminus, and snowmelt flushing from the surrounding soils early in the melt season may have contributed to the high terrestrial fluorescence signature of the DOM. Furthermore, their glacier meltwater sampling site was downstream from a lake, so the increased microbial signature in late season DOC may be influenced by lacustrine microbial activity and the production of microbially-

derived DOC. However, if Bow Glacier subglacial meltwater DOM is similar to Outre Glacier DOM, that is to say derived from supraglacial snow and icemelt, then Bow Glacier subglacial meltwater would be "microbial" in character.

A variation in the molecular characteristics of DOM is not uncommon in freshwater aquatic ecosystems. The flushing of terrestrial OM from leaf litter and soils into rivers in response to snowmelt and rainfall events is well documented (e.g. Boyer et al., 1997). While OM flushing from glacier systems in response to precipitation would also be expected to occur, due to snowpack flushing and increased water flux to the subglacial drainage system, OM flushing of different OM pools in response to melt events also occurs, as was documented at Outre Glacier. As such, a more consistent input of relatively labile (microbial) OM to aquatic ecosystems from subglacial and supraglacial sources in glacier fed streams relative to non-glacier fed streams would be anticipated.

5.2.2. Ice.

Both meteorically-derived glacier ice and basal ice contain a significant microbially-derived OM component at both JEG and VUG. The ubiquitous presence of the tyrosine fluorophore in JEG and VUG basal ice DOM, which is independent of fluorophores that are indicative of humic material, suggests recent microbial activity that is not a consequence of the incorporation of overrun sediment. With the exception of the ubiquitous tyrosine fluorescence, the spectrofluorometric analysis indicates that the molecular characteristics of DOC change spatially within glacier and basal ice. At VUG and JEG, basal ice spectra exhibited fluorophores that are associated with humic material whereas these fluorophores were less common in VUG glacier ice spectra. These humic fluorophores were interpreted as indicating the presence of humic material that was likely derived from overrun soil or sediment. The presence of the tyrosine-like fluorophore in the JEG and VUG DOM indicates that the DOM has a labile component which could represent a substrate for microbial metabolism in downstream ecosystems when the ice melts.

DOM in basal ice at Outre Glacier displayed fluorescence characteristics that were similar to those of DOM in seepage water flowing from a moss-covered alpine meadow in a nearby non-glacial catchment. This suggests that OM in overrun vegetation and soil had been incorporated, and is being sequestered in, Outre Glacier basal ice.

The micro-FTIR analysis of the DCM-extractable POM from JEG and VUG indicates the presence of a lipid-like component in the POM in basal ice from each site. Potential sources of OM at the VUG and JEG sites were expected to be different because of the presence of vascular plants and soils at JEG (and thus the presence of aromatic compounds) and the absence of both in Victoria Valley. The fact that no significant aromatic moieties were detected at each site suggests that the detected lipid-like component is microbially-derived. Furthermore, this microbially-derived POM was present in all of the basal ice samples that were taken. While the DCM extraction is biased towards extracting lipid-like compounds, the fact that the microbially-derived lipid exists ubiquitously suggests that there is a strong microbial component to basal ice POM.

5.3. Factors that influence the flux of OM exported from glacier systems to downstream aquatic environments.

Glacier hydrology and meltwater flow routing are the primary influences on the export of OM to downstream ecosystems. The hydrological characteristics of the glacier meltwater drainage system control the mobilization of different subglacial and supraglacial OM pools. At JEG, the first subglacial meltwater that is released at the beginning of the melt season is extremely solute-rich and exhibits a strongly microbial fluorescence signature. This water has likely experienced prolonged storage in a subglacial environment where subglacial microbial communities are active. As the melt season progresses and the subglacial drainage system evolves from a distributed to a more channelized configuration, terrestrially-derived DOC is exported. As the channelized system continues to develop, intermittent hydrological connections between the main conduit and the residual distributed system flush pools of subglacially stored meltwater, which has a microbial fluorescence signature, into the bulk subglacial flow.

At Outre Glacier, a large portion of the subglacial meltwater flow is likely confined to N-channels that have been incised into bedrock. Increased surface melt and the resultant increased flux of supraglacial meltwater to the subglacial channelized system cause a rise in channel hydraulic pressure and the establishment of a hydraulic connection between the channelized and distributed systems. As the hydraulic pressure gradient reverses with decreased supraglacial meltwater input and decreased channel flow, OM in subglacial meltwater from the distributed system flows into the channelized system and is detected in the bulk subglacial meltwater DOM.

Given the hydrologic control on the mobilization of glacier system OM, and existence of different OM pools within a single glacier system, prediction of the characteristics of the DOM exported from the glacier systems investigated here should be possible. For example, at JEG, the initial subglacial meltwater that emerges each year should be microbially-derived. Thus, to sample OM that is produced by subglacial microbes, the initial subglacial meltwater should be targeted. Likewise, at Outre Glacier, to obtain a sample that is representative of glacially overrun OM, subglacial meltwater should be sampled on the descending limb of the discharge hydrograph after the establishment of a hydraulic connection between the distributed and channelized hydraulic system.

5.4. Conclusions.

There are very few reports of the abundance and characteristics of organic carbon in glacier systems (e.g. Lafreniere and Sharp, 2004). Viable microbial populations have been identified in the supraglacial snowpack and cryoconite holes, subglacial meltwater, basal ice and accreted ice above subglacial lakes. Active microbial activity in glaciers has been inferred using geochemical approaches. If microbial populations are active in glacier systems, then they alter their metabolic substrates and create new metabolic products.

Organic matter plays an important ecological role in aquatic systems and glaciers are the source of water for many aquatic ecosystems. As stated in the Introduction 1) glaciers supply freshwater to major rivers globally, 2) viable subglacial heterotrophic microbial communities may produce, consume and or alter OM which is exported to downstream aquatic ecosystems, 3) increased glacier melt in response to global climate warming will increase the flux of glacier meltwater to downstream ecosystems, 4) the abundance and molecular characteristics of OM exert a fundamental influence on aquatic ecosystem processes. Thus there is a need to determine the abundance and characteristics of OM in, and released from, glacier systems.

This study demonstrates that there is OM in glacier systems that have different thermal and hydrological regimes and that have different potential sources of OM. OM that is exported from glaciers in subglacial meltwater may be different from that which is produced supraglacially which indicates that a subglacial pool of OM may exists beneath some glaciers in overrun sediment, soils and vegetation, isolated areas of the distributed subglacial meltwater drainage

system or in basal ice. Access and mobilization of these subglacial OM pools is controlled by the development of the subglacial drainage system over the course of the melt season.

Subglacially exported OM has both microbial and terrestrial characteristics which is influenced by OM source. Microbial OM is associated with microbial production in the supraglacial snowpack and cryoconite holes, subglacially routed supraglacial meltwater that does not mix with subglacial pools of "terrestrial" OM, and subglacial meltwater with long subglacial residence times. Terrestrial OM is associated with overrun sediment, soil and vegetation, and windblown sediment that accumulates in supraglacial cryoconite holes.

OM is also incorporated and sequestered in basal ice. The spatial distribution of OM in glacier and basal ice is heterogeneous and there is evidence for the in situ production of microbial OM in basal and meteorically derived glacier ice. Surprisingly, at JEG, the DCM-extractable POM was microbial in character and similar to the VUG POM extract suggesting a common and ubiquitous microbially-derived component to basal ice POM in glaciers. Microbial OM is generally considered to be more environmentally labile than terrestrial OM. The existence of microbial OM which is stored and exported from glacier systems suggests that labile organic compounds are exported in meltwater from glacier systems to downstream ecosystems.

5.4.1. Implications for global carbon cycling.

Concerns regarding global climate change have focused attention on arctic tundra ecosystems and their effect on global climate (e.g. Billings et al., 1982; Jones et al., 2000). Since the 1980s, an increase in tundra surface temperature has resulted in a thickening of the active layer which has resulted in an increase in the rate of soil organic matter decomposition. The annual rate of decomposition now exceeds the annual rate of primary production and tundra ecosystems in the northern hemisphere are a source of CO_2 to the atmosphere. The same observation has been reported in alpine taiga ecosystems (e.g. Welker et al., 1999). CO_2 is a greenhouse gas and a product of heterotrophic microbial metabolism. Thus the microbial heterotrophic metabolism of tundra and taiga soil OM is contributing to a positive feedback as soil microbial activity increases with increasing soil temperature and active layer thickening.

The same phenomenon occurs in aquatic ecosystems where increased concentrations of OM result in an increased rate of heterotrophic metabolism and an increased flux of CO_2 to the

atmosphere (Schlesinger, 1997). Until now, there was no evidence of a positive feedback to this cycle in aquatic systems. However, the export of labile OM from glacier systems to downstream aquatic environments may contribute to a positive feedback with the atmospheric CO_2 flux.

Results reported here indicate that OM that is produced, stored and exported from glacier systems has a microbially-derived component. OM export from glaciers is not simply the result of a mobilization of overrun OM in soils, sediment and vegetation by the subglacial drainage system to downstream ecosystems. The DOM that is exported in subglacial meltwater is predominantly autochthonous microbially-derived in some glaciers (Chapter 3). Microbially-derived OM is generally considered to be more labile than terrestrially-derived OM due to a relative lack of recalcitrant biopolymers, such as cellulose (Repeta et al., 2002). As such it is more easily metabolized by heterotrophic microorganisms to CO_2. Microbially-derived DOM and POM appear to occur ubiquitously in meteorically derived glacier ice and basal ice (Chapters 1 and 4), and subglacial meltwater DOC concentrations do not vary diurnally in the glacier systems investigated here (Chapters 2 and 3), and DOC concentration do not vary with discharge (e.g. Outre Glacier (Chapter 2)). This suggests that glacier systems are a consistent source of microbially-derived OM and that the flux of this OM would be expected to increase with increased meltwater flux due to climate warming.

Thus, the following feedback may exist: climate warming increases glacier melt and glacier meltwater discharge to downstream aquatic ecosystems. The flux of labile microbially-derived OM, from supraglacial snow and ice melt, to downstream aquatic ecosystems also increases with increased meltwater discharge. This increase in labile OM increases aquatic ecosystem respiration which increases the flux of CO_2 to the atmosphere. This increased CO_2 flux from glacier-fed aquatic systems contributes to the greenhouse effect exerted by increasing levels of atmospheric CO_2 which, in turn, contributes to climate warming and increased glacier melt. Currently, the flux of OM in glacier meltwater has not been quantified, nor has the downstream microbial mineralization of glacially-derived aquatic OM, so the importance of this feedback is unknown. However, the apparent ubiquity of labile OM that is produced, stored and exported from glacier systems and the fact that glaciers are melting at accelerating rates suggests that this potential CO_2 feedback will become progressively more significant in the future.

5.5. Directions for future research.

Glacier systems sequester and export OM which contains compounds which are considered to be labile and could be ecologically reactive in downstream aquatic ecosystems. However, how this exported OM reacts in downstream environments remains unknown. The biogeochemical processing of OM that is exported in glacier meltwater could have important consequences including metal and nutrient availability (e.g. Cabaniss, 1992). While fluorescence and FTIR spectroscopy proved to be useful techniques for characterizing portions of glacier system OM (e.g. fluorescing compounds in DOM, DCM-extractable compounds in POM), it is likely that a portion of the OM remains uncharacterized. For example, humic material and proteins typically represent a fraction of the total OM. The existence of the unidentified fluorescence peak in VUG basal ice (317 nm) supports the hypothesis that only a fraction of the DOM has been identified. Furthermore, polar compounds (e.g. polar proteins), were excluded from the POM characterization. Also, only analyzing POM in basal ice ignores the contribution of POM to the total OM that is exported from glacier systems (e.g. POM in snow and ice melt). A more rigorous characterization of OM in glacier systems would be useful for elucidating potential downstream biogeochemical processes. For example, the analysis of isolated DOM by ^{13}C-NMR ^{1}H-NMR (proton nuclear magnetic resonance) would provide a more comprehensive indication of the quantity and characteristics of compounds that are present in the sample (e.g. polysaccharides, lipid, humic material; Repeta et al 2002). Additionally the application of chemical extraction techniques, in combination with gas chromatography, could yield information about actual suitability of glacier system-derived OM for use as a substrate for downstream microbial metabolism (e.g. determination of carbohydrate content by acid hydrolysis and gas chromatography (Guggenberger et al., 1994)). Furthermore, the determination of factors such as OM redox potential would provide an indication of OM reactivity. Such analyses typically require a large sample. For example, ^{13}C-NMR requires ~5 g carbon to produce a reliable spectrum (Quideau, pers comm). For this study, logistical considerations precluded the collection and transport of large sample volumes. The development of techniques for filtering and concentrating the OM from large volumes of glacier meltwater on-site would help to obtain the sample concentrations necessary for more in depth analysis.

Furthermore, while the results of this investigation indicate the production of microbially-derived OM in basal ice, the biogeochemical processes responsible for this production, and the rates at which they occur remain unknown. Subglacial environments provide a Martian polar analogue

on Earth. The elucidation of englacial biogeochemical processes would be useful for identifying biomarkers which could then be targeted by investigations that seek evidence of biological activity on extraterrestrial icy planets. Additionally, if glacier system biomarkers are unique to subglacial biogeochemical OM cycling, which might be expected given the unique conditions that subglacial environments impose (e.g. lack of sunlight, stable temperature near 0 °C) then these biomarkers could be sought in ocean sediment to provide an estimate of the magnitude of glacier system biogeochemical OC cycling on glacier-interglacial timescales (e.g. Crowley, 1995).

Additionally, the characterization of OM in the supraglacial environment would be useful. This research focus would a) permit the characterization of supraglacially-derived OM that is input to the subglacial environment. By comparing the OM which is added to the subglacial pool to that which is output from the subglacial environment, the magnitude of subglacially-derived OM to the net OM flux may be possible, b) assess the importance of long-range atmospheric OM transport to glacier systems, c) assess the susceptibility of supraglacial organic matter to photodegratation and photopolymerization, relative to subglacially-exported OM, as it relates to environmental reactivity and bioavailability.

5.6. References.

Barrett, J.E., Virginia, R.A., Parsons, A.N., Wall, D.H. 2005. Potential soil organic matter turnover in Taylor Valley, Antarctica. *Arctic, Antarctic and Alpine Research* 37(1): 108-117.

Bhatia, M., Sharp, M., Foght, J., 2006. Distinct bacterial communities exist beneath a high Arctic polythermal glacier. *Applied and Environmental Microbiology* 72(9): 5838-5845.

Billings, W.D., Luken, J.O., Mortensen, D.A., Peterson, K.M. 1982. Artic tundra: a source or sink for atmospheric carbon dioxide in a changing environment. *Oecologia* 53(1): 7-11.

Bingham, R.G., Nienow, P.W., Sharp, M.J., Boon, S. 2005. Subglacial drainage processes at a High Arctic polythermal valley glacier. *Journal of Glaciology* 51(172): 15-24.

Bomblies, A., McKnight, D.M., Andrews, E.D. 2001. Retrospective simulation of lake-level rise in Lake Bonney based on recent 21-yr record: indication of recent climate change in the McMurdo Dry Valleys, Antarctica. *Journal of Paleolimnology* 25(4): 477-492.

Boyer, E.W., Hornberger, G.M., Bencala, K.E., McKnight, D.M. 1997. Response characteristics of DOC flushing in an alpine catchment. *Hydrological Processes* 11(12): 1635-1647.

Cabaniss, S.E. 1992. Synchronous fluorescence spectra of metal-fulvic acid complexes. *Environmental Science and Technology* 26(6): 1133-1139.

Crowley, T.J. 1995. Ice age terrestrial carbon changes revisited. *Global Biogeochemical Cycles* 9(3): 377-389.

Downes, M.T., Howard-Williams, C., Vincent, W.F. 1986. Sources of dissolved organic nitrogen, phosphorous and carbon in Antarctic streams. *Hydrobiologia* 134(3): 215-225.

Guggenberger, G., Zech, W., Schulten, H.-R. 1994. Formation and mobilization pathways of dissolved organic matter: evidence from chemical structural studies of organic matter fractions in acid forest floor solutions. *Organic Geochemistry* 21(1): 51-66.

Jones, M.H., Fahnestock, J.T., Stahl, P.D., Welker, J.M. 2000. A note on summer CO_2 flux, soil organic matter, and microbial biomass from different high arctic ecosystem types in northwestern Greenland. *Arctic, Antarctic and Alpine Research* 32(1): 104-106.

Lafreniere, M.J., Sharp, M.J. 2004. The concentration and fluorescence of dissolved organic carbon (DOC) in glacial and nonglacial catchments: interpreting hydrological flow routing and DOC sources. *Arctic, Antarctic and Alpine Research* 36(2): 156-165.

Matsumoto, G.I. 1989. Biogeochemical study of organic substances in Antarctic lakes. *Hydrobiologia* 172(1): 265-289.

McKnight, D.M., Tate, C.M. 1997. Canada stream: a glacial meltwater stream in Taylor Valley, South Victoria Land, Antarctica. *Journal of the North American Benthological Society* 16(1): 14-17.

Quideau, S. 2003. *personal communication.*

Repeta, D.J., Quan, T.M., Aluwihare, L.I., Accardi, A.-M. 2002. Chemical characterization of high molecular weight dissolved organic matter in fresh and marine waters. *Geochimica et Cosmochimica Acta* 66(6): 955-962.

Schlesinger, W.H. 1997. Biogeochemistry: an analysis of global change (2nd ed). Academic Press, London: 588 pp.

Stedmon, C.A., S. Markager and R. Bro. 2003. Tracing dissolved organic matter in aquatic environments using a new approach to fluorescence spectroscopy. *Marine Chemistry* 82(3-4): 239-254.

Thurman, E.M. 1985. Organic geochemistry of natural waters. Martinus Nijhoff/Dr W. Junk Publishers, Dordrecht: 497 pp.

Welker, J.M., Brown, K.B., Fahnestock, J.T. 1999. CO_2 flux in arctic and alpine dry tundra: comparative field responses under ambient and experimentally warmed conditions. *Arctic, Antarctic, and Alpine Research* 31(3): 272-277.